1976-06

The frequency response and operating characteristics of the XR-3 loads and motions program

Booth, Bryant Fred

Monterey, California. Naval Postgraduate School

THE FREQUENCY RESPONSE AND OPERATING CHARACTERISTICS OF THE XR-3 LOADS AND MOTIONS PROGRAM

Bryant Fred Booth

NAVAL POSTGRADUATE SCHOOL
Monterey, California

THESIS

THE FREQUENCY RESPONSE
AND
OPERATING CHARACTERISTICS
OF THE
XR-3 LOADS AND MOTIONS PROGRAM

by

Bryant Fred Booth III

June 1976

Thesis Advisor: A. Gerba, Jr.

SECURITY CLASSIFICATION OF THIS PAGE (When Date Entered)

REPORT DOCUMENTATION PAGE		READ INSTRUCTIONS BEFORE COMPLETING FORM
1. REPORT NUMBER	2. GOVT ACCESSION NO.	3. RECIPIENT'S CATALOG NUMBER
4. TITLE (and Subtitle) The Frequency Response and Operating Characteristics of the XR-3 Loads and Motions Program		5. TYPE OF REPORT & PERIOD COVERED Master's Thesis June 1976 6. PERFORMING ORG. REPORT NUMBER
7. AUTHOR(s) Bryant Fred Booth III		8. CONTRACT OR GRANT NUMBER(s)
9. PERFORMING ORGANIZATION NAME AND ADDRESS Naval Postgraduate School Monterey, California 93940		10. PROGRAM ELEMENT, PROJECT, TASK AREA & WORK UNIT NUMBERS
11. CONTROLLING OFFICE NAME AND ADDRESS Naval Postgraduate School Monterey, California 93940		12. REPORT DATE June 1976 13. NUMBER OF PAGES 160
14. MONITORING AGENCY NAME & ADDRESS(if different from Controlling Office) Naval Postgraduate School Monterey, California 93940		15. SECURITY CLASS. (of this report) Unclassified 15a. DECLASSIFICATION/DOWNGRADING SCHEDULE

16. DISTRIBUTION STATEMENT (of this Report)

** Approved for public release; distribution unlimited.

17. DISTRIBUTION STATEMENT (of the abstract entered in Block 20, if different from Report)

18. SUPPLEMENTARY NOTES

19. KEY WORDS (Continue on reverse side if necessary and identify by block number)

20. ABSTRACT (Continue on reverse side if necessary and identify by block number)

The XR-3 Loads and Motions Program, a digital computer simulation of the six degrees-of-freedom equations of motion for the XR-3 captive air bubble test craft, is subjected to a wide range of regular and irregular wave excitations. The operating characteristics of the simulated craft and the frequency response functions for the heave, pitch, and roll responses in ahead, abeam, and following seas are obtained

DD FORM 1 JAN 73 1473 EDITION OF 1 NOV 65 IS OBSOLETE
S/N 0102-014-6601 |
(Page 1)

SECURITY CLASSIFICATION OF THIS PAGE (When Date Entered)

for regular wave excitations. The ahead seas frequency response functions are verified with irregular wave excitation.

The Frequency Response and Operating Characteristics of the XR-3 Loads and Motions Program

by

Bryant Fred Booth III
Lieutenant, United States Navy
B.S.E.E., Iowa State University, 1970

Submitted in partial fulfillment of the
requirements for the degree of

MASTER OF SCIENCE IN ELECTRICAL ENGINEERING

from the

NAVAL POSTGRADUATE SCHOOL
June 1976

ABSTRACT

The XR-3 Loads and Motions Program, a digital computer simulation of the six degrees-of-freedom equations of motion for the XR-3 captive air bubble test craft, is subjected to a wide range of regular and irregular wave excitations. The operating characteristics of the simulated craft and the frequency response functions for the heave, pitch, and roll responses in ahead, abeam, and following seas are obtained for regular wave excitations. The ahead seas frequency response functions are verified with irregular wave excitation.

TABLE OF CONTENTS

LIST OF TABLES

LIST OF FIGURES

ACKNOWLEDGEMENT

The author wishes to express his sincere appreciation to Associate Professor Alex Gerba for the continuous guidance and encouragement he provided during this study. Also acknowledged is the helpful assistance rendered by Ms. Kristina Butler, Mr. M. Anderson, and Mr. Ed Donnellan of the W. R. Church Computer Center.

I. INTRODUCTION

A. BACKGROUND

Since 1973 work has been ongoing at the Naval Postgraduate School on a digital computer model that simulates the forces generated in and the motion experienced by the school's two ton XR-3 captive air bubble test craft. The origin of this model was the "SES Loads and Motions Program" developed for the U.S. Navy by Oceanics Inc. for the Bell 100 ton (100-B) surface effect ship [Ref. 1]. Since there were major design differences between the 100-B and the XR-3, Leo and Boncal [Ref. 2] converted the 100-B model to an initial representation of the XR-3 test craft.

In 1974 Finley [Ref. 3] refined the bow and stern seal subroutines of the XR-3 model and developed new lift fan maps in order to improve the model's performance by providing more realistic air flow rates. At the same time Forbes [Ref. 4] measured various variables of the actual XR-3 test craft while in operation and compared them with the computed values from the XR-3 model. Forbes also introduced several modifications to various subroutines of the model. By the end of 1974 there were three versions of a program to simulate the XR-3.

During 1975 Menzel [Ref. 5] undertook a comparison of Finley's and Forbes's versions by looking at their pitch and roll characteristics. Based on the results of this study,

Menzel introduced program modifications to improve the computed pitch and roll behavior of the simulated XR-3. Menzel's version is considered to be the best to date but there are still portions of the model that require study.

Before additional modifications are made, however, it was deemed desirable to provide a baseline with which further versions could be compared. In addition it was noted that the majority of the past work had been performed while operating the model in calm water conditions. Although the model includes a "sea-state generator," relatively few runs had been made simulating the XR-3 craft in the presence of waves. Two reasons account for this. Past work has been primarily concerned with developing the force interactions within the model where the response of the model to wave forcing actions was not desired. Second, a large amount of CPU time was necessary to simulate a few seconds of simulated run time. The response of the craft, however, to various wave inputs provides a commonly used baseline for future comparisons.

B. OBJECTIVE

The objective of this study was to investigate the dynamic and operational characteristics of Menzel's model when subject to many differing operating conditions. In particular it was desired to obtain the frequency response of the model, i.e., the response of such characteristics as heave, pitch, and roll as functions of wave frequency and amplitude. In

support of this primary objective it was desired to review the characteristics of ocean waves and the interaction of waves and craft in the XR-3 digital model.

II. FREQUENCY RESPONSE FUNCTIONS

The fundamental principle of linear systems is that in the frequency domain the response of a system, Y(w), is equal to the excitation, X(w), multiplied by the system's transfer function, H(w):

$$Y(w) = X(w)H(w).$$

Also

$$|Y(w)| = |X(w)|\,|H(w)|$$

$$\angle Y(w) = \angle X(w) + \angle H(w)$$

where $|\ |$ denotes the magnitude and $\angle$ the phase and

$$S_y(w) = S_x(w) \cdot |H(w)|^2$$

where $S_x(w)$ and $S_y(w)$ represent either the power spectral density or energy spectral density of the excitation and response respectively.

This concept, ingrained in the electrical engineer, is also used by naval architects and marine engineers to describe the motion of a displacement type vessel in a random sea and was first proposed for such use by St. Denis and Pierson [Ref. 6]. The marine engineer refers to the transfer function as the "frequency response function" and $|H(w)|^2$ as the "Response Amplitude Operator," (RAO). The excitation is the ocean wave and the excitation frequency is given in terms of the encounter frequency (see Appendix A). Using this

concept, the vessel can be represented as a single input, multiple output system as shown in Figure 1. The frequency response functions thus describe the vessel in terms of several linear input-output relationships. There can be a separate frequency response function for each degree of freedom. They can be obtained either theoretically or experimentally by such techniques as towing a model in regular waves in a towing tank and measuring the response of interest.

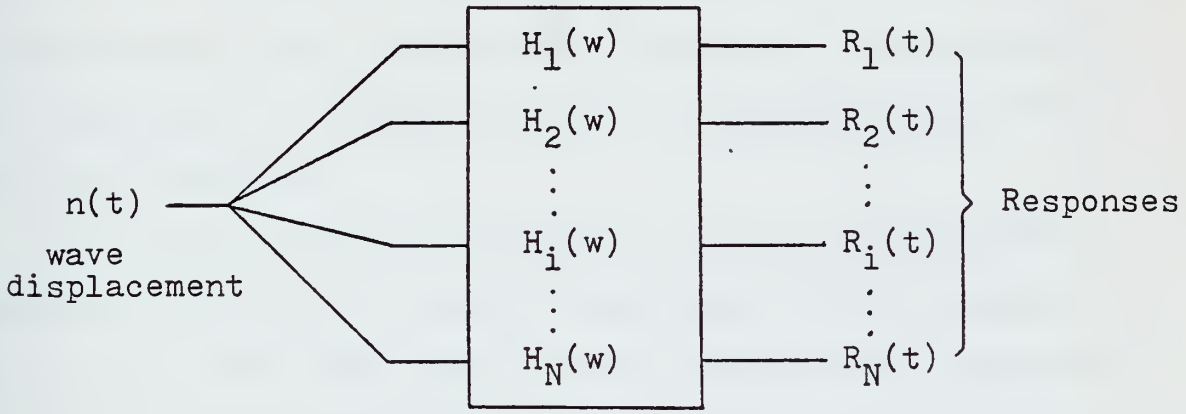

Craft Input-Output Relationship

Figure 1

The assumption that the excitation-response relationship is linear is not true for the SES craft since the hydrodynamic and aerostatic characteristics of the SES are inherently non-linear. However a theoretical frequency response model for the XR-3 was developed by the Aerojet-General Corp. [Ref. 7] using a four degree-of-freedom representation of the craft (responses in surge, heave, pitch, and roll). It was assumed that the response motions were small enough so that the deviation from the linear response was negligible for the motions in the vertical plane.

The frequency response characteristics obtained from this model are reproduced in Appendix B and discussed further in Chapter IV. The predictions were compared to the results from ½ scale model towing tests and, in general, the experimental and theoretical frequency response information was found to show good agreement.

The purpose of this study was to obtain the frequency response functions for the XR-3 Loads and Motions program, a time-domain model that simulates the craft in six degrees-of-freedom and provides time domain outputs of the craft's motions and forces for the on-bubble mode of operation. Since the model provides time-domain outputs, determination of the response characteristics was basically an experimental process consisting of running the model in a sinusoidal wave many times for different wave frequencies, amplitudes, and craft speeds. The desired responses were observed, measured, and

plotted as functions of the encounter frequency. The process and results are discussed in detail in Chapter IV.

However, because the program provides for all six degrees-of-freedom, the inherent nonlinearities of the SES craft are incorporated into the model, particularly in the coupling of the various degrees of freedom. The generality of the frequency response obtained is therefore dependant on the significance of the nonlinearities.

III. WAVE SIMULATION IN THE MODEL

The XR-3 Loads and Motions program has the capability of simulating the craft's motion in regular and irregular seas. The purpose of this section is to review briefly the characteristics of ocean waves and their modeling in the computer program.

A. WAVE CHARACTERISTICS

The outstanding characteristic of the open ocean is its irregularity which can be described by statistical methods on the assumption that a large number of regular (sinusoidal) waves having different wavelengths, frequencies, directions, phase, and amplitudes are superimposed to form the randomly varying sea. Consequently a brief look at the properties of regular waves is necessary.

It is common to characterize wave motion by the direction of the field displacement; waves are either transverse or longitudinal. In the transverse wave the field intensity oscillates in a direction perpendicular to the direction of wave travel, as in the electromagnetic wave. In the longitudinal wave the particles of the medium move in a direction parallel to the motion of the wave itself as in the sound wave. However ocean waves can be considered a combination of the motion experienced in both the transverse and longitudinal waves since the path of an individual water particle is circular as a wave moves by.

The properties of regular waves are well defined by gravity-free surface wave theories. It is assumed that the wave crests are straight, infinitely long, parallel and equally spaced and that wave heights are constant. The wave advances in a direction perpendicular to the line of the crests at a uniform velocity, C, often referred to as "celerity" to emphasize that it is the wave form rather than the water particles that advances.

For convenience the regular wave is normally modeled as a sinusoid with the following properties:

Wave Velocity: $$C = \left(\frac{g\lambda}{2\pi}\right)^{\frac{1}{2}} = \frac{gT}{2\pi} = \frac{g}{w} \qquad \text{(III-1)}$$

Frequency: $$w = \left(\frac{2\pi g}{\lambda}\right)^{\frac{1}{2}} = \frac{2\pi C}{\lambda} \qquad \text{(III-2)}$$

Wavelength: $$\lambda = \frac{2\pi g}{w^2} \qquad \text{(III-3)}$$

Wave surface profile:

$$A(x,t) = A_o \cos\left(\frac{2\pi x}{\lambda} - wt + \varepsilon\right) \qquad \text{(III-4)}$$

where w = angular frequency (radians/sec)

λ = wavelength

T = wave period

g = gravitational constant

x = distance along the direction of propagation from a defined origin

ε = phase angle at the origin

A_o = maximum wave amplitude

The slope of the wave surface is obtained by differentiating (III-4):

$$\frac{A(x,t)}{x} = \frac{-2\pi A_o}{\lambda} \sin\left(\frac{2\pi x}{\lambda} - wt + \varepsilon\right)$$

The maximum wave slope is then:

$$v = \frac{2\pi A_o}{\lambda} \text{ radians} = \frac{360\ A_o}{\lambda} \text{ degrees} \qquad \text{(III-5)}$$

An important property of the regular wave is the energy associated with it consisting of kinetic energy associated with the orbital motion of the water particles and potential energy resulting from the change in water levels in wave hallows and crests. The average energy per unit area of surface for a regular wave is [Ref. 8]:

$$E = \tfrac{1}{2}\ k\ A_o^2 \qquad \text{(III-6)}$$

where k is a water density constant.

The irregular elevation or amplitude of the sea surface is considered to be composed of a theoretically infinite number of small amplitude sine waves of different frequencies. Since the wave frequencies differ, the velocities of propagation differ (III-1) so that at a particular spot on the ocean the phases of the individual waves are uniformly distributed over 2π radians. The wave amplitude at that spot is the sum of the individual wave amplitudes and is therefore also random.

Oceanographers describe the random amplitude of the sea by use of an energy density spectrum. This indicates the amount of energy in the different component waves which have

combined to produce the observed irregular pattern. It is a plot of the energy density per unit frequency, S(w), versus frequency, (w). S(w) is equal to $E/\delta w$ where E is the energy per unit area of the wave surface and δw is an incremental frequency element.

The area under the spectrum represents the total energy per unit surface area of the sea surface since:

$$\int_0^w \frac{E}{w}\, dw = \int_0^w S(w)dw = E$$

The area between any two frequencies, w_1, and w_2, represent the energy density associated with all waves between the two frequencies. It can be shown that the total energy in this frequency increment δw at a central frequency w_n is [Ref. 8]:

$$kS(w_n)\, \delta w.$$

Since the regular waves the energy per unit surface area is proportional to the square of the wave amplitude (III-6) it follows that the square of the amplitude of a wave having the same energy as all the wave components in a band of frequencies represented by δw is:

$$A_n^2 = 2S(w_n)\, \delta w \qquad \text{(III-7)}$$

This allows the construction of an approximate energy density spectrum from a finite number of regular wave components for a given sea condition.

Certain visible properties of the random sea that can be measured by trained observers have also been related to the total energy E and are listed in Table I [Ref. 9]. The most commonly referred to property is the Significant Wave Height, defined as the average of the heights of the highest third of the waves observed and usually written as $\bar{H}_{1/3}$.

Several mathematical models of the energy density spectrum have been proposed but the most widely used model today for wind generated sea states is the Pierson-Moskowitz spectrum [Ref. 10]. It is given by the equation

$$S(w) = \frac{0.0081\, g^2\, e^{-0.74(w_o/w)^4}}{w^5} \qquad \text{(III-8)}$$

where $w_o = (0.210 \cdot g/\bar{H}_{1/3})^{\frac{1}{2}}$.

and is plotted in Figure 2 as a function of significant wave height.

Pierson and Moskowitz also developed a relationship between the significant wave height and wind velocity, U, as:

$$\bar{H}_{1/3} = 0.210\, \frac{U^2}{g}. \qquad \text{(III-9)}$$

TABLE I

Approximate Wave Height Data

Most frequent wave height	$1.41\sqrt{E}$
Average wave height	$1.77\sqrt{E}$
$\bar{H}_{1/3}$	$2.83\sqrt{E}$
$\bar{H}_{1/10}$	$3.60\sqrt{E}$

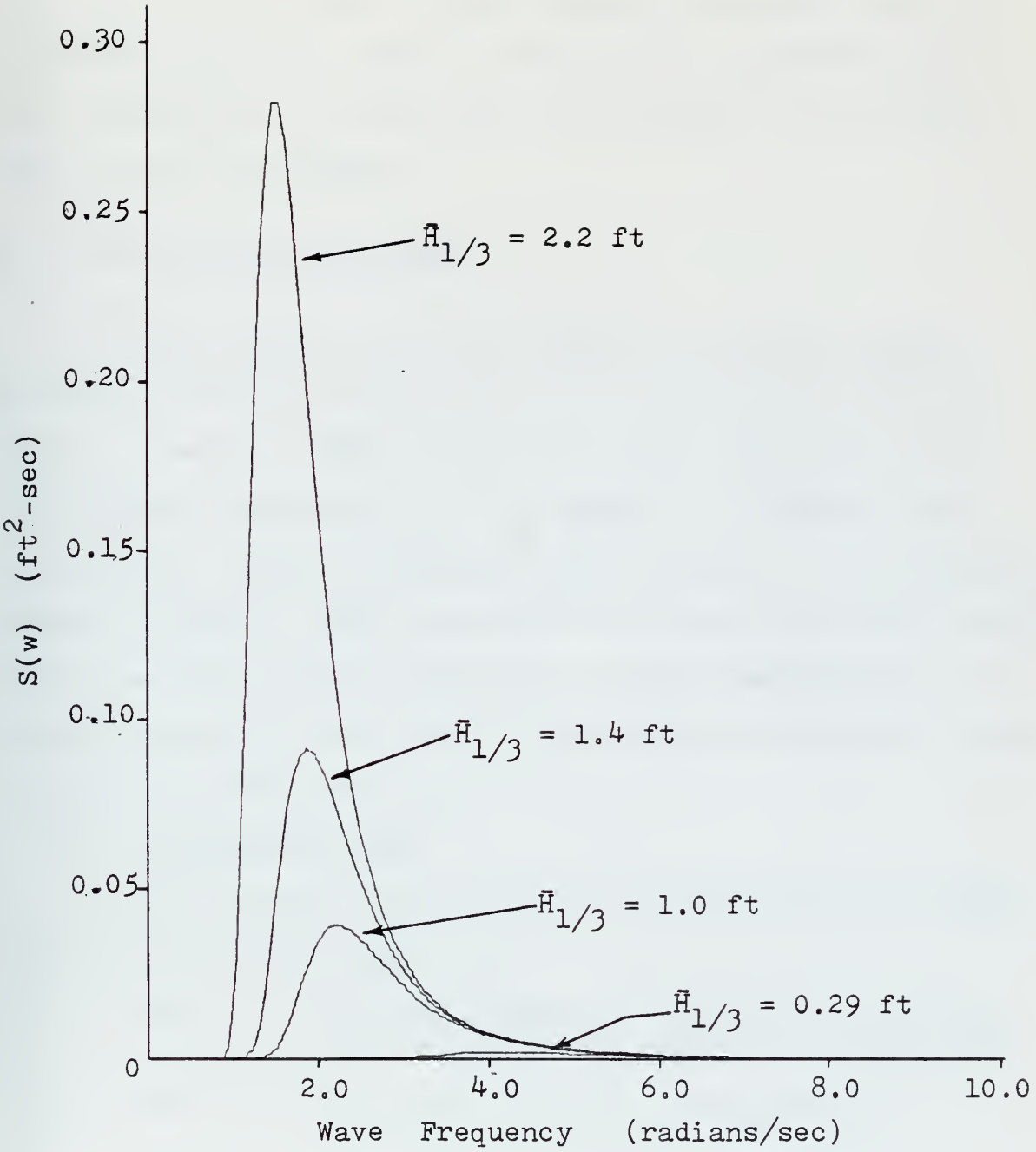

Figure 2. Pierson-Moskowitz Energy Density Spectrums

Substitution of equation III-9 into III-8 yields

$$S(w) = \frac{0.081g^2 \cdot e^{-0.74g^4/(wU)^4}}{w^5} \qquad \text{(III-10)}$$

It is this form of the Pierson-Moskowitz spectrum that can be used in the XR-3 model to generate wave components for the simulation of a random sea as discussed in the following section and Chapter V.

B. SIMULATION IN THE MODEL

Two subroutines of the XR-3 Loads and Motions program, INCON and WAVES, are involved in the construction and simulation of waves. INCON develops the wave components to be used in the construction of the regular or irregular seas and prepares the wave parameter table section of the program's summary listing. WAVES calculates the wave forces and moments acting on the craft and generates the wave amplitudes at the various stations around the hull as well as the bubble volume lost due to wave elevation.

1. Subroutine INCON

Four options are available to define the wave component frequencies and amplitudes.

Option 1: The amplitudes and frequencies (rad/sec) of up to 10 wave components are specified.

Option 2: The amplitudes and wavelengths of up to 10 wave components are specified.

Option 3: The significant wave height ($\bar{H}_{1/3}$) and significant range of periods are specified.

Option 4: The significant wave height and range of significant wave frequencies are specified.

Options 1 and 2 allow the user to construct the regular wave with one component or irregular seas composed of up to 10 components. In option 3 and 4 the program calculates the wave components from the Pierson-Moskowitz energy density spectrum based on the $\bar{H}_{1/3}$ and the range of frequencies in the spectrum. If option 3 is used the upper and lower period limits specified are converted to the lower (w_l) and upper (w_u) frequency limits of the spectrum.

The desired number of component amplitudes and frequencies are developed from the spectrum as follows. The frequency range is divided into as many increments as there are desired wave components. The width of each component is $w_l c^n$ where n is the increment number and c is a weighted scaling factor defined as

$$c = \left(\frac{w_u}{w_l}\right)^{1/N}$$

where N is the number of wave components.

The central frequency of each increment, w_n, is determined by finding the midpoint of the increment, and the energy density per unit frequency, S(w), is calculated from equation III-10 for each w_n. The central frequencies of each of the increments are then used as the component frequencies. The component wave amplitudes are found by taking the square root of equation III-7, i.e.,

$$A_n = (2S(w_n) \cdot \delta w)^{\frac{1}{2}}.$$

The above computations are performed in INCON from statement INCN3600 to INCN4100.

After the frequency and amplitude of each wave component is determined, the waveslope, initial encounter frequency, and encounter period of each wave component is calculated (statements INCN4720 through INCN4920). This information is listed in the wave parameters table section of the program's summary listing. It should be stressed that the encounter frequencies listed are only true if during the simulation the speed is maintained at the initial condition speed.

2. Subroutine WAVES

Once the regular wave components with the appropriate distribution of amplitude and frequency have been determined in INCON, subroutine WAVES constructs the irregular sea simply by adding together the regular wave components as time progresses. It's important to note that this is not a true random sea since the irregular wave formed by the sum of several periodic regular waves must also be periodic unless of course one of the regular wave frequencies is an irrational number. However, it is also apparent that the period of the irregular wave may be exceptionally long as compared to that of any of the regular waves and that in the course of the simulation, one cycle of the irregular wave may not be completed. Therefore the irregular sea developed by adding together the component regular waves may be considered pseudo-random.

WAVES generates the wave amplitudes at the various stations around the sidewalls and seals relative to calm water. The wave elevation relative to any point on the craft is represented for the n^{th} component wave by

$$ETA_n(x,y) = A_n \sin \frac{2\pi}{\lambda_n} (-x\cos\Upsilon - y \sin\Upsilon) + f_n(t) \quad \text{(III-11)}$$

where

$$f_n(t) = w_n t + \frac{2\pi}{\lambda_n} (-X_o \cos\beta - Y_o \sin\beta) \quad \text{(III-12)}$$

X_o and Y_o represent the position of the center of gravity of the craft with respect to the inertial reference frame and are time-varying quantities as the craft moves. β is the angle between the normal to the wave crests and the inertial frame X axis as shown in Figure 3. The craft axes are x and y and the two define any point on the craft in the horizontal plane. The angle Υ is the angle between the ship x axis and the normal to the wave crests and is defined as

$$\Upsilon = \beta - \Psi$$

It is not difficult to see how the relative motion between the craft and wave is accounted for in equation III-11. Assume that the wave height at the center of gravity is desired for a craft heading straight into the waves. Then x = 0, y= 0, $\beta = 180^o$, and $\Psi = 0^o$. Equations III-11 and III-12 then reduce to one equation

$$ETA_n(c.g.) = A_n \sin (w_n t + \frac{2\pi}{\lambda_n} X_o).$$

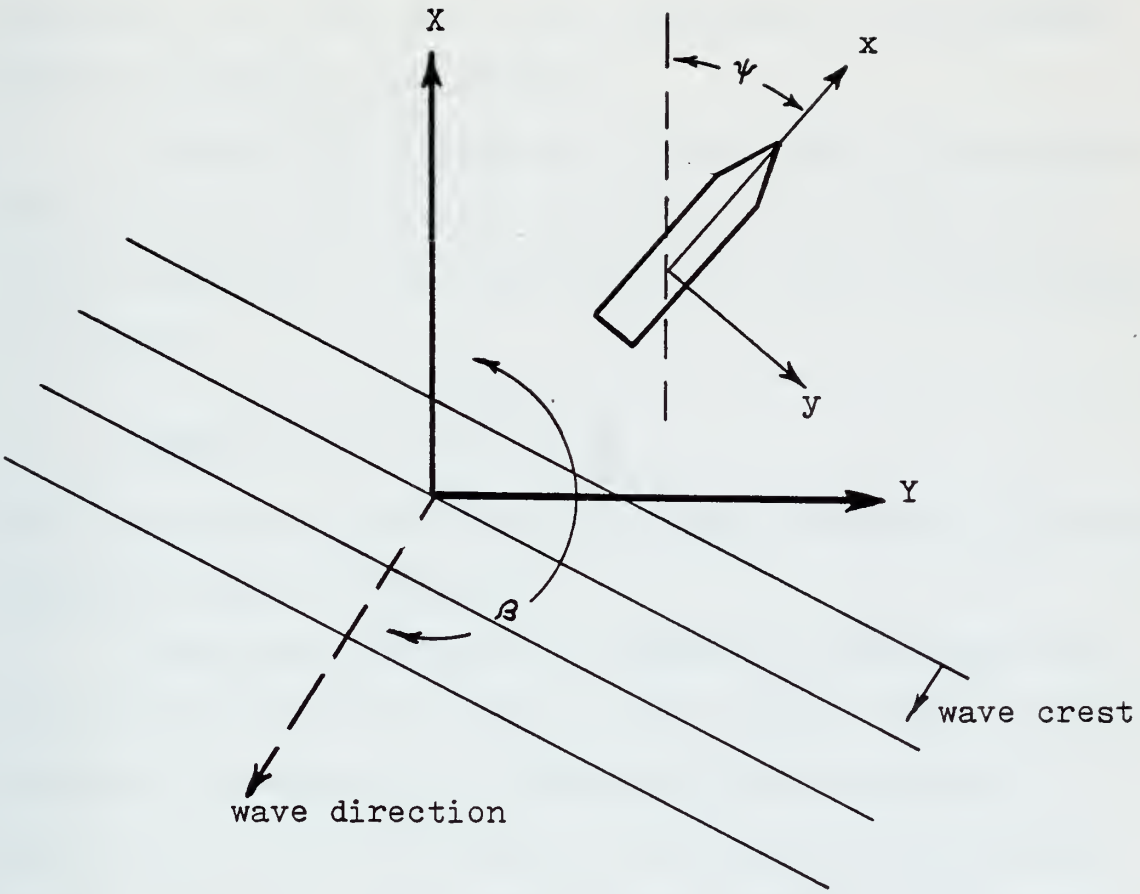

Figure 3. Relation between ship axes, wave direction, and inertial reference frame.

But X_o is Vt, where V is the craft velocity, and $w_n = \frac{2\pi C}{\lambda_n}$ (Eq. III-2) giving

$$ETA_n(c.g.) = A_n \sin\left(\frac{2\pi C}{\lambda_n} + \frac{2\pi V}{\lambda_n}\right)t.$$

The argument of the sine is therefore the encounter frequency times time were $w_{e_n} = (C + V)\frac{2\pi}{\lambda}$ as shown in equation A-3.

Equations III-11 and III-12 are represented by statements WAVS2530, WAVS0540, and WAVS0910.

Because the integration routine used in the program cannot calculate an instantaneous rise in the build-up of the wave amplitude, the amplitude of the wave is restrained by a factor

$$AMPFAC = 1.0 - e^{-t/1.30287}.$$

This restriction of the wave amplitude is evident in the time responses shown in chapter 4.

The primary function of WAVES is to calculate the wave forces and moments acting on the craft. This is described in detail in reference 1. WAVES also has the option of printing the wave elevations at the various stations and center of gravity, the plenum volume lost due to the waves , and the wave forces and moments.

IV. REGULAR SEA RESPONSE CHARACTERISTICS

A. PROCEDURE

Determination of the response characteristics of the XR-3 Loads and Motions computer program was basically an experimental process. In brief, a particular value of craft speed, wave amplitude, and wave heading was chosen and held constant while the model was repeatedly run in a sinusoidal regular wave, each run having a new wave frequency. The desired oscillatory response was measured for each run and plotted as a function of the encounter frequency. A new value of either craft velocity, wave amplitude, or wave direction was chosen and the runs were repeated.

The craft velocities used were 10, 20, and 30 knots which covered the speed range of the actual XR-3 test craft. Three wave headings of 180, 90, and 0 degrees were chosen thereby simulating the craft in ahead, abeam, and following seas respectively. The wave frequencies were chosen to cover the range of frequencies contained in a random sea and present integer values of encounter frequency to the craft as discussed in Appendix A. The responses of primary interest were roll, pitch, and heave at the center of gravity.

The XR-3 model can be run with constant speed or constant thrust options. With the constant speed option the thrust is varied as necessary to maintain the required speed. With the

constant thrust option, the thrust is held constant and the speed is allowed to vary as the simulation progresses. The data presented here was obtained while operating the program with the constant thrust option as it simulates the operation of the actual XR-3 test craft more closely. However the constant speed option was used frequently to obtain initial operating conditions as is explained later in this chapter.

The program's initial conditions in pitch, draft, plenum pressure, and thrust were determined as a function of speed and are given in Appendix C. Appendix D lists the craft parameters used. The model was normally run for 35 seconds to ensure that the steady-state responses had been obtained. The responses were assumed to have reached steady-state when their peak-to-peak and average values remained constant for at least ten seconds. The responses were normally sampled and printed every 0.05 seconds to ensure that the minimum Nyquist rate was more than satisfied at the higher encounter frequencies.

1. Ahead Seas Runs

The initial runs were performed with a craft speed of 20 knots in ahead seas ($\beta = 180^{\circ}$). A wave amplitude of 0.2 feet was chosen as the excitation and the 20 knot calm water thrust of 186.72 lbs. per side was used. Steady-state values of heave and pitch were obtained rapidly for encounter frequencies of 1, 2, and 3 radians per second. However at $w_e = 4$ steady-state responses could not be obtained merely

by running the model for a greater period of time. As shown in Figures 4-A through 4-C, as time progressed the draft increased significantly while the pitch oscillations diverged. Concurrently the speed had dropped in 60 seconds from an initial 20 knots to approximately 15.6 knots thereby reducing the frequency of encounter with the wave excitation. More important was the fact that the plenum volume and pressure were found to have decreased significantly as shown in Figures 4-D and 4-E.

Intuitively the above can be explained as follows. As the plenum volume and pressure fell, the craft sank deeper into the water, increasing the drag on the sidewalls and reducing the speed. The only possible source for the loss of pressure and volume was believed to be associated with the leakage of air through gaps formed between the sidewalls and the water surface or the bow seal and water surface. It was found that the most forward section of the sidewall, and therefore presumably the bow seal also, did rise in and out of the water allowing air leakage through the gap formed as discussed in Appendix E.

However it should be noted that the pressure-volume relationship inside the plenum is an adiabatic process which would have the pressure increase instead of decrease for constant air mass with a reduced volume. Therefore for pressure and volume to both drop, the mass of the air must be decreasing at a rate faster than the volume. Since the

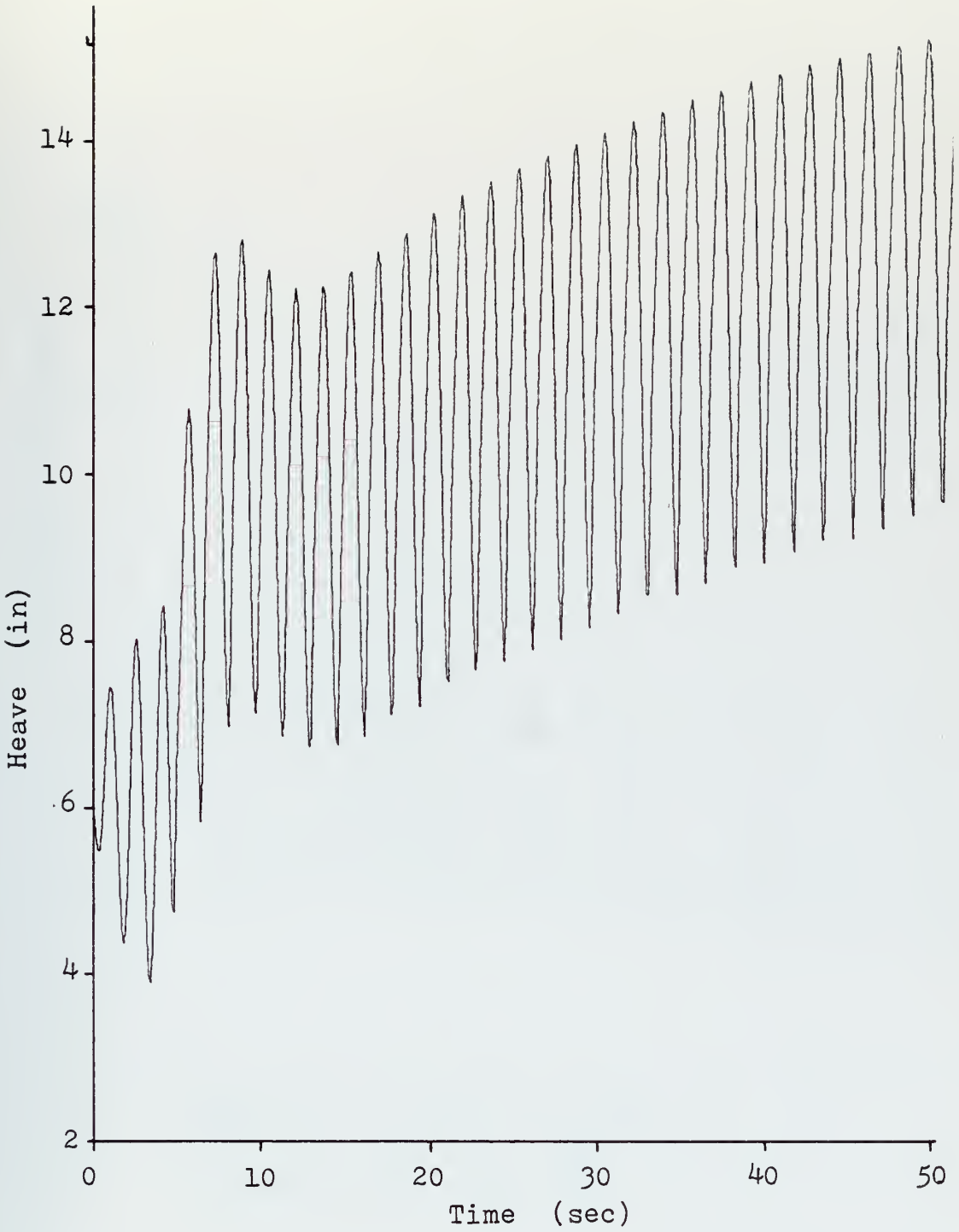

Figure 4-A. Heave vs. Time
V=20 kts, A=0.2 ft, w_e=4
Constant Thrust, β =180°

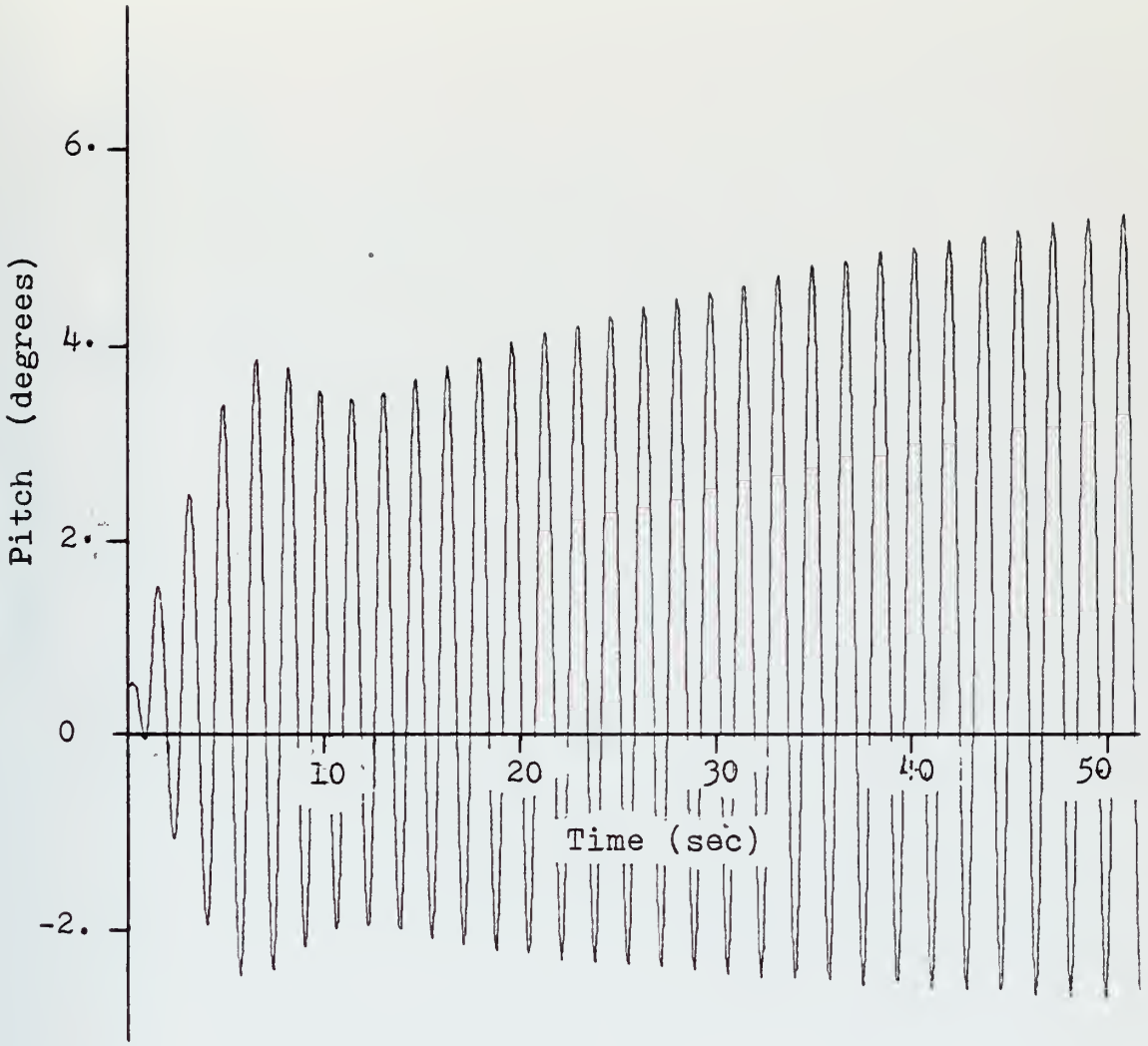

Figure 4-B. Pitch vs. Time
V=20 kts, A=0.2 ft, w_e=4
Constant Thrust, β=180°.

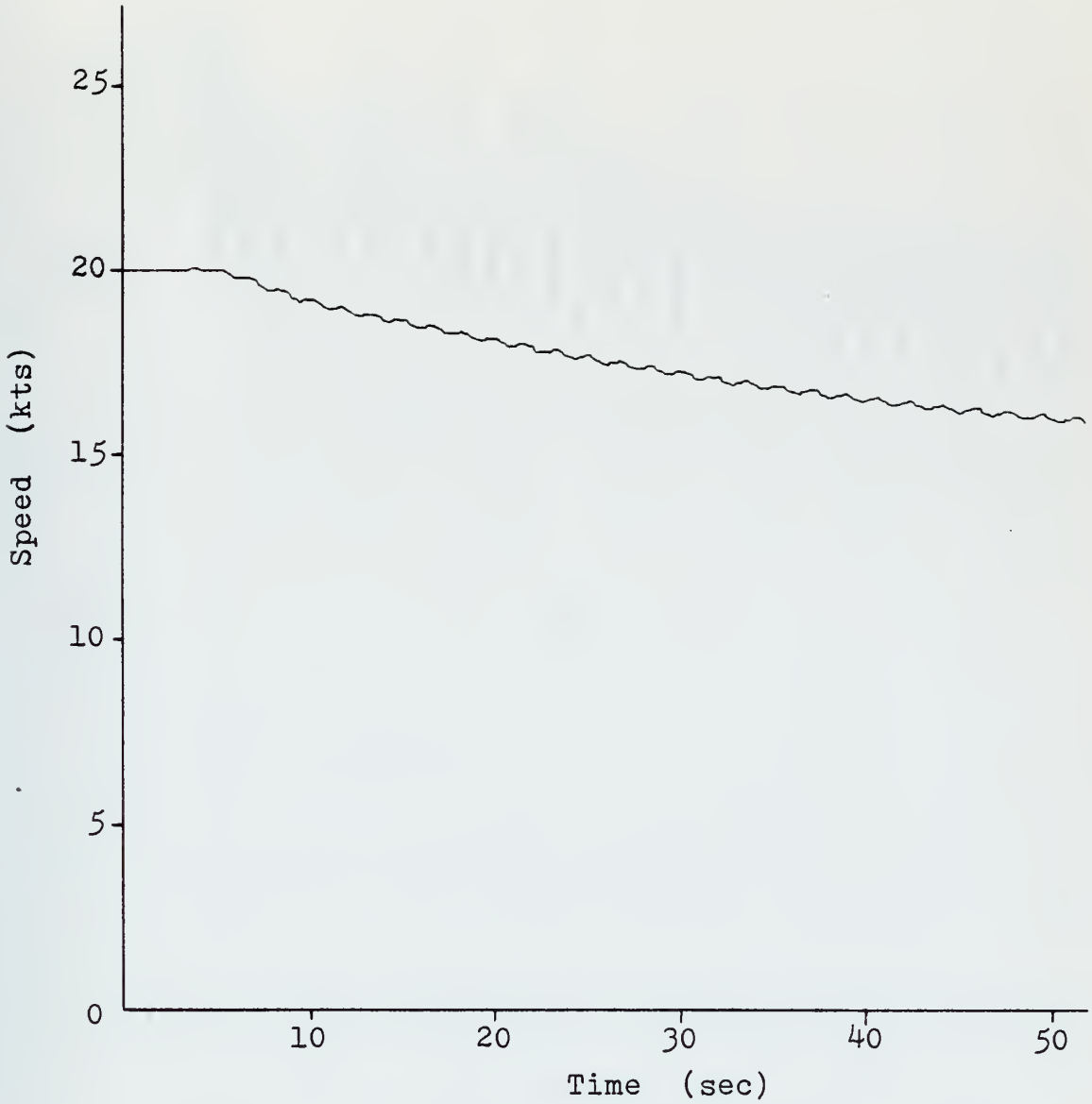

Figure 4-C. Speed vs. Time
V=20 kts, A=0.2 ft, w_e=4
Constant Thrust, β =180°

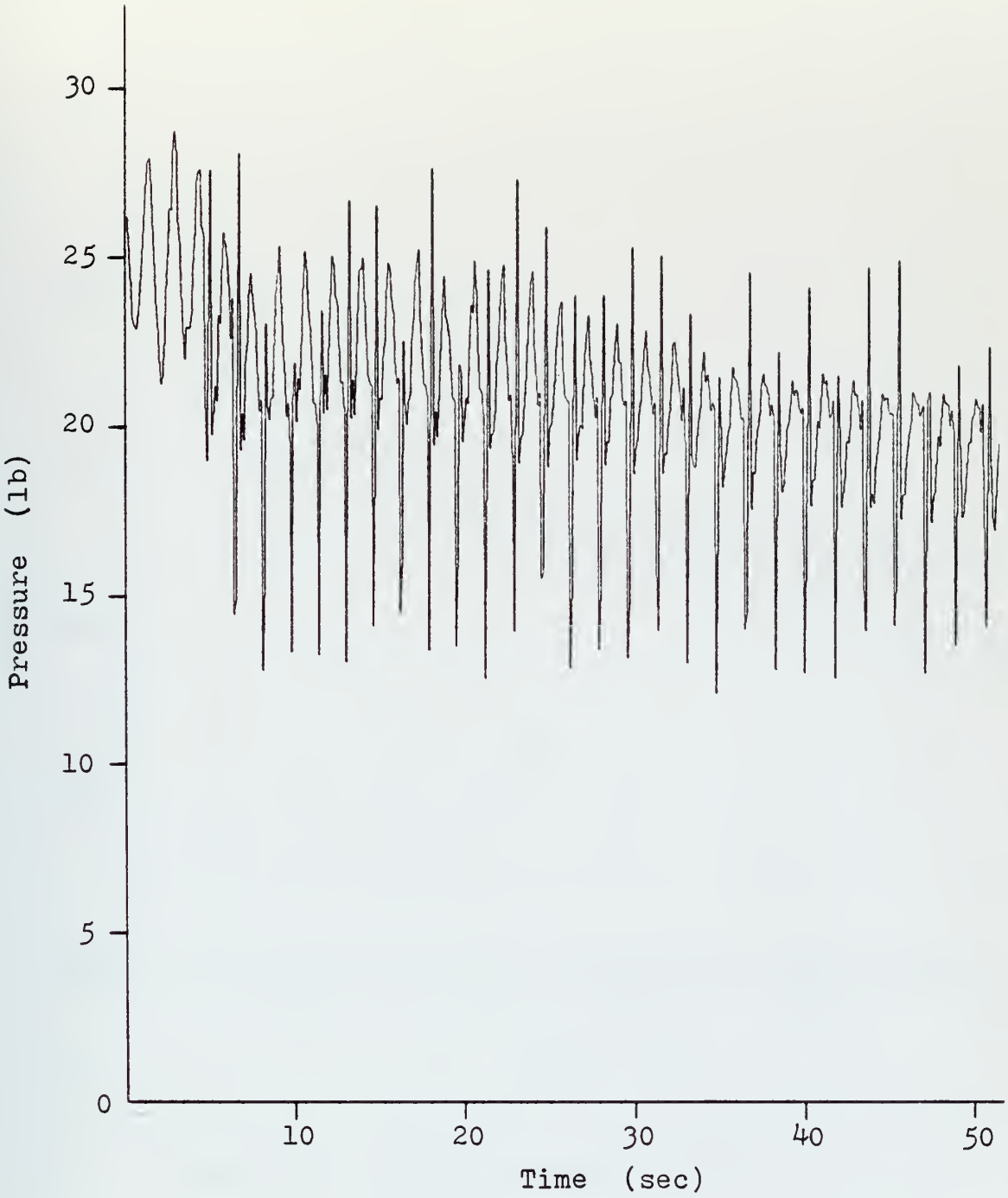

Figure 4-D. Plenum Pressure vs. Time
V=20 kts, A=0.2 ft, w_e=4
Constant Thrust, β =180°

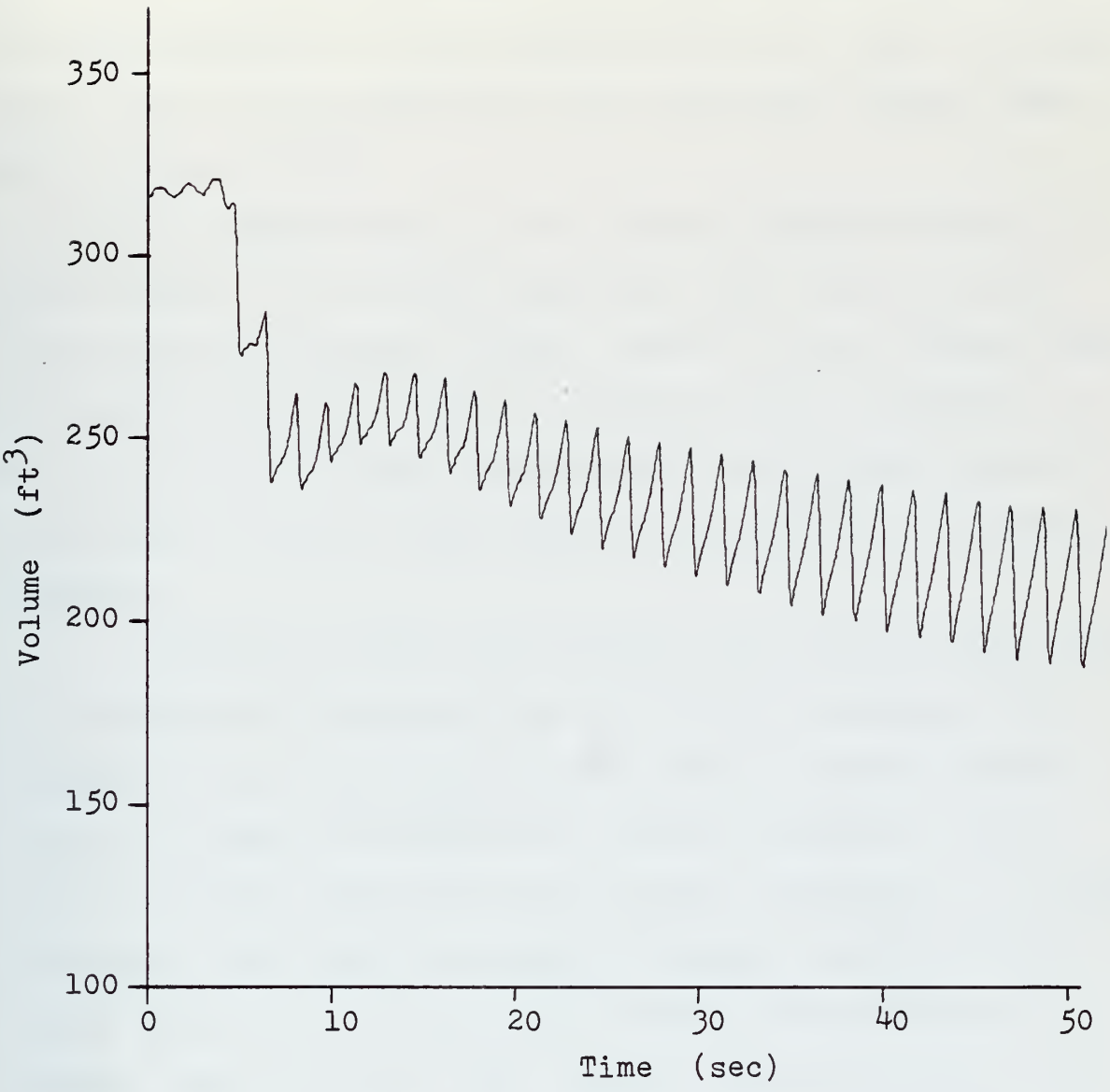

Figure 4-E. Plenum Volume vs. Time
V=20 kts, A=0.2 ft, w_e=4
Constant Thrust, β =180°

air flow rate into the plenum will saturate due to the air fan map limitations, high leakage rates would cause the mass of the air to drop faster than the volume and thereby cause the pressure to drop.

Of interest also is the initial transient portion of the responses. As the wave amplitude rises exponentially, the responses are almost linear. However as the coupled heave and pitch amplitudes increase, gapping begins, resulting in the rapid drop in volume and therefore causing the nonlinear saturation of the air fans which is reflected in the pressure response.

Clearly the calm water thrust value was not sufficient to overcome the increased drag due to the increasing draft. Because of this, the model was ran with the constant speed option in order to determine the thrust necessary to maintain the 20 knot speed and the encounter frequency of 4 radians per second. The result is shown in Figure 5 where the necessary thrust is a not quite sinusoidal variable with an average value of 215 lbs. and lagging the wave excitation by approximately 240 degrees. The model was then run with a constant thrust value of 215 lbs. per side and steady-state responses were obtained as shown in Figure 6. Note that the craft still sinks somewhat deeper into the water than for calm water conditions and that the plenum pressure and volume have reached a steady-state condition.

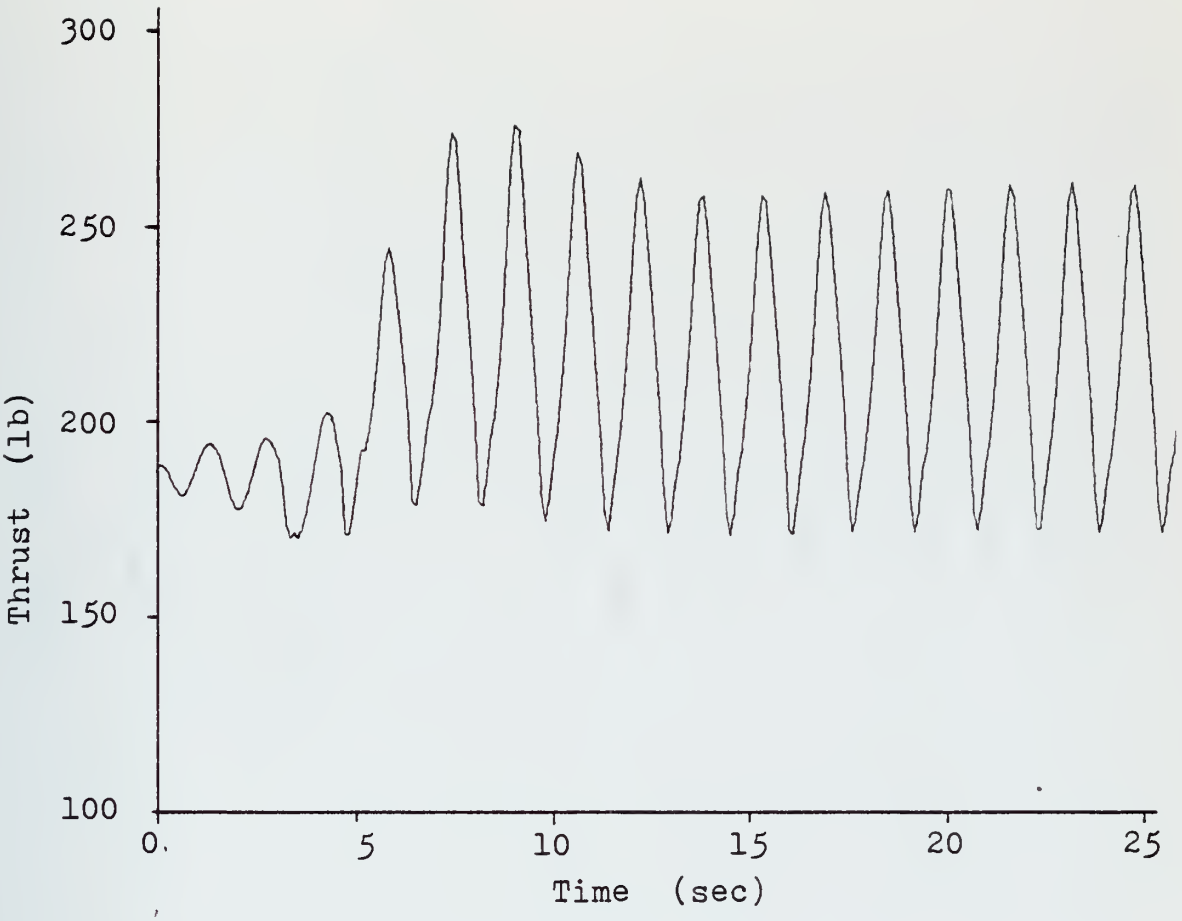

Figure 5. Starboard Thrust vs. Time
V=20 kts, A=0.2 ft, w_e=4
Constant Speed, β =180°

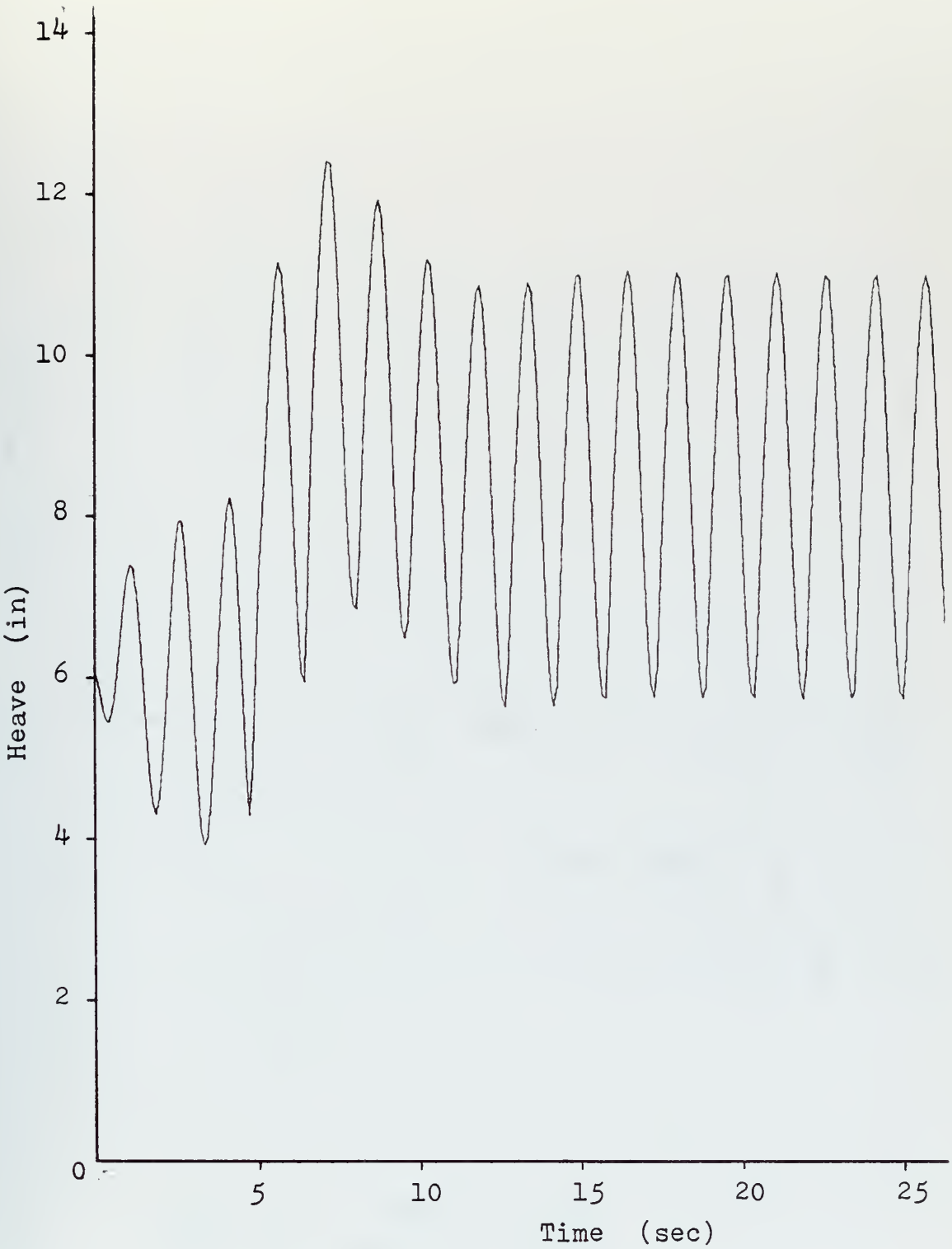

Figure 6-A. Heave vs. Time
V=20 kts, A=0.2 ft, w_e=4
Constant Thrust=215 lb, β =180°

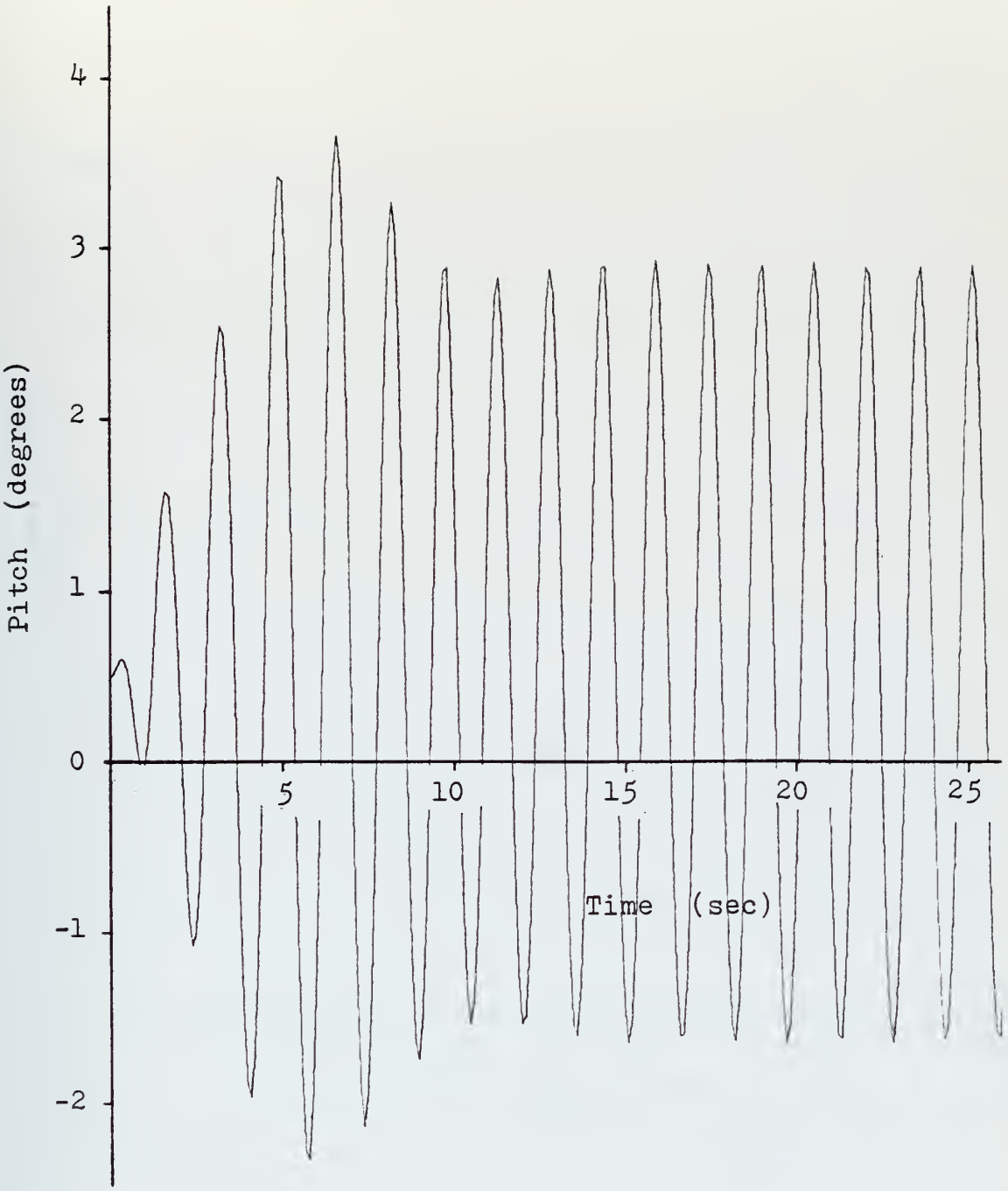

Figure 6-B. Pitch vs. Time
V=20 kts, A=0.2 ft, w_e=4
Constant Thrust =215 lb, β =180°

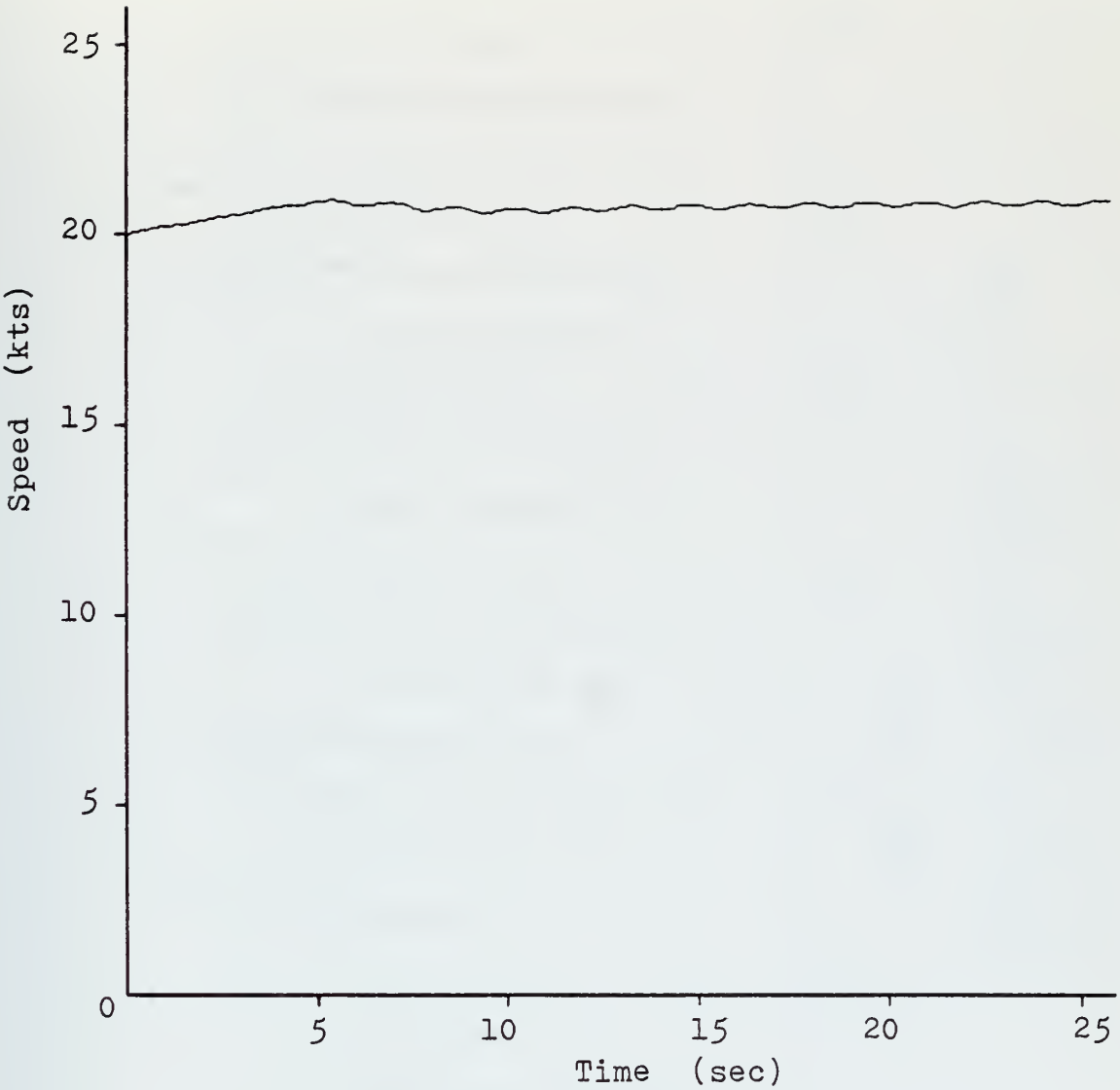

Figure 6-C. Speed vs. Time
V=20 kts, A=0.2 ft, w_e=4
Constant Thrust =215 lb, β =180°

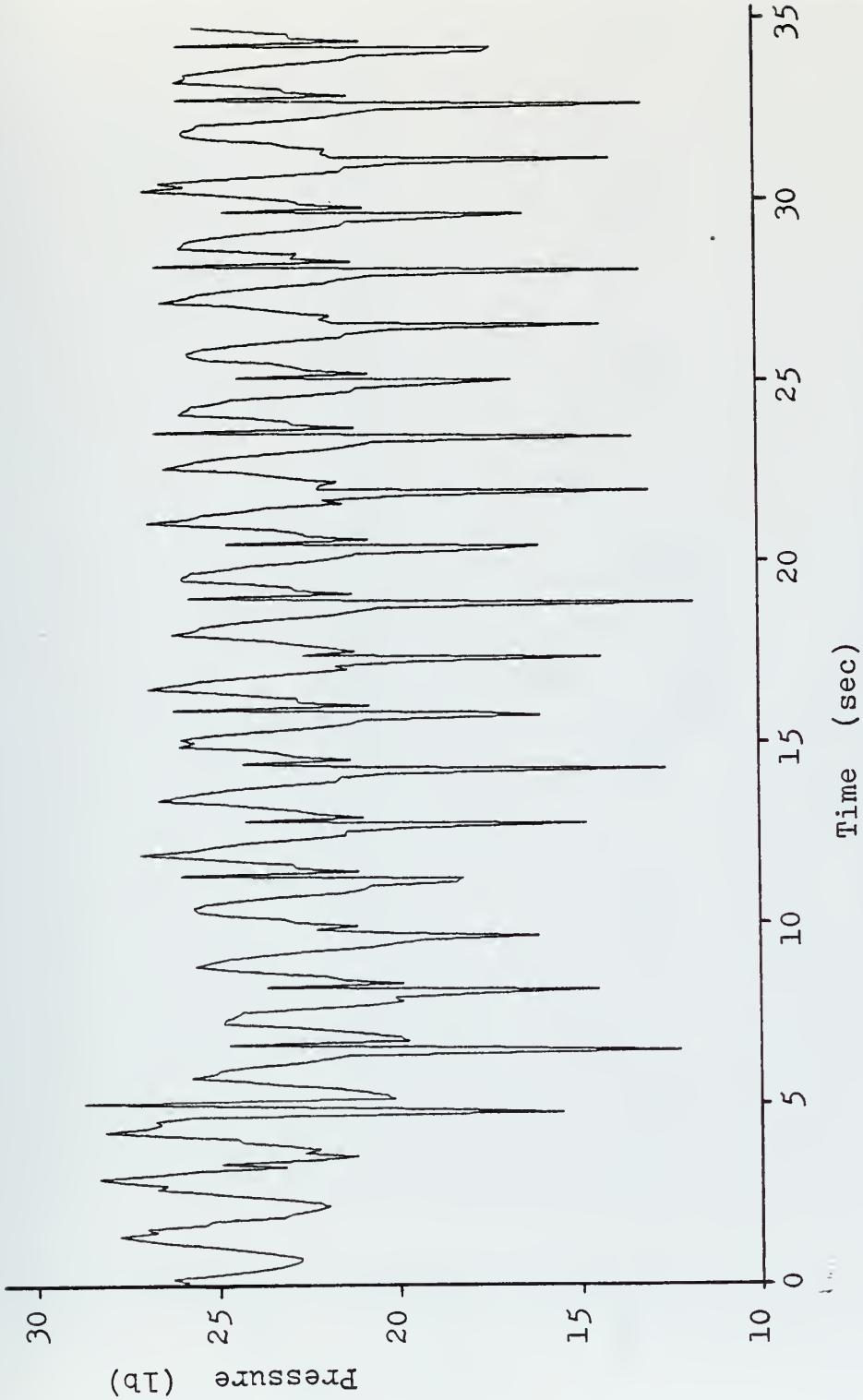

Figure 6-D. Plenum Pressure vs. Time
V=20 kts, A=0.2 ft, w_e=4
Constant Thrust =215 lb, β =180°

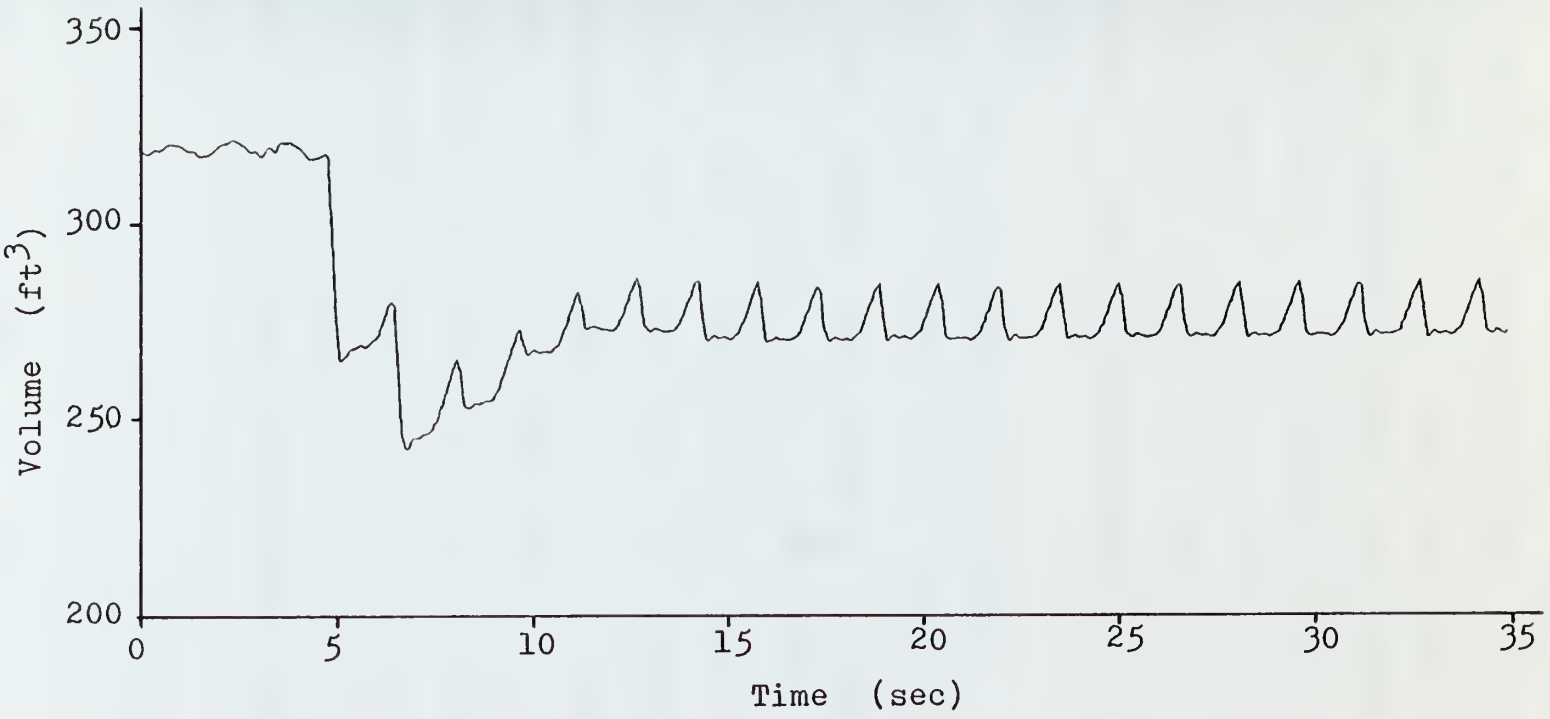

Figure 6-E. Plenum Volume vs. Time
V=20 kts, A=0.2 ft, w_e=4
Constant Thrust =215 lb, β =180°

From the initial 20 knot runs a general procedure was developed for obtaining steady-state responses. The model was initially run with the constant thrust option using the calm water thrust for the desired speed. The pitch, heave, and roll responses and craft speed were observed. If steady-state values were not reached within thirty-five seconds the model was rerun with the constant speed option. The average value of thrust from this run was then used as the thrust for a second constant thrust run. This would normally produce steady-state heave and pitch responses for speeds of 20 and 30 knots.

Obtaining steady-state responses for a craft speed of 10 knots required several more iterations of the thrust, however. For example, at an encounter frequency of six radians per second, the calm water thrust of 200.31 lbs. per side drove the craft to a speed of 11.5 knots in 20 seconds and resulted in a decreasing draft and converging heave and pitch oscillations. A constant speed run produced an average thrust of 194 lbs. per side but when this was applied as the input to a constant thrust run, the speed dropped below hump speed. A choice midway between the two values (198 lbs.) again produced an increasing speed and unsteady oscillations. A final thrust value of 196 lbs. produced the desired steady-state responses.

All runs performed at 10 knots were found to be extremely sensitive to small changes in thrust. This is due to operating the program in a region where the drag versus

speed has a minima, allowing small variations in thrust to significantly effect the craft speed. This problem was also noted by Cagle [Ref. 11] in his study of the original 100-B digital model.

2. Abeam Seas Runs

To obtain the frequency response functions for the roll characteristics of the digital model, the program was run simulating the craft in abeam seas, i.e., the angle between the normal to the wave crests (in the direction of propagation) and the craft's X_o - axis was 90 degrees. The craft was run at 20 and 30 knots using the calm water thrust values and the constant thrust option. The wave amplitude was 0.2 feet.

A typical set of responses obtained while operating the program in this manner is shown in Figures 7-A through 7-E where neither the heave, pitch, nor roll reached steady-state. Figure 7-E provided the explanation for the responses. As the craft encountered the waves a yaw oscillation was induced. As time progressed the average value of the yaw became non-zero and the craft gradually turned into the wave, changing the wave excitation-craft response relationship. To obtain steady-state pitch, roll, and heave conditions, it was clear that it was necessary to first have a stable yaw response.

To obtain steady-state yaw a rudder map, i.e., a set of data points that describe the rudder angle as a function of time, was added to the model in order to turn the craft

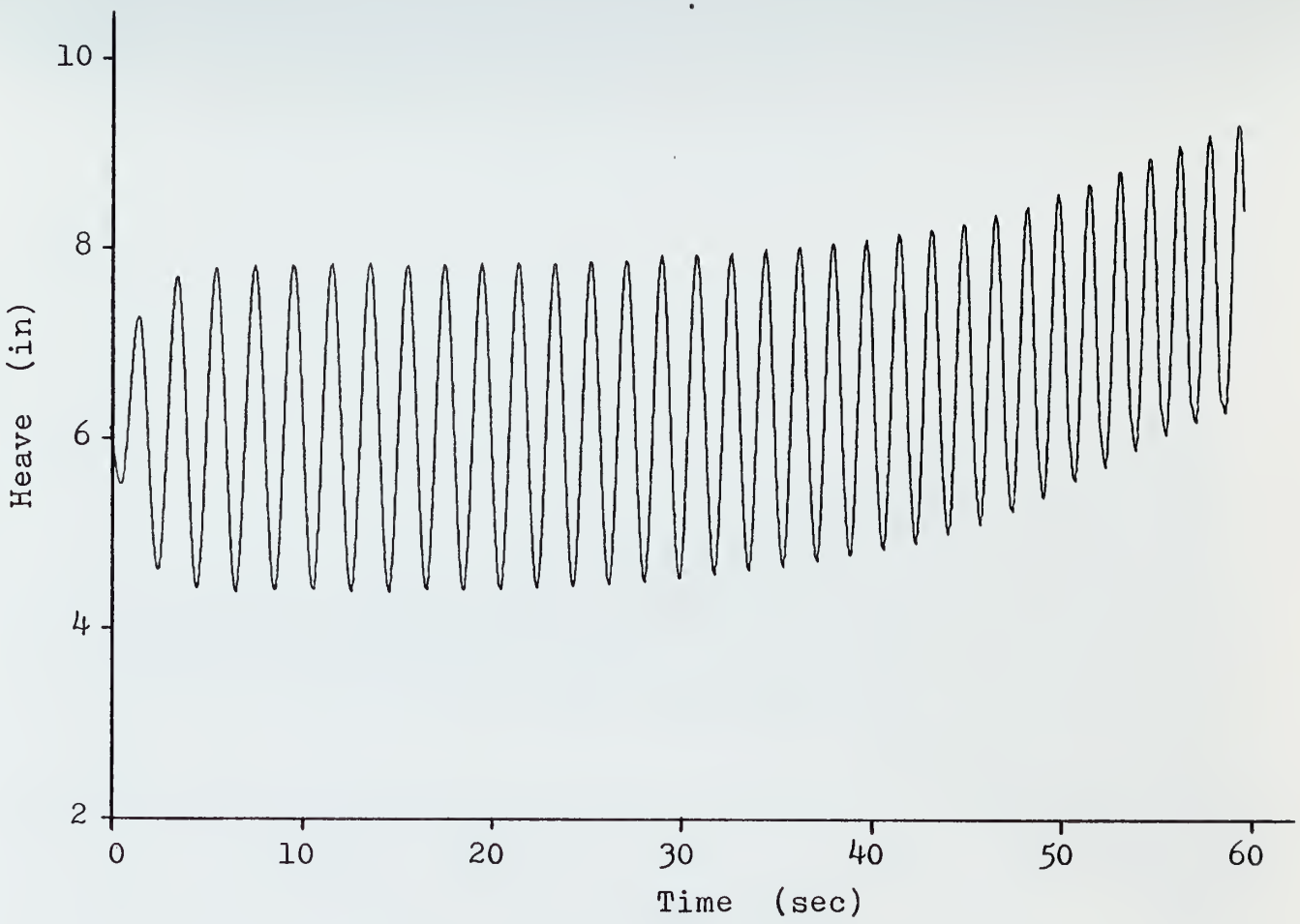

Figure 7-A. Heave vs. Time
V=20 kts, A=0.2 ft, w_e=3
$\beta = 90^{o}$, Constant Thrust

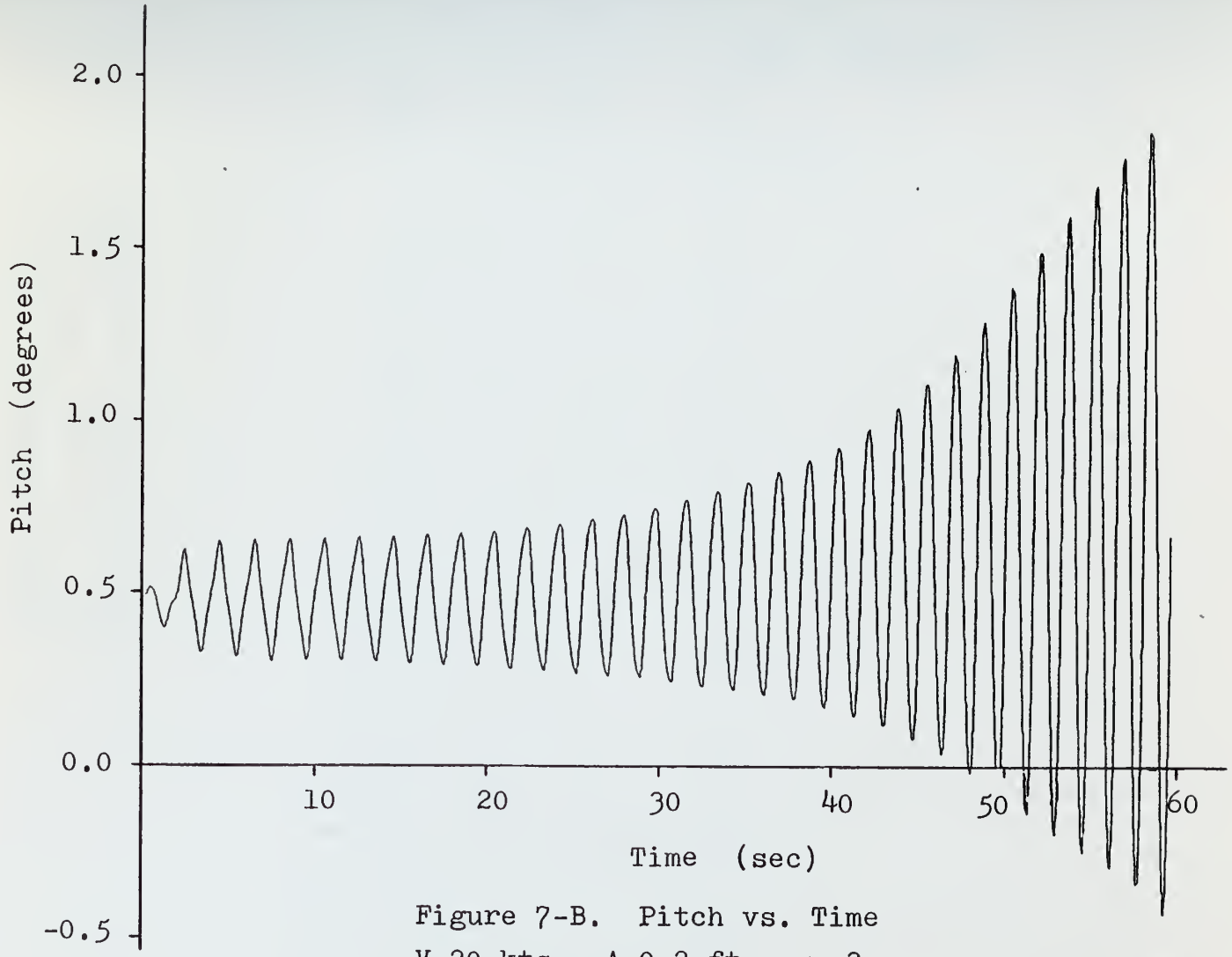

Figure 7-B. Pitch vs. Time
V=20 kts, A=0.2 ft, w_e=3
$\beta = 90^\circ$, Constant Thrust

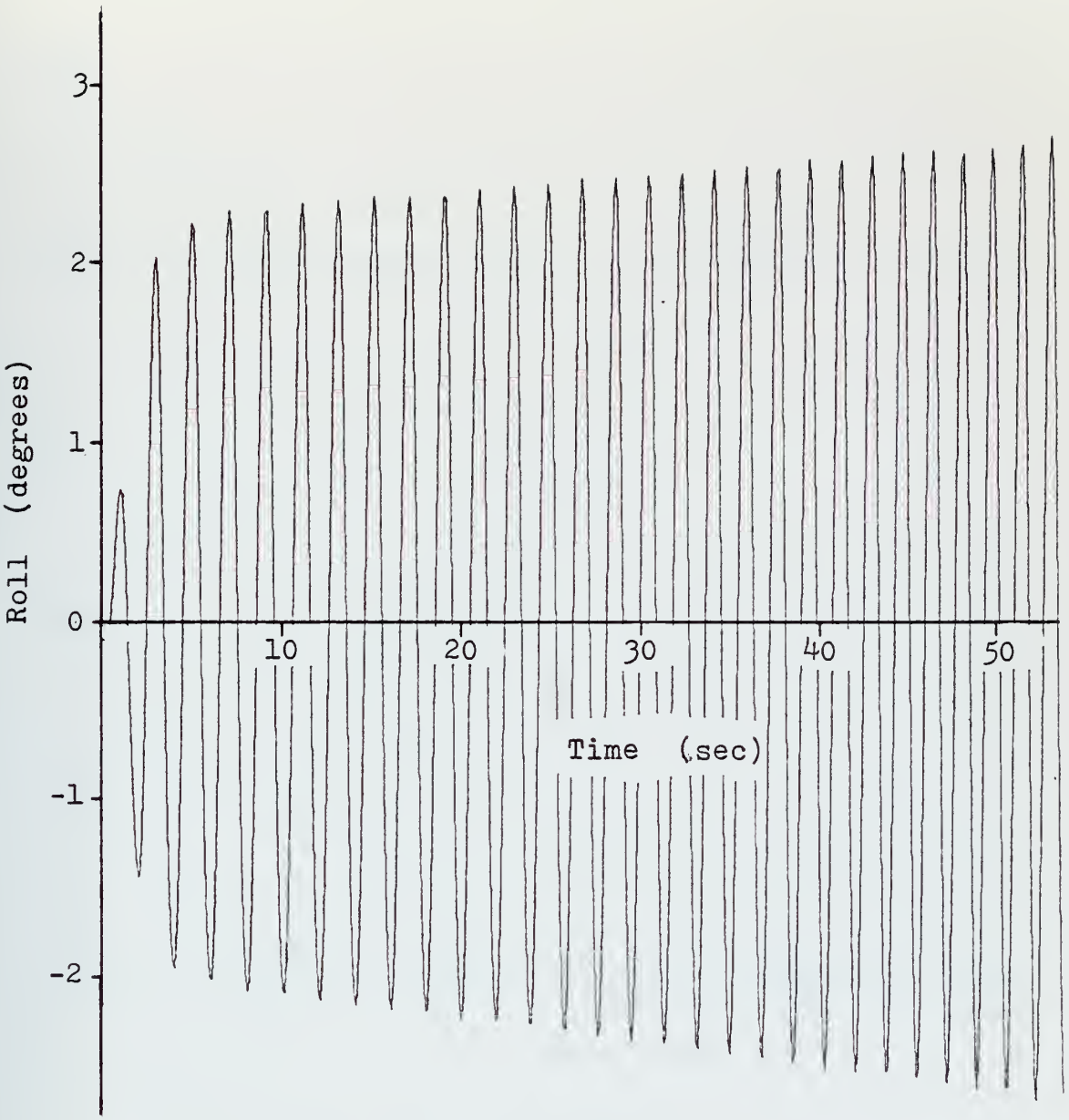

Figure 7-C. Roll vs. Time
V=20 kts, A=0.2 ft, w_e=3
$\beta = 90^{\circ}$, Constant Thrust

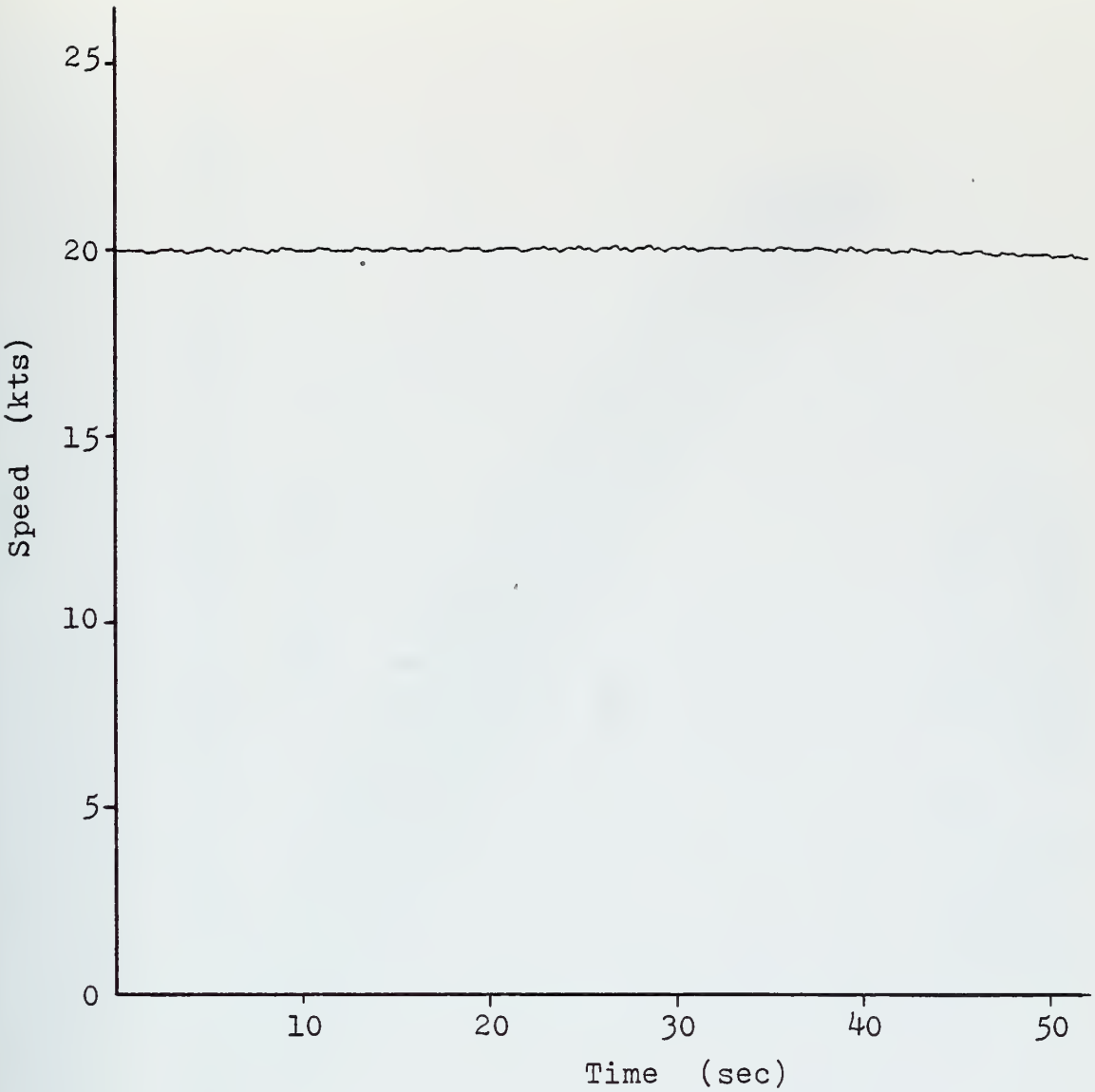

Figure 7-D. Speed vs. Time
V=20 kts, A=0.2 ft, w_e=3
β = 90°, Constant Thrust

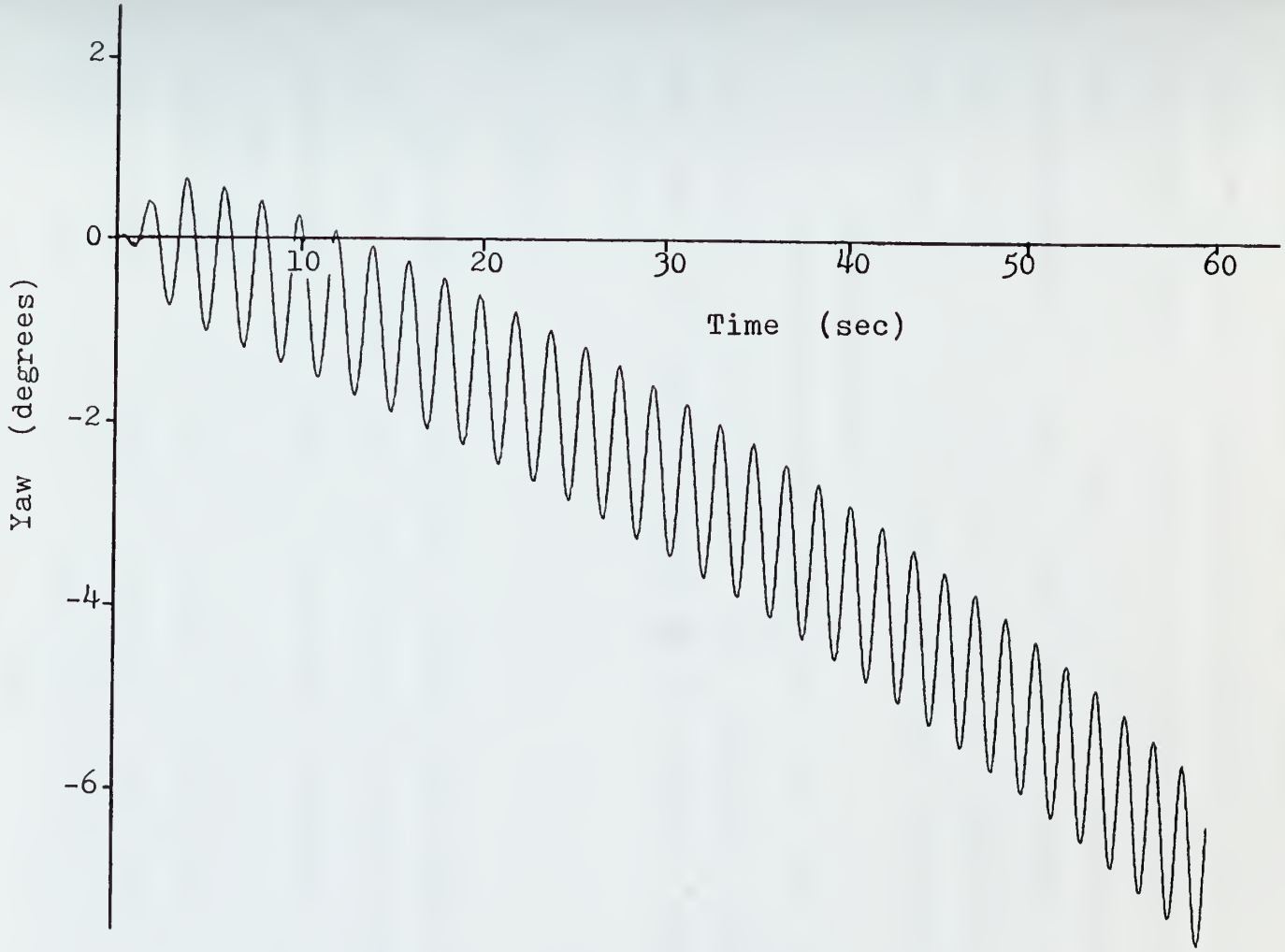

Figure 7-E. Yaw vs. Time
V=20 kts, A=0.2 ft, w_e=3
$\beta = 90^{\circ}$, Constant Thrust

in a direction opposite that which was induced by the wave. Several iterations of this process were required before steady-state responses were reached. It was determined that a small rudder angle, typically less than a degree, of constant magnitude would allow steady-state operation to be reached. For the example given in Figure 7, a constant rudder map of -0.2 degrees as shown in Figure 8-A produced steady-state responses as exemplified in Figure 8-B and 8-C. Although the average value of the yaw is still not zero, its magnitude is considerably less than initially when the rudder angle was zero.

3. Following Seas Runs

Following seas are encountered when the craft and waves travel in the same direction. The procedures described for ahead seas were used to determine the desired response characteristics.

B. RESULTS

The responses of primary interest were heave, pitch, and roll. Once steady-state conditions had been reached, the peak-to-peak and average values were determined and are listed in Appendix G. Since heave is a function of vertical wave displacement, the ratio of the two was obtained and plotted as a function of encounter frequency. Similiarily the ratio of pitch amplitude and roll amplitude to their excitation, the wave slope, was found and plotted.

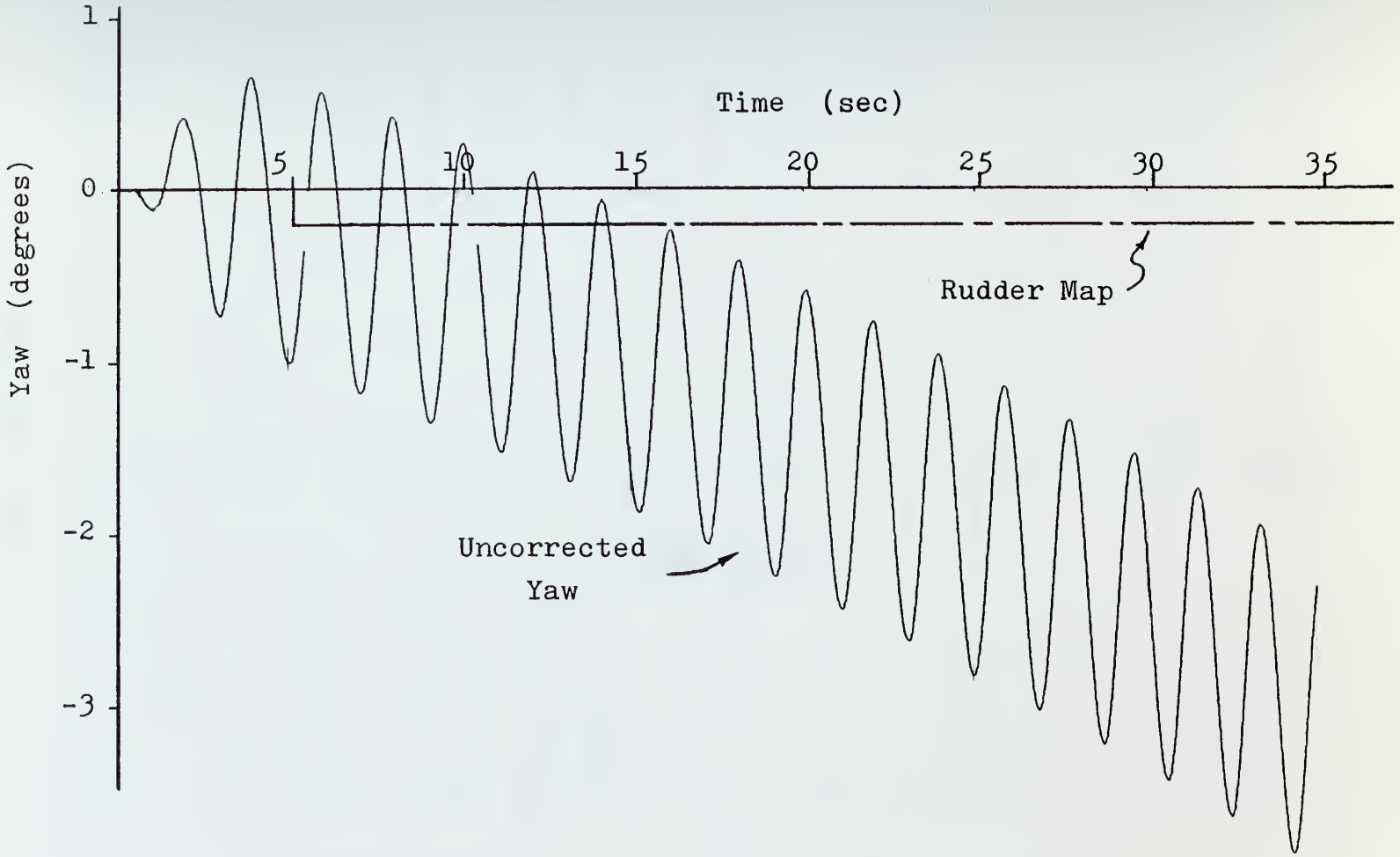

Figure 8-A. Yaw vs. Time & Rudder Map
V=20 kts, A=0.2 ft, w_e=3
$\beta = 90^{o}$, Constant Thrust

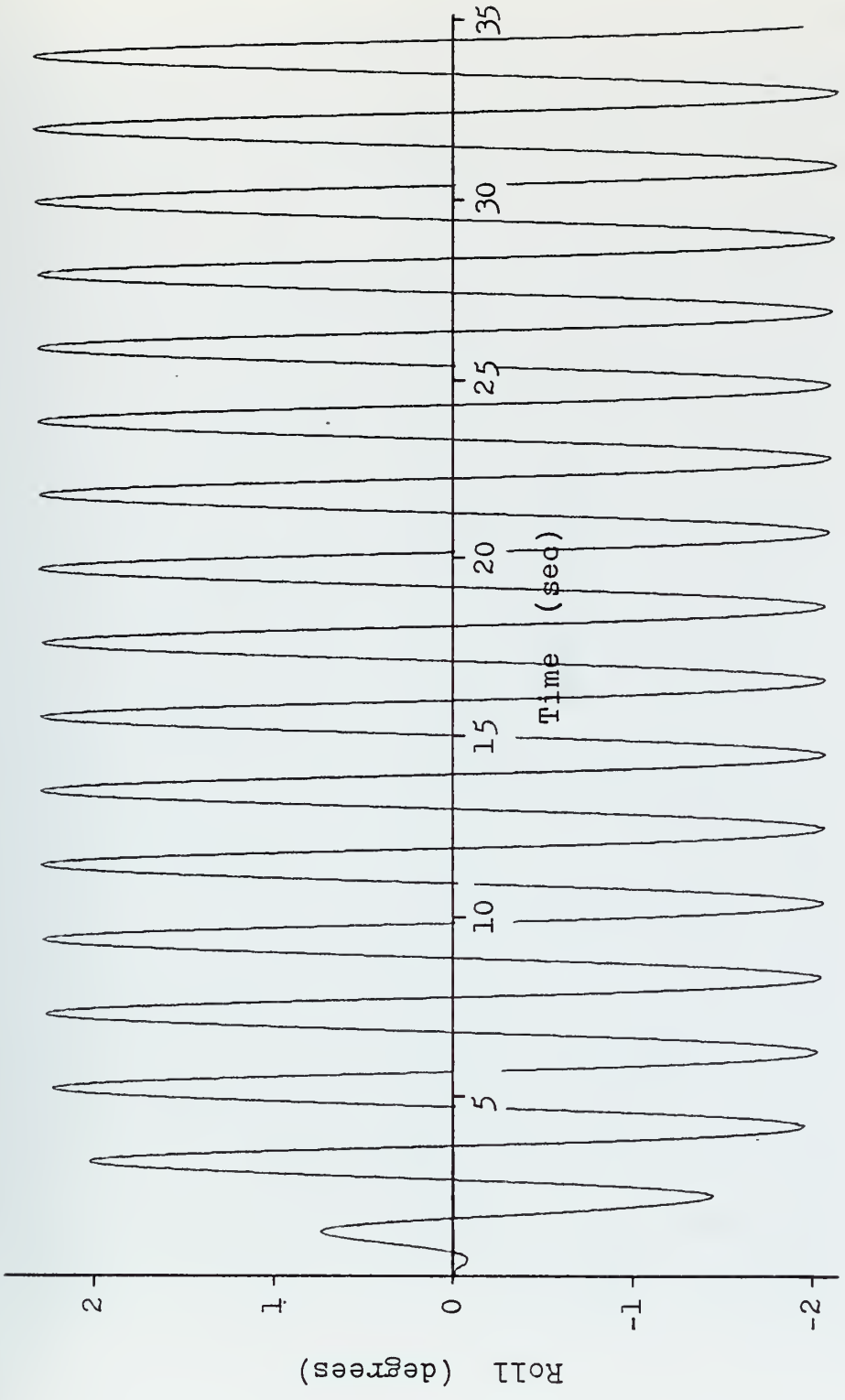

Figure 8-B. Roll vs. Time
V=20 kts, A=0.2 ft, w_e=3
β = 90°, Constant Thrust

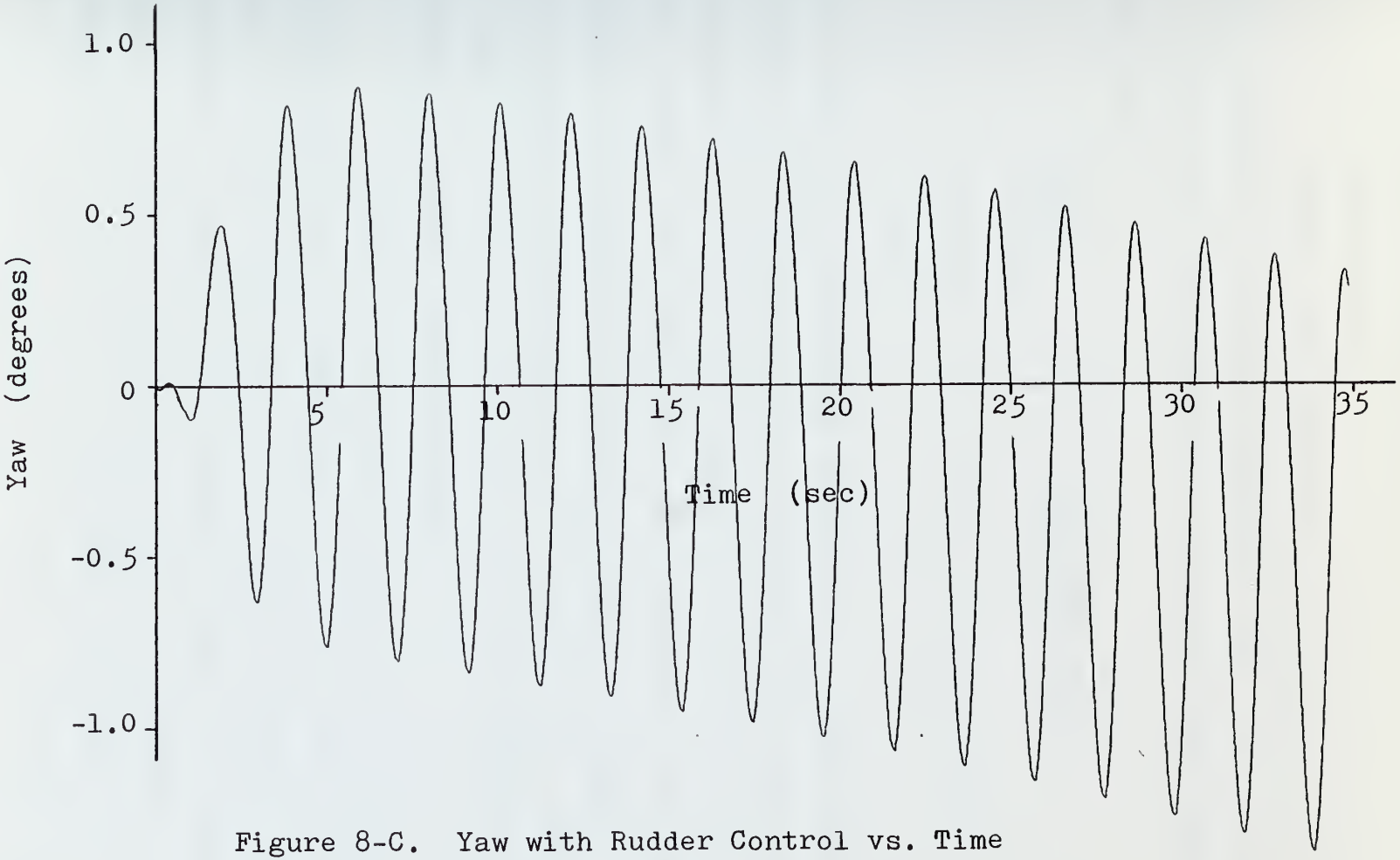

Figure 8-C. Yaw with Rudder Control vs. Time
V=20 kts, A=0.2 ft, w_e=3
$\beta = 90^{\circ}$, Constant Thrust

1. Frequency Response Functions

a. Ahead Seas

Program runs simulating ahead seas conditions over a range of encounter frequencies from 1 to 20 radians per second were conducted at the following craft speeds and wave heights.

Speed	Wave Amplitude
10 knots	0.2 ft
20 knots	0.1, 0.2, 0.3, 0.5 ft
30 knots	0.2, 0.3 ft

Given that with a sinusoidal excitation a linear system should produce a sinusoidal response, in general the heave and pitch responses were found to be linear for the ahead seas conditions. Small nonlinearities were noted at w_e=1 in the pitch response, two examples of which are shown in Figure 9. The only extreme occurrence was at V=20 knots, w_e=4, and A=0.5 ft. As shown in Figure 10 both pitch and heave displayed large nonlinear response characteristics.

Figures 11 through 17 present the frequency response functions for heave and pitch for the seven combinations of craft speed and wave heights simulated. The predominate characteristic in all of them is the resonant peak in the pitch response near w_e=4. A comparison of the responses as a function of waveheight for speeds of 20 and 30 knots is shown in Figures 18 and 19. The heave response is nearly independent of waveheight except for the region

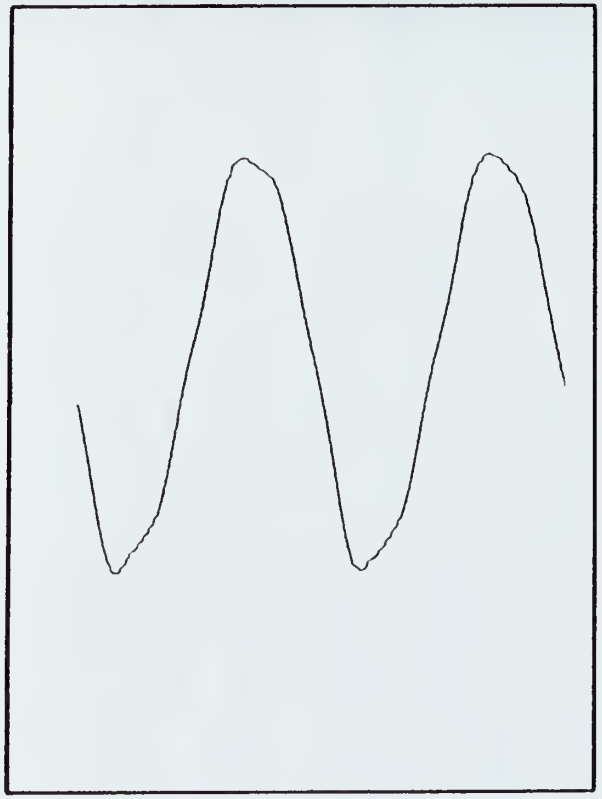

V = 20 kts, A = 0.2 ft

w_e = 1

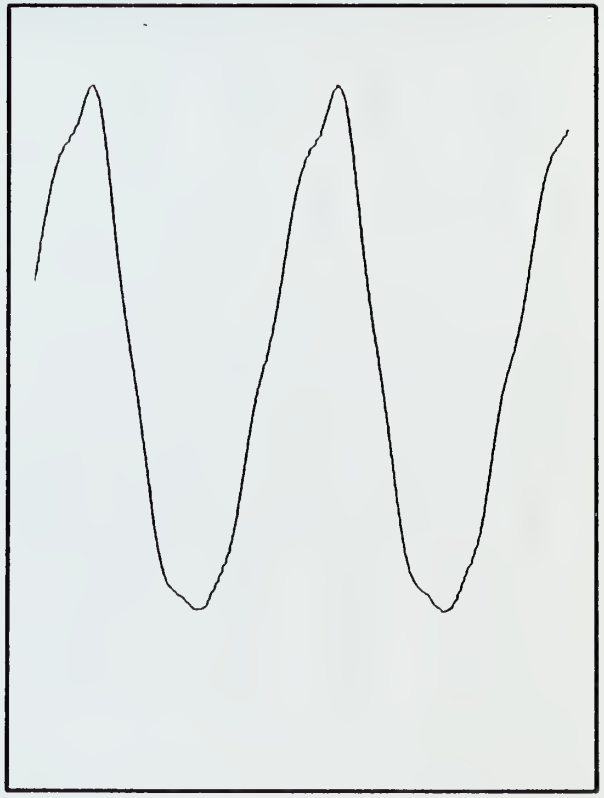

V = 30 kts, A = 0.3 ft

w_e = 1

Figure 9. Ahead Seas Pitch Nonlinearities

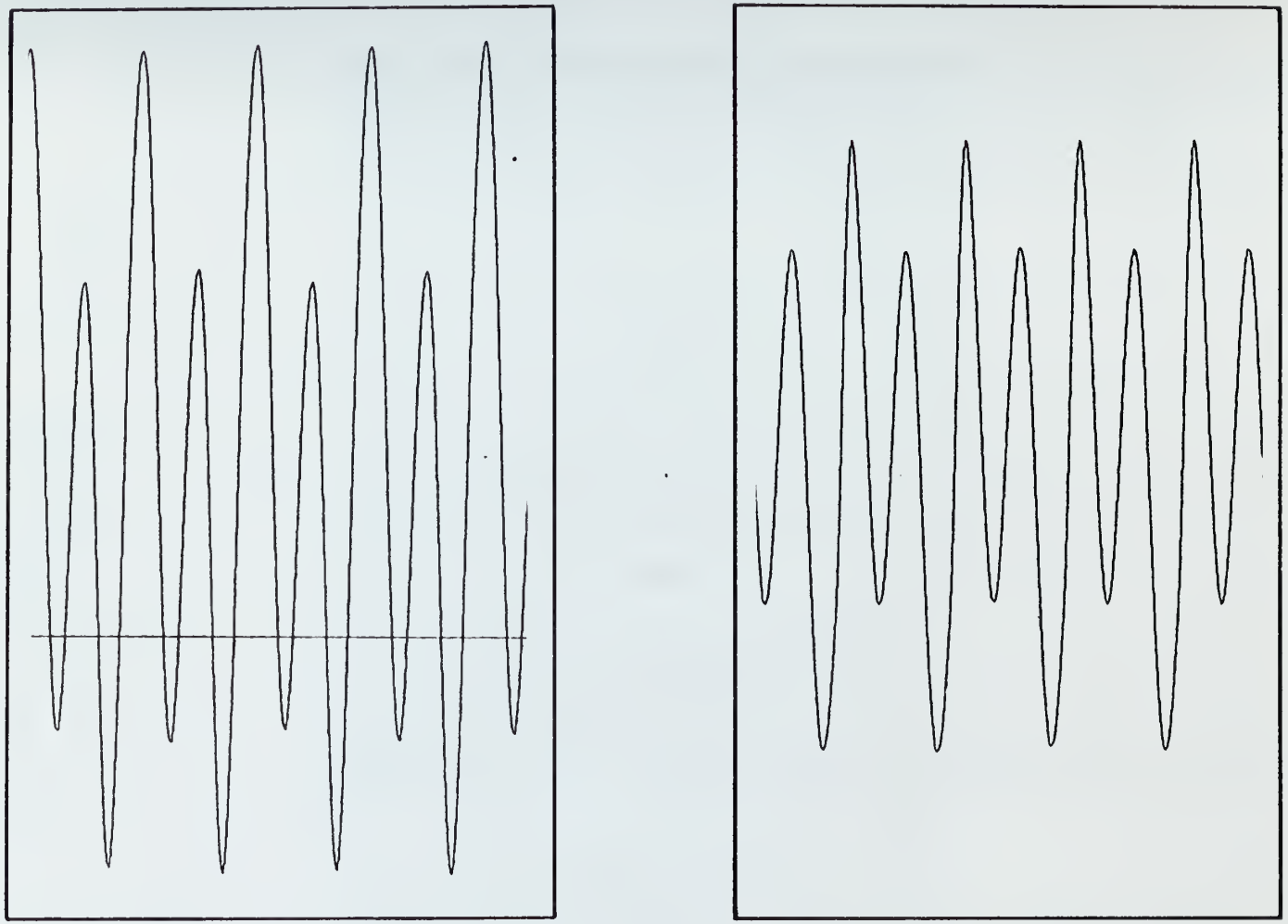

Pitch Heave

Figure 10. Ahead Seas Pitch & Heave Nonlinearities

V = 20 kts, A = 0.5 ft, $w_e = 4$

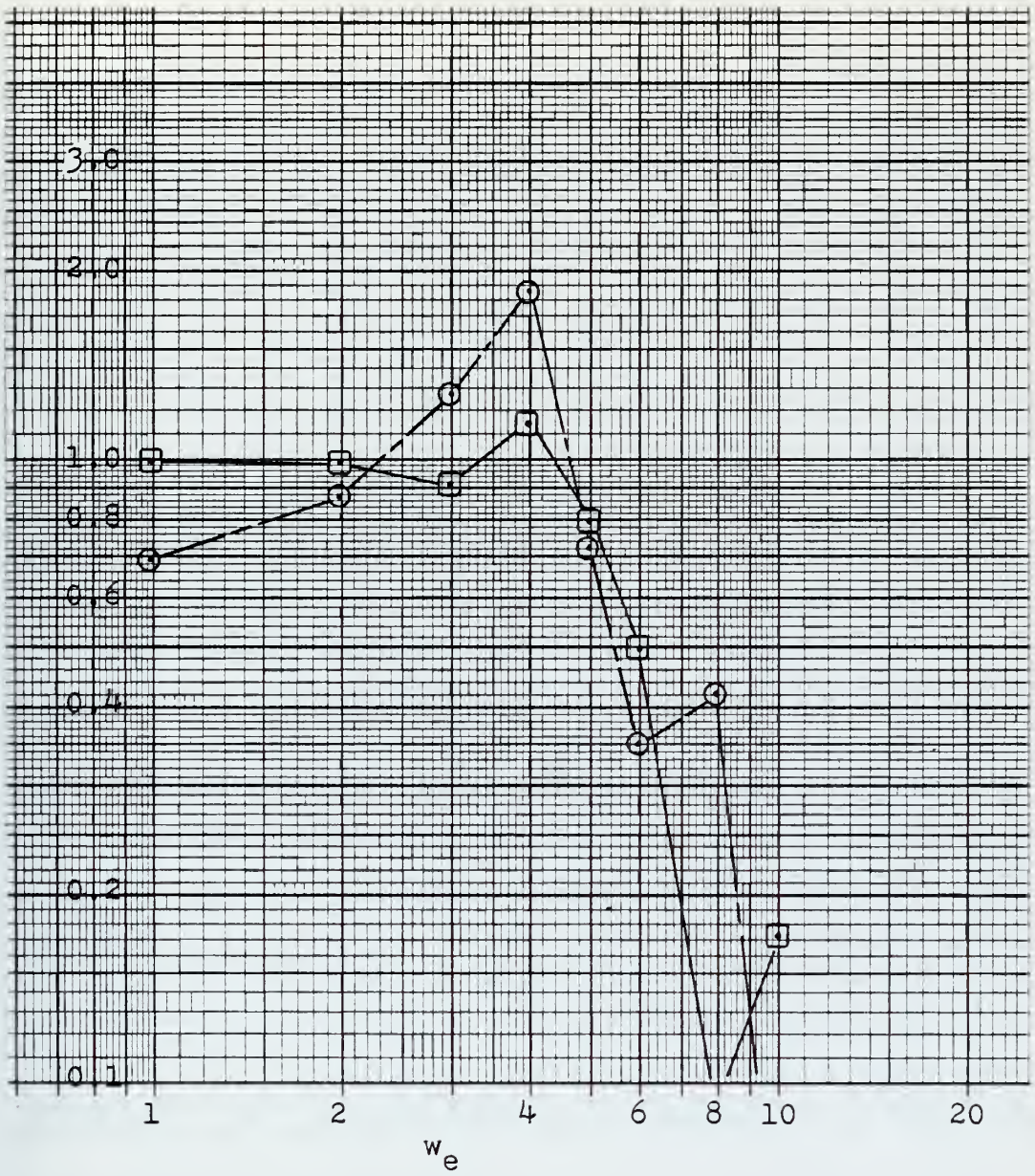

Figure 11. V=10 kts, A=0.2 ft,
Ahead Seas
⊡ = Heave Frequency Response
⊙ = Pitch Frequency Response

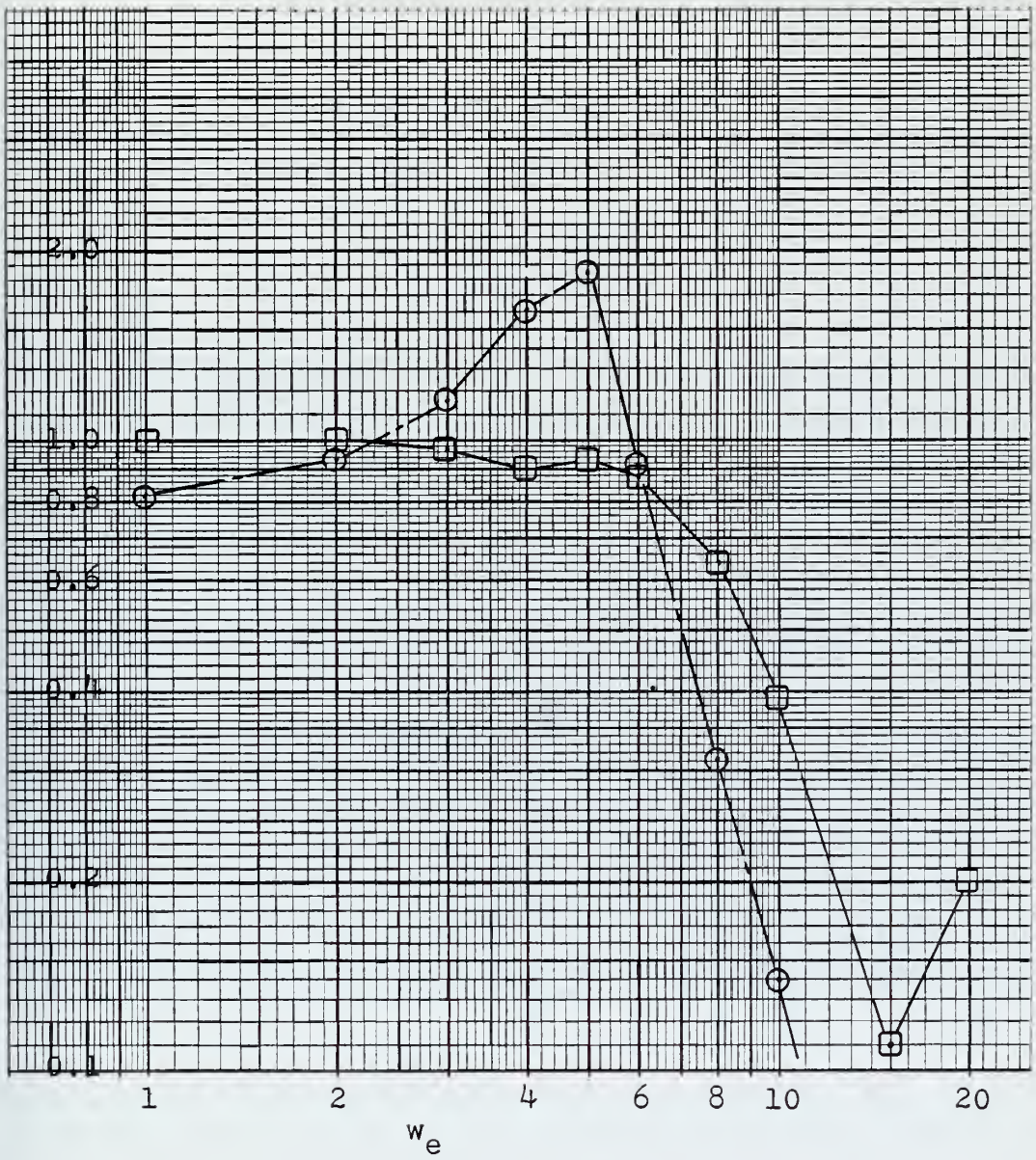

Figure 12. V=20 kts, A=0.1 ft,
Ahead Seas
⊡ = Heave Frequency Response
⊙ = Pitch Frequency Response

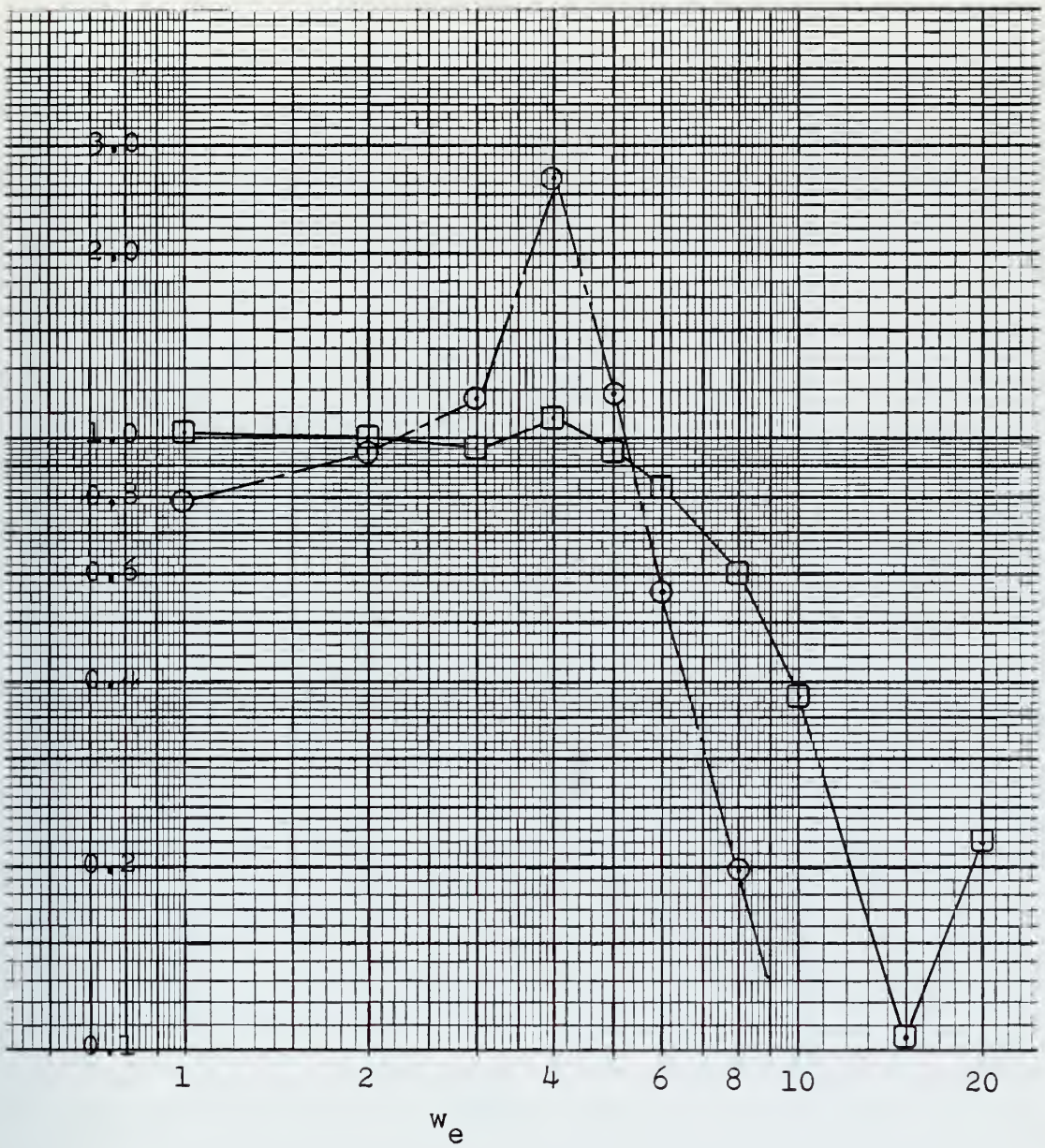

Figure 13. V=20 kts, A=0.2 ft,
Ahead Seas,
⊡ = Heave Frequency Response
⊙ = Pitch Frequency Response

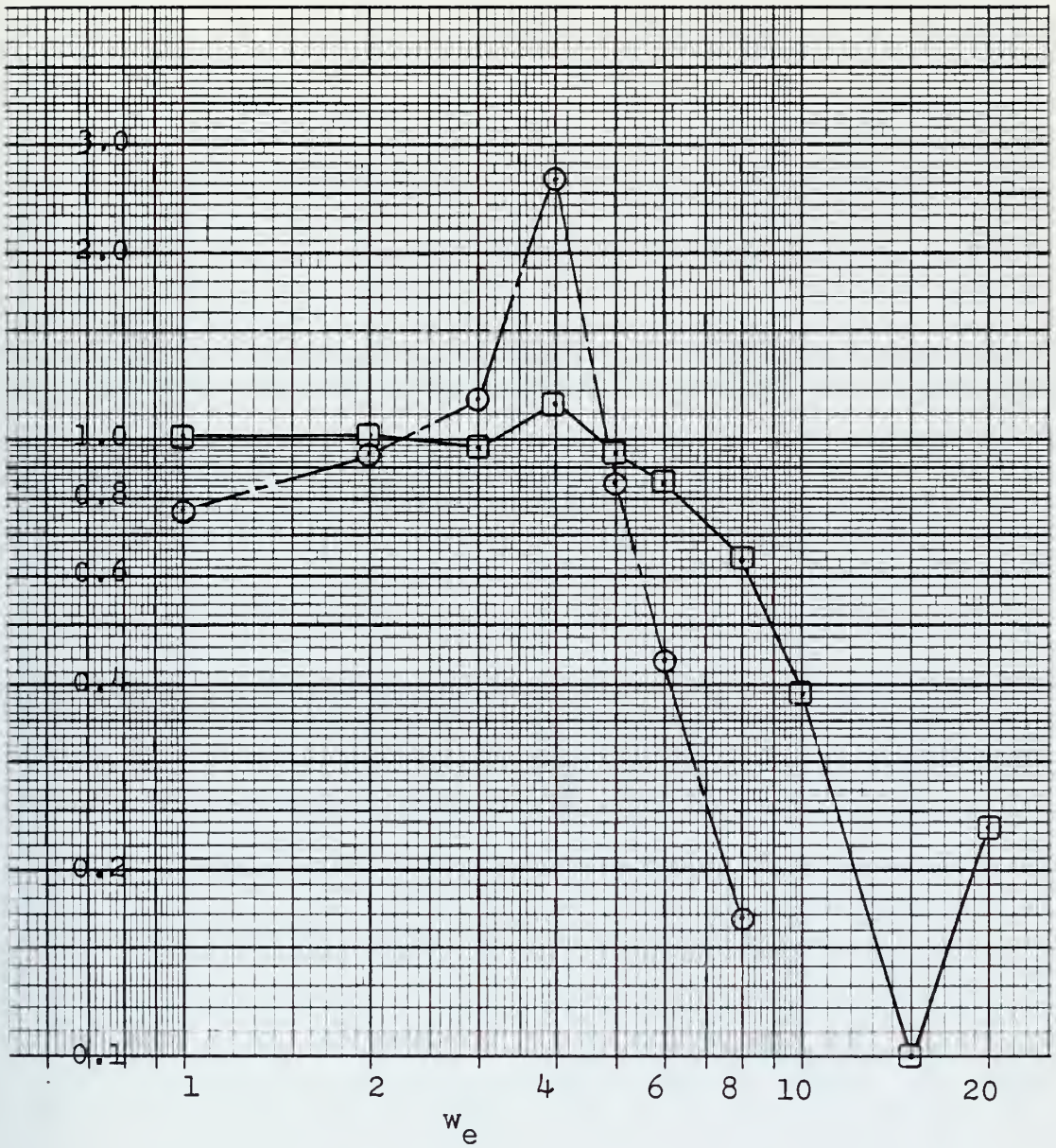

Figure 14. V=20 kts, A=0.3 ft,
Ahead Seas
⊡ = Heave Frequency Response
⊙ = Pitch Frequency Response

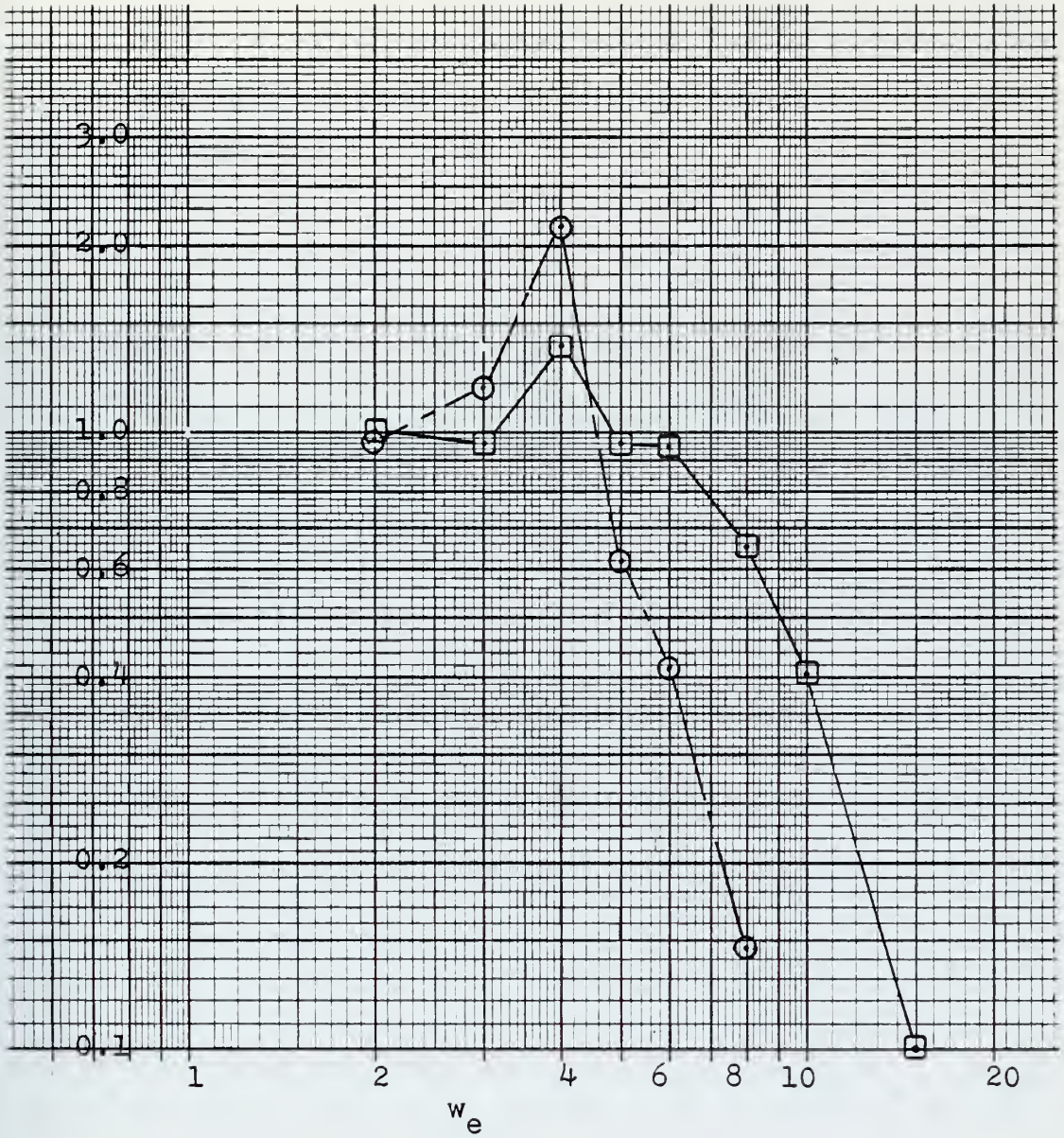

Figure 15. V=20 kts, A=0.5 ft,
Ahead Seas
⊡ = Heave Frequency Response
⊙ = Pitch Frequency Response

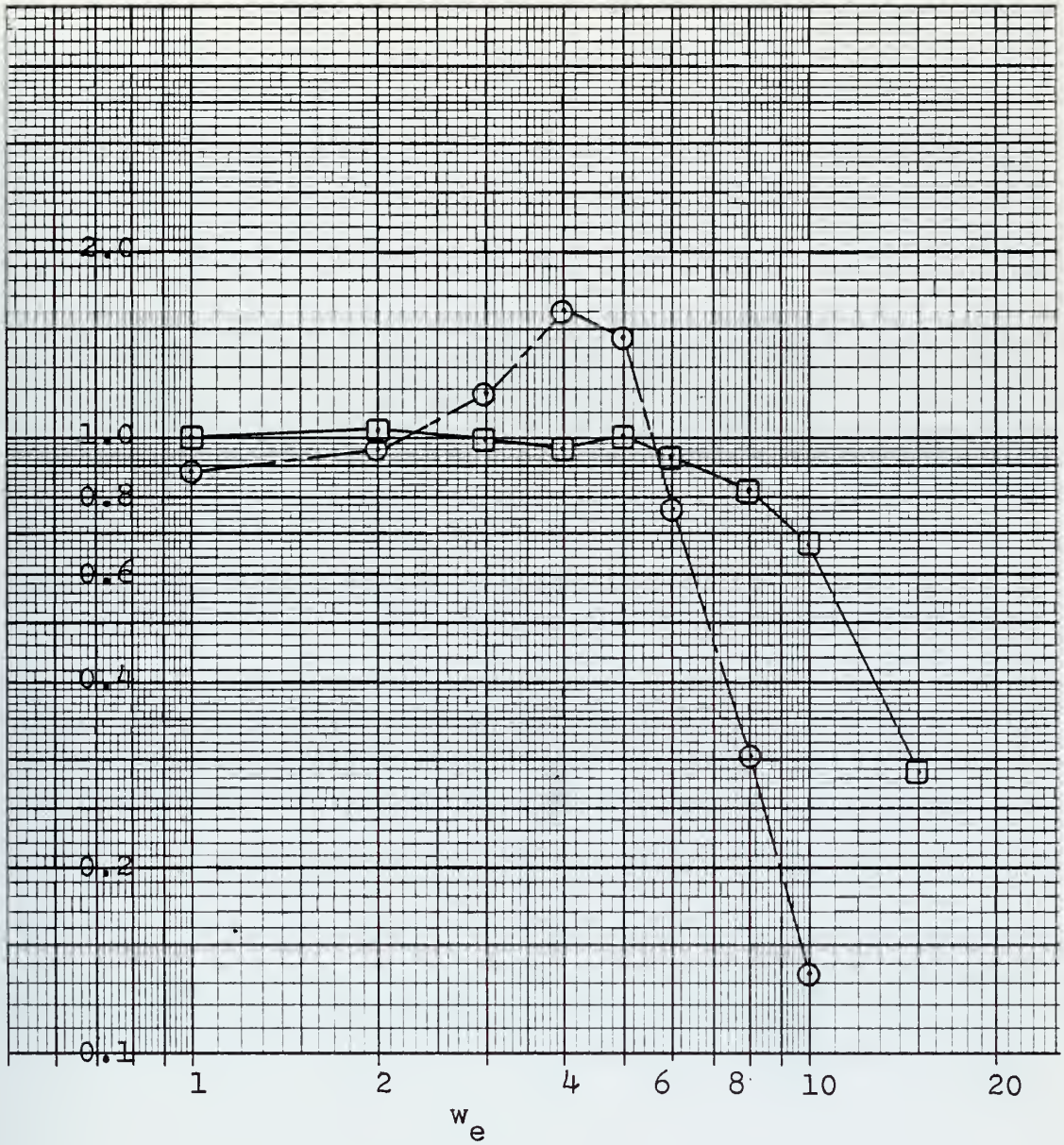

Figure 16. V=30 kts, A=0.2 ft,
Ahead Seas
⊡ = Heave Frequency Response
⊙ = Pitch Frequency Response

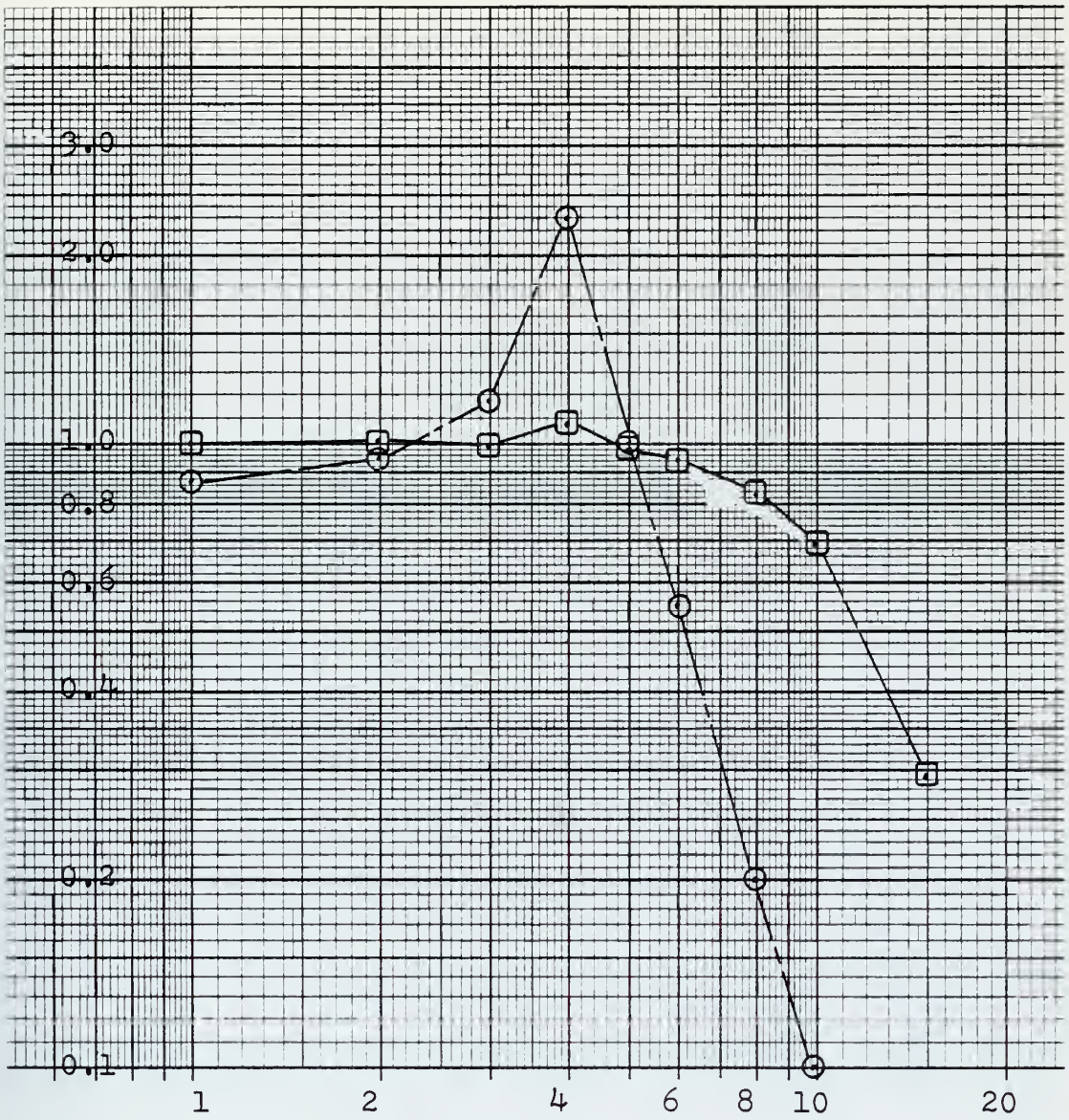

Figure 17. V=30 kts, A=0.3 ft,
Ahead Seas
⊡ = Heave Frequency Response
⊙ = Pitch Frequency Response

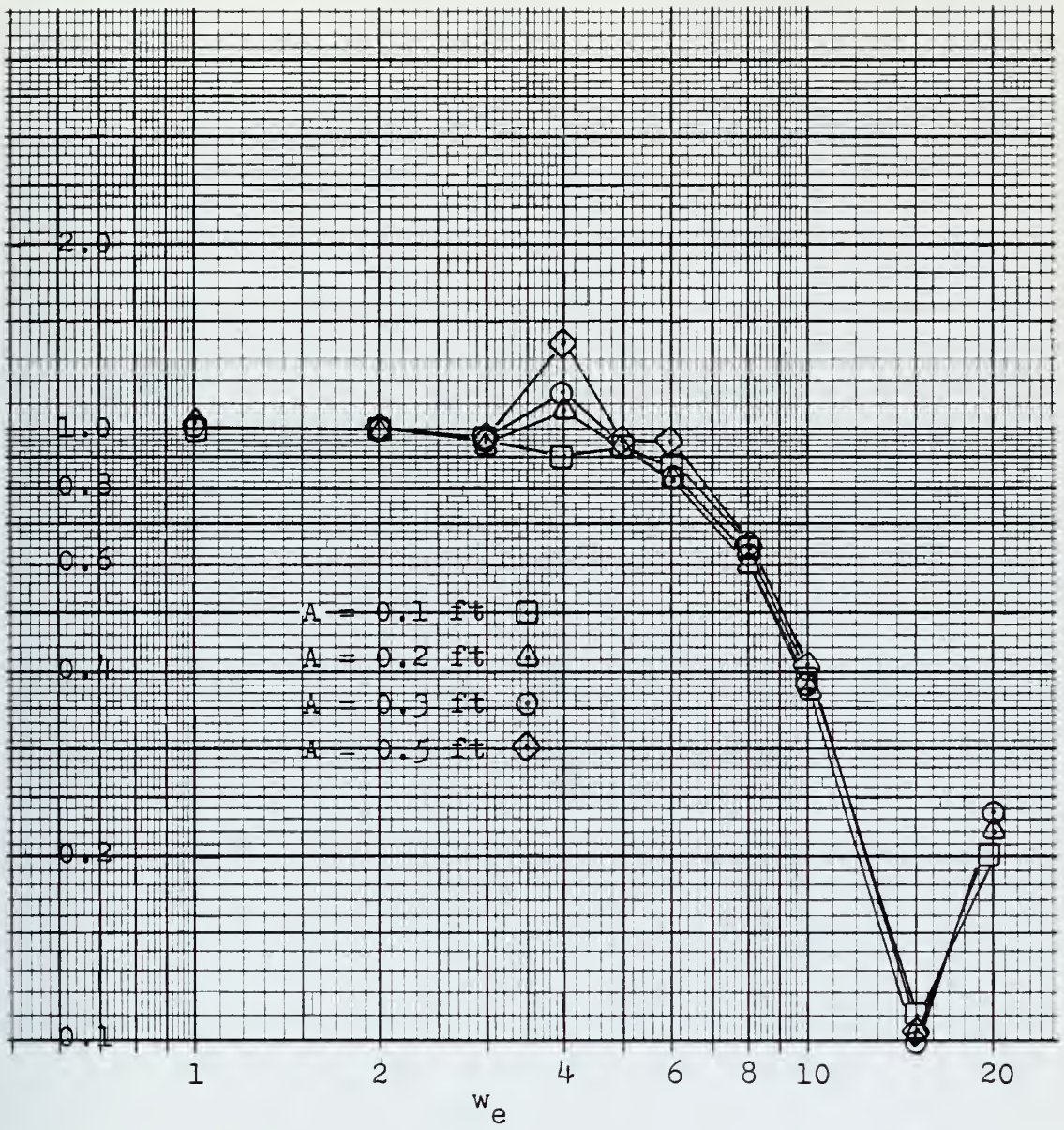

Figure 18-A. Heave Frequency Response vs. Wave Height, V=20 kts

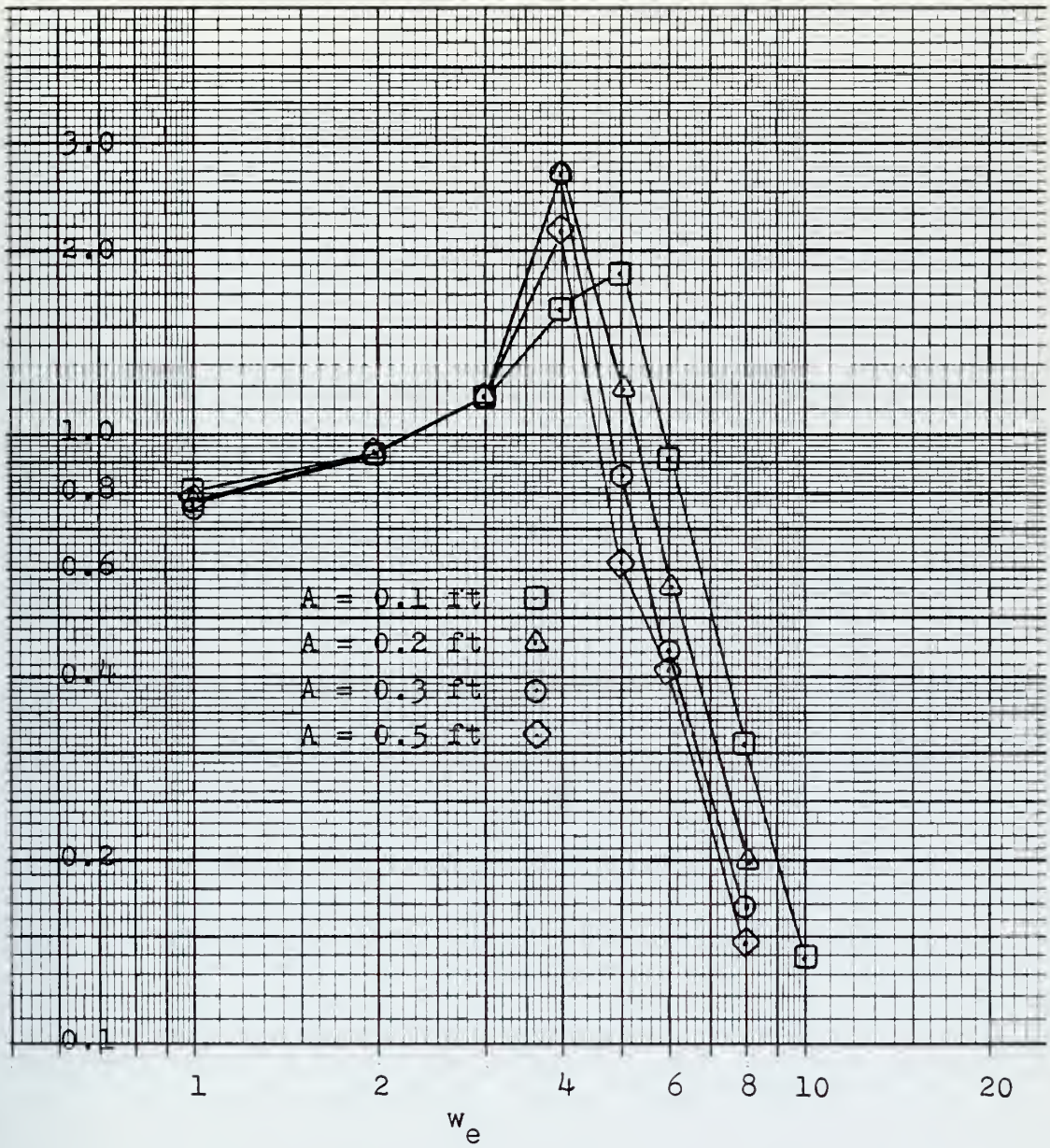

Figure 18-B. Pitch Frequency Response vs. Wave Height, V=20 kts

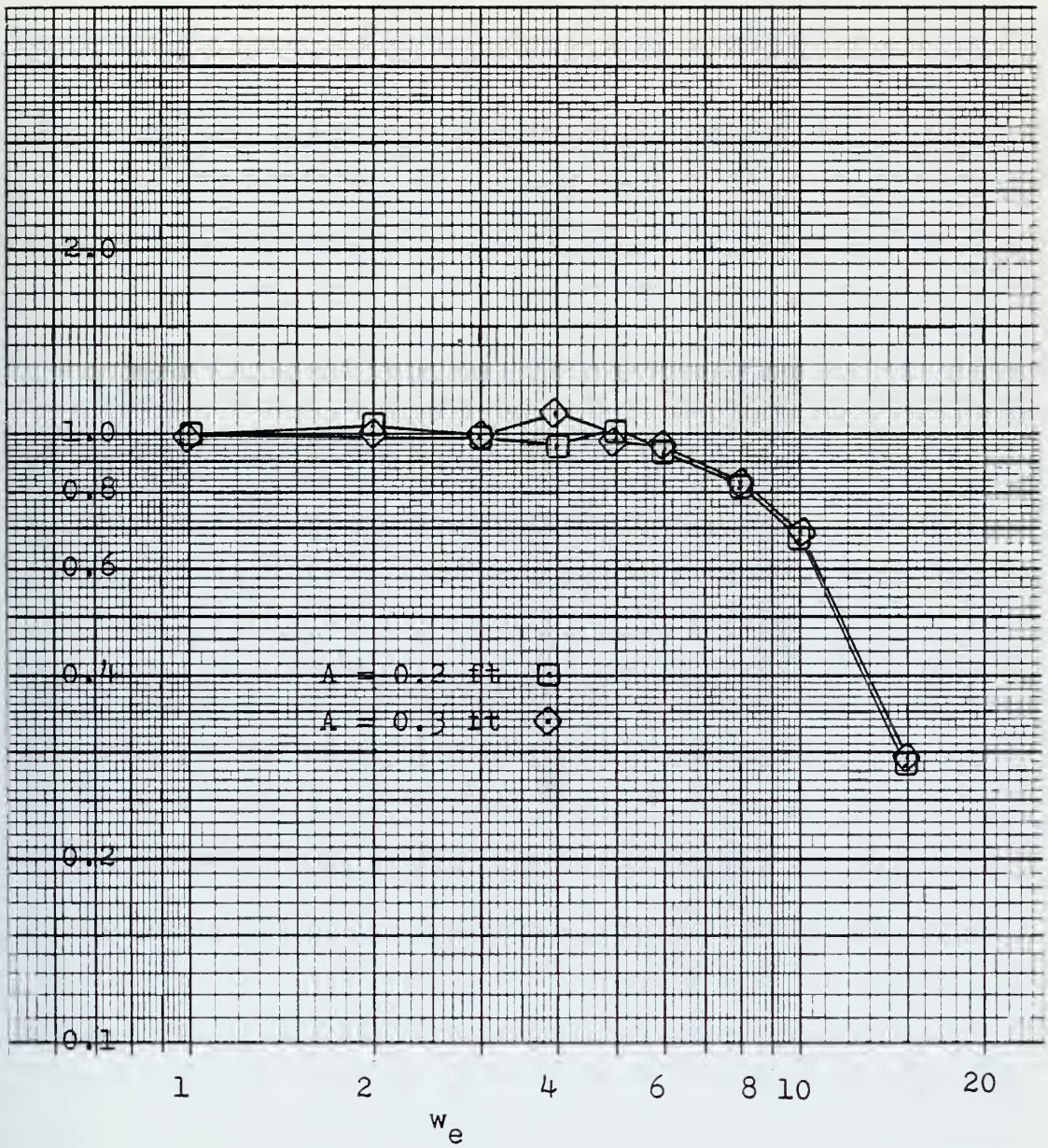

Figure 19-A. Heave Frequency Response vs. Wave Height, V=30 kts

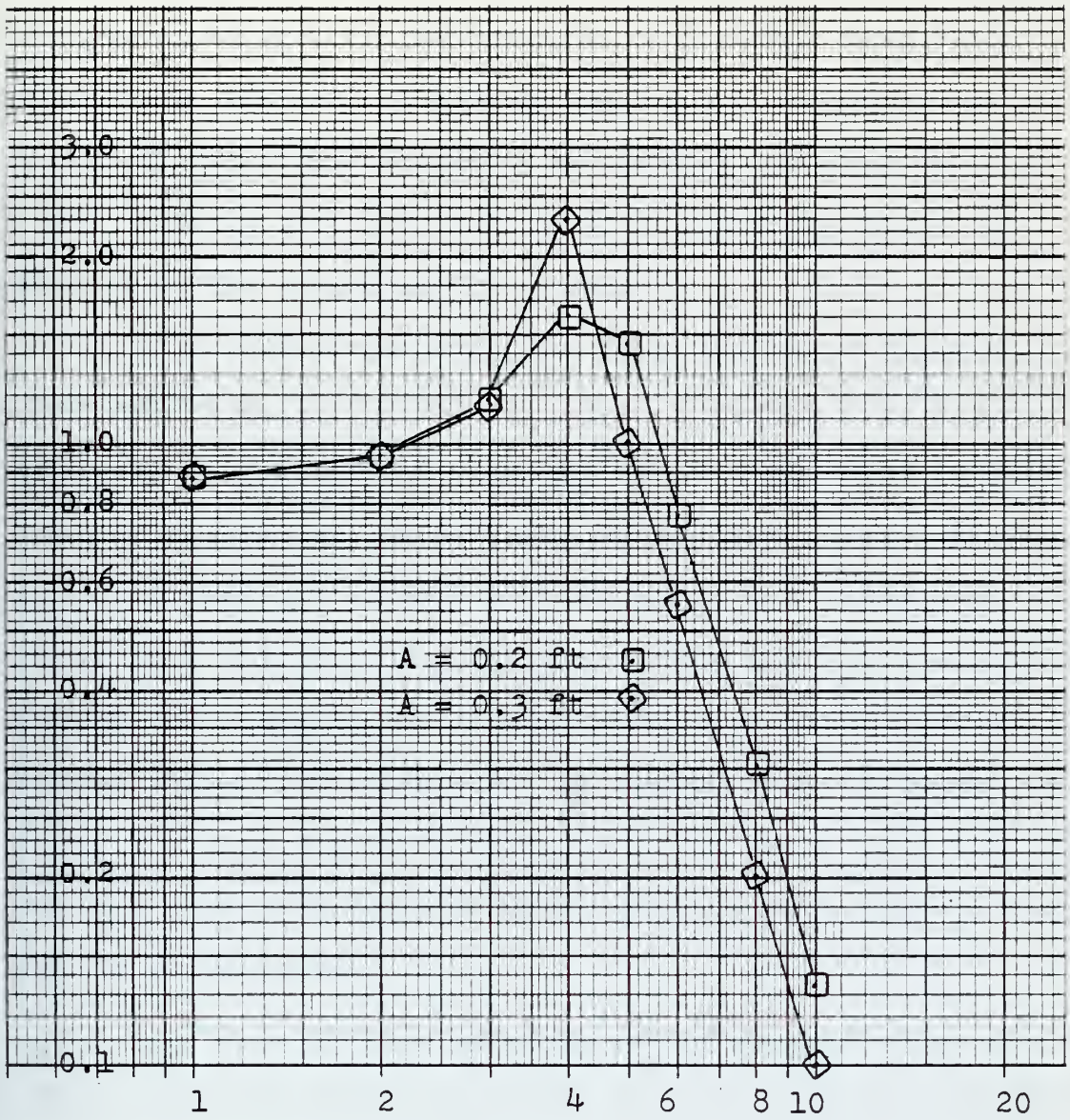

Figure 19-B. Pitch Frequency Response vs. Wave Height, V=30 kts

near w_e=4. This is not true for the pitch response where at the higher frequencies the response falls off faster for greater wave heights. A comparison of the responses as a function of speed for constant waveheight is shown in Figure 20. Clearly the response in both heave and pitch is dependent on the speed of the craft.

A comparison with the four degree-of-freedom theoretical response in Figure B-1 in Appendix B is also of interest. Both models show the speed dependence of heave but not of pitch. In general the theoretical response characteristics fall off slower in both pitch and heave then that obtained from the XR-3 digital simulation and the theoretical responses would appear to be independent of waveheight at resonance. Also noteworthy is the second peak in heave near w_e=8 for the four degree-of-freedom model which does not appear in the six degree-of-freedom model until a much higher frequency is encountered.

The frequency response functions obtained from the XR-3 Loads and Motions program show that at low frequencies representing waves with large wavelengths as compared to the craft length, or the length of the bubble chamber for the CAB type craft, the simulated XR-3 will follow the wave surface and slope. At high frequencies the wavelength is small relative to the plenum length and the craft will tend to not follow the waves but will "platform" over them. Intermediate to these two conditions is a range of resonant frequencies for which wave inputs, particularly the wave slope,

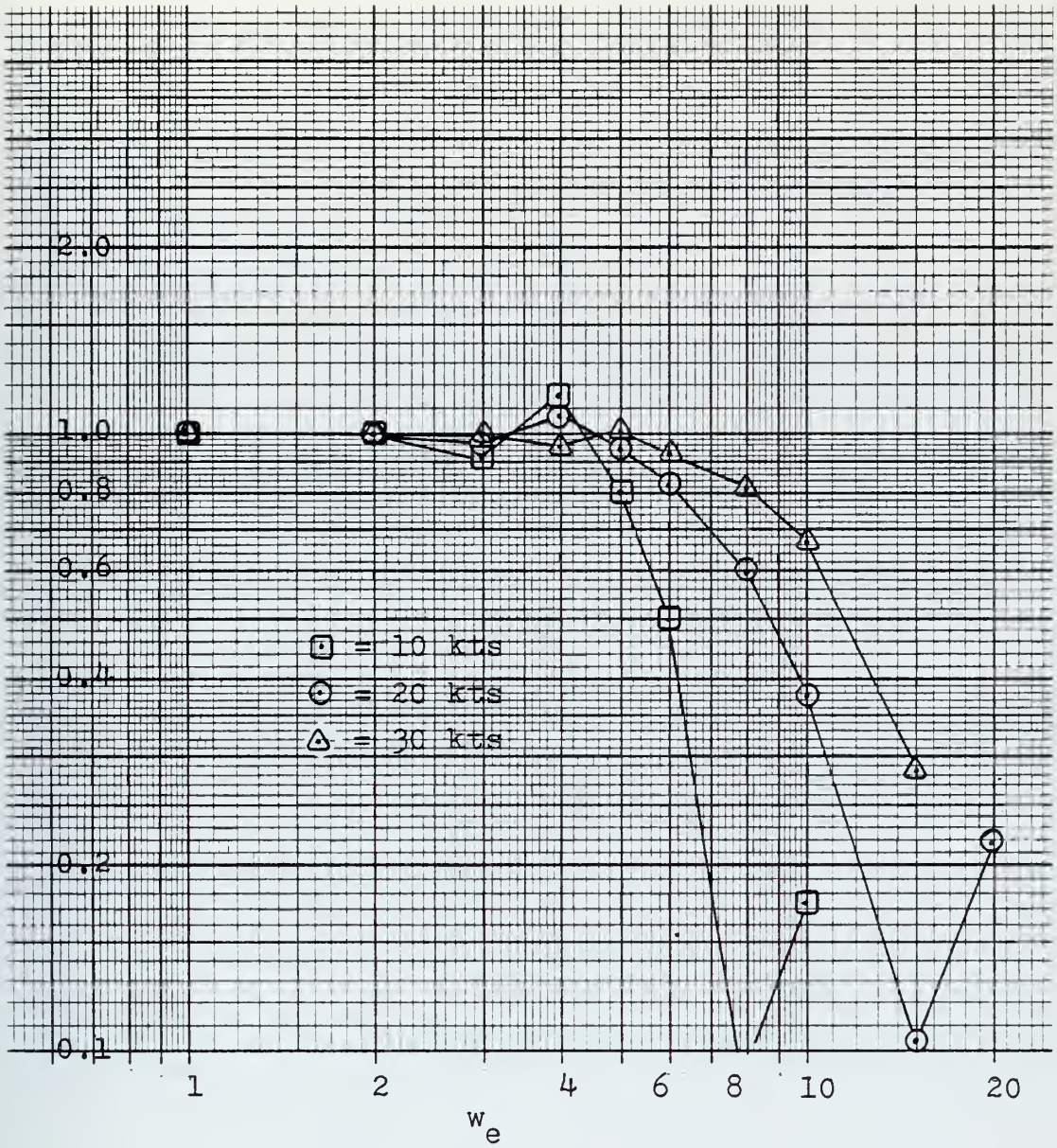

Figure 20-A. Heave Frequency Response Vs. Speed, A=0.2 ft

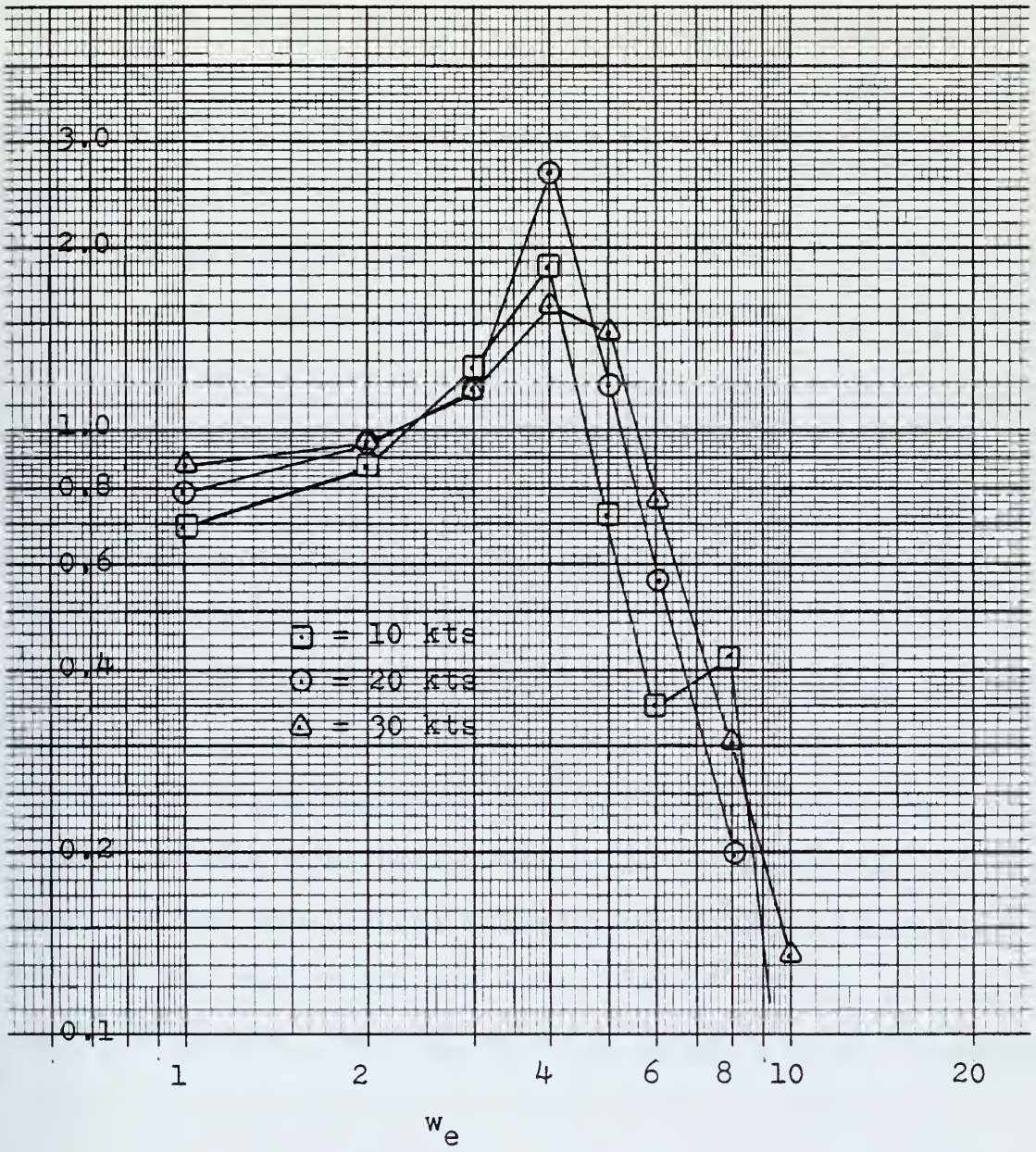

Figure 20-B. Pitch Frequency Response vs. Speed, A-0.2 ft

would be amplified to result in craft motions that could be significantly larger than the input values. Figure 21 plots the dependence of heave and pitch on the wavelength to plenum length ratio. Note that in terms of this ratio, heave is fairly independent of speed.

b. Following Seas

Following seas runs were simulated for craft speeds of 10 and 20 knots with a wave amplitude of 0.2 feet. Steady-state conditions could not be obtained for V=10 knots, w_e=8. Nonlinearities were noted primarily at 10 knots in heave for the lower encounter frequencies. Figure 22 presents representative examples.

The frequency response functions for the following seas simulations are presented in Figures 23 and 24. The 10 knot response characteristics can be compared with the four degree-of-freedom theoretical response in Figure B-2. As can be seen the two bear little resemblance to each other. In particular the magnitudes are considerably smaller for the digital simulation. The digital simulation's pitch response has the general features of the theoretical response, in particular the notch above w_e=2 is evident in both, but the heave response of the digital simulation has a resonant peak in contrast to the notch in the theoretical response.

c. Abeam Seas

Runs simulating abeam seas conditions were conducted with a wave amplitude of 0.2 feet for craft speeds of 20 and 30 knots. For abeam seas the frequency of encounter is not

Heave Amplitude / Wave Amplitude
1.4
1.0
0.9
0.8
0.7
0.6
0.5
0.4
0.3
0.2
0.1
0
1
2
3
4
5
6
7
8
9
10
11
12
13
14
λ/L
40 kts
20 kts
30 kts
λ = wave length
L = plenum length
Figure 21-A. Heave Response vs. λ/L

Figure 21-E. Pitch Response vs. λ/L
λ = wave length
L = plenum length
Peak-to-Peak Pitch Amplitude (degrees)
5.0
4.0
3.0
2.0
1.0
0
2
3
4
5
6
7
8
9
10
11
12
13
14
λ/L
10 kts = ○
20 kts = □
30 kts = △

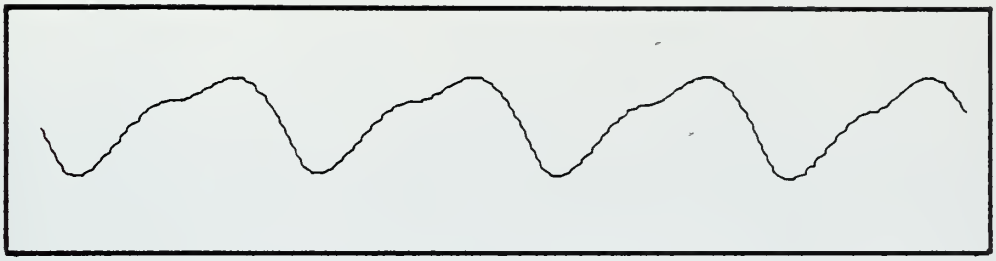

V = 10 kts, A = 0.2 ft, w_e = 1

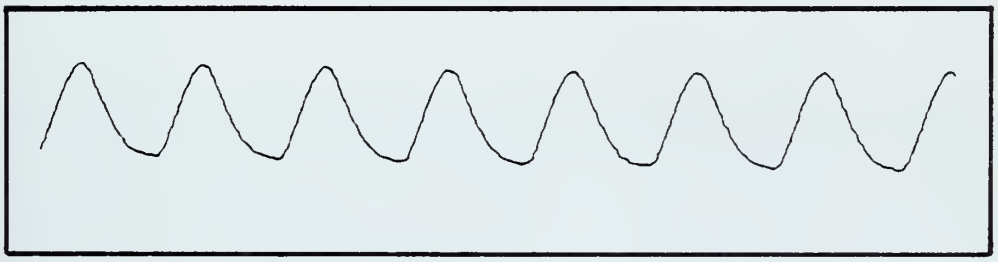

V = 10 kts, A = 0.2 ft,. w_e = 2

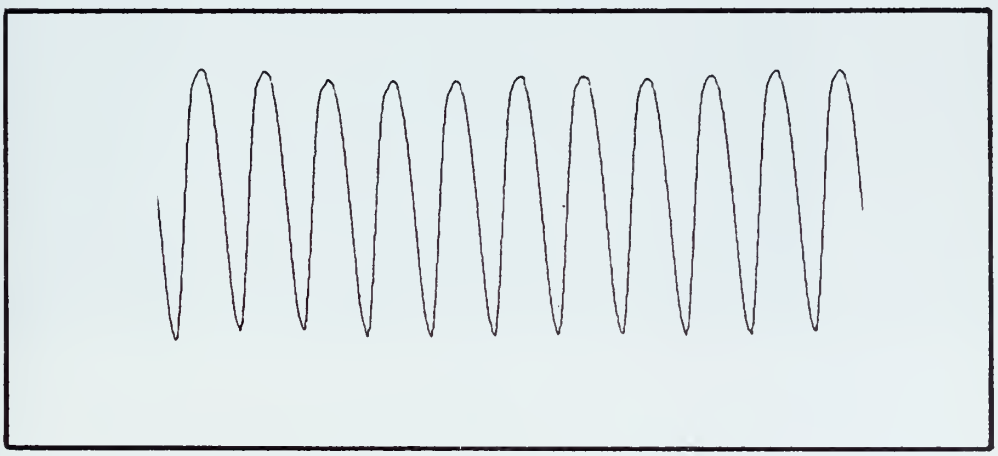

V = 10 kts, A = 0.2 ft, w_e = 4

Figure 22. Heave Nonlinearities
Following Seas

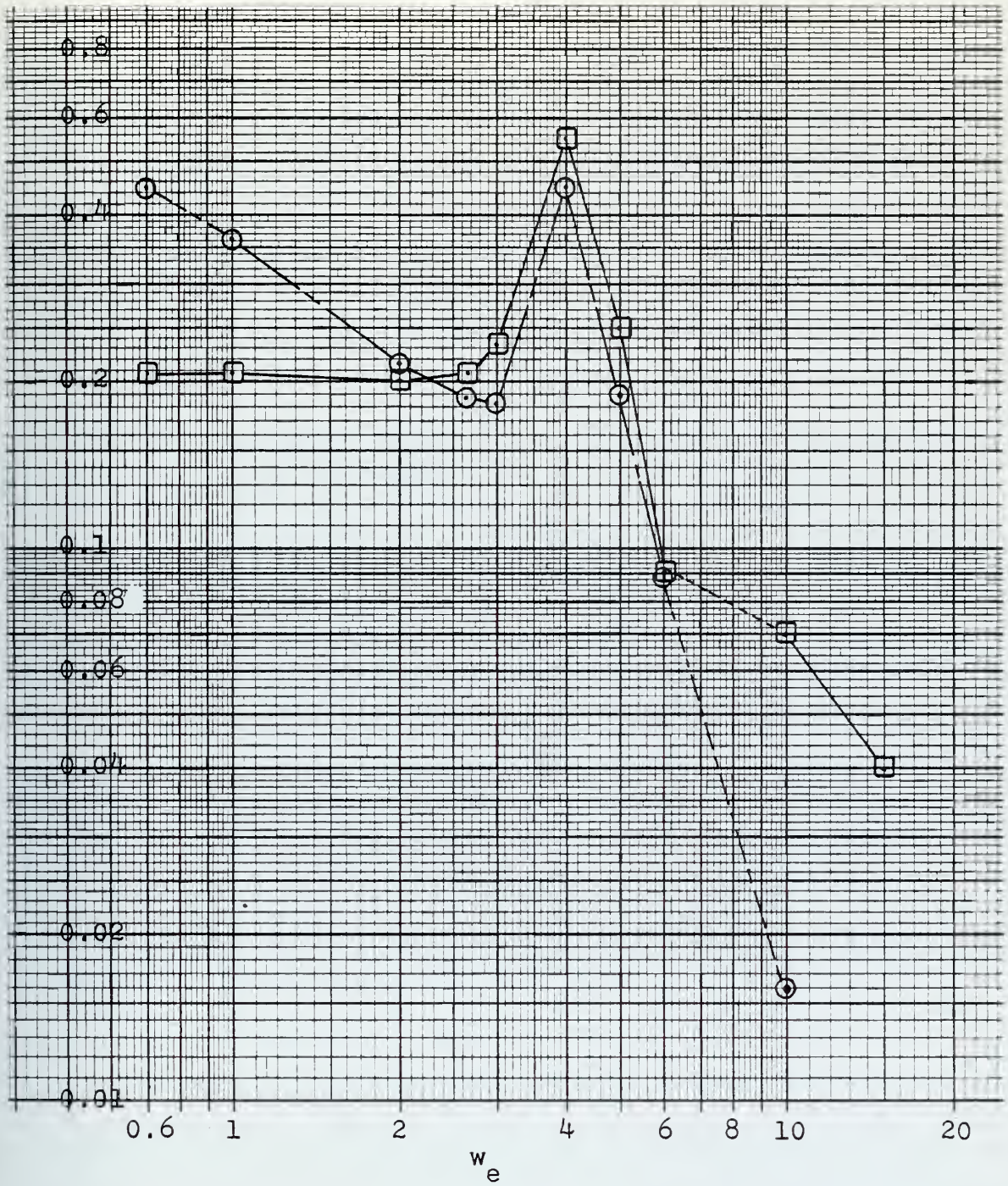

Figure 23. V=10 kts, A=0.2 ft,

Following Seas

⊡ = Heave Frequency Response

⊙ = Pitch Frequency Response

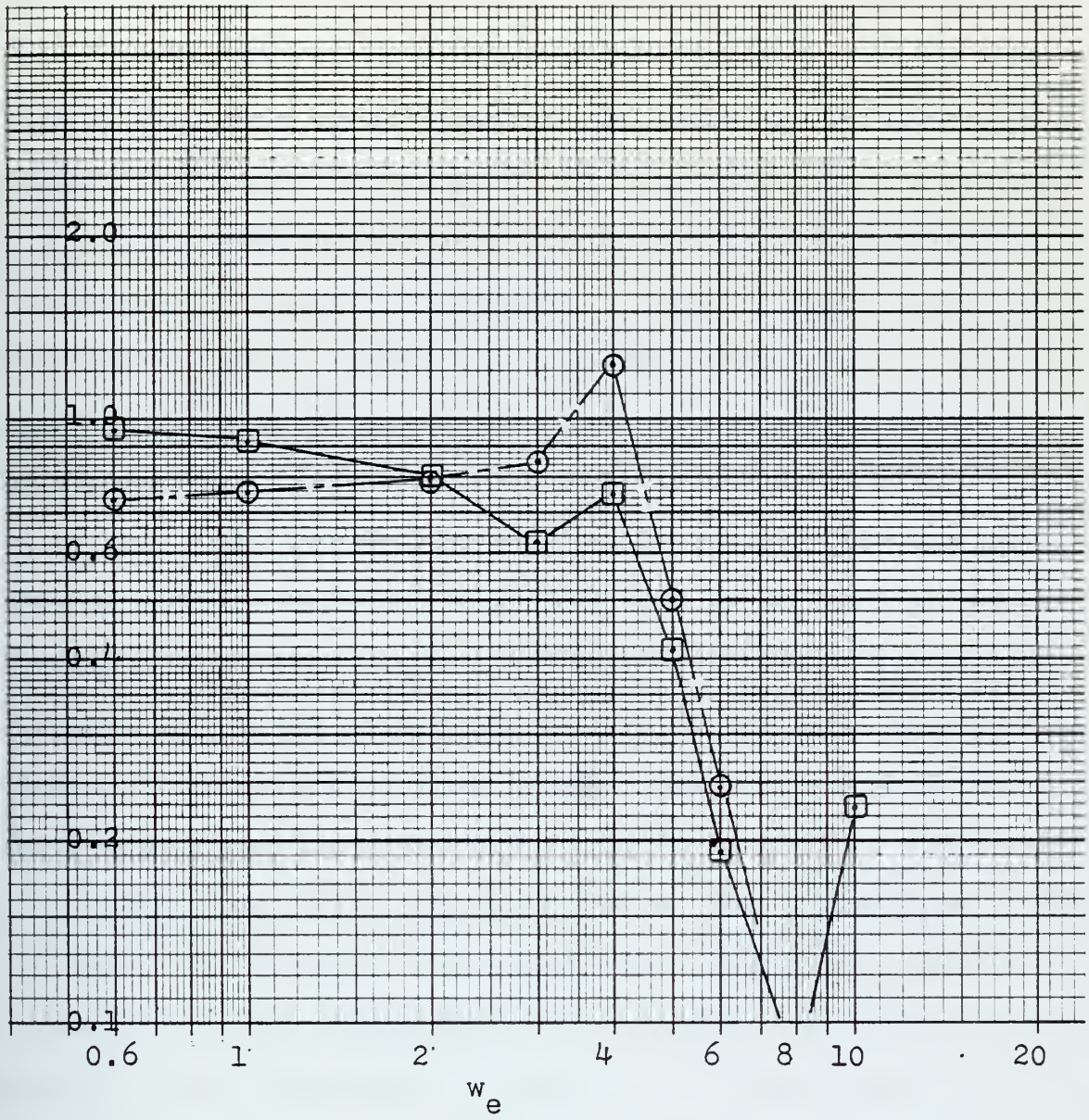

Figure 24. V=20 kts, A=0.2 ft

Following Seas

⊡ = Heave Frequency Response

⊙ = Pitch Frequency Response

a function of the craft speed but is the actual wave frequency. This has the effect of producing considerably greater wave slopes than were encountered in the ahead or following seas conditions.

Nonlinearities were found in pitch and roll at the lowest encounter frequencies. However since pitch is coupled to both the roll and yaw, nonlinearities in its response were to be expected. Typical responses are presented in Figure 25.

The heave frequency responses for the two speeds were so nearly identical that they can be plotted as one as in Figure 26. The frequency response functions for pitch and roll are given in Figures 27 and 28 and also show a high degree of independence from speed. Comparisons with the theoretical responses are not possible since they are based on a craft speed of 10 knots. However the theoretical pitch response does deserve some attention. The pitch frequency response function shows that for the lower encounter frequencies the pitch amplitude is equal to the wave slope. If there were no yaw, as believed to be the case for the four degree-of-freedom model, the pitch of the craft would be minimal, much as is characterized by the responses from the digital simulation.

2. Operating Characteristics

The operating characteristics of the XR-3 program were defined as the average draft, average pitch, and the thrust necessary to maintain the desired speed. Figures 29

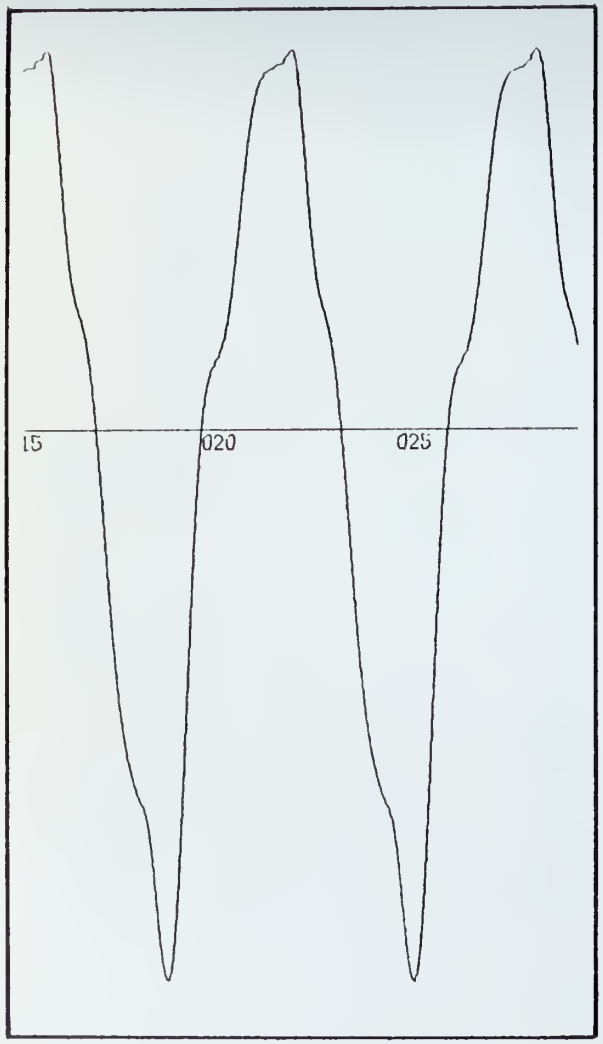

Roll
V = 20 kts
A = 0.2 ft
w_e = 1

Pitch
V = 30 kts
A = 0.2 ft
w_e = 2

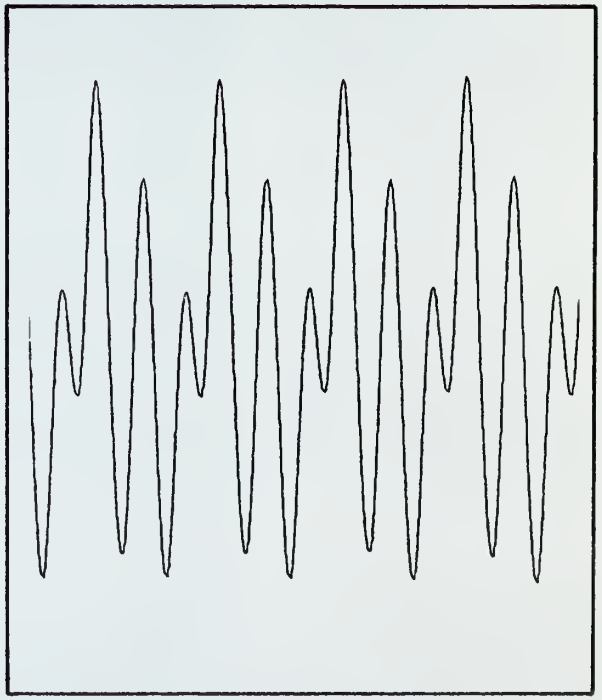

Figure 25. Abeam Seas Nonlinearities

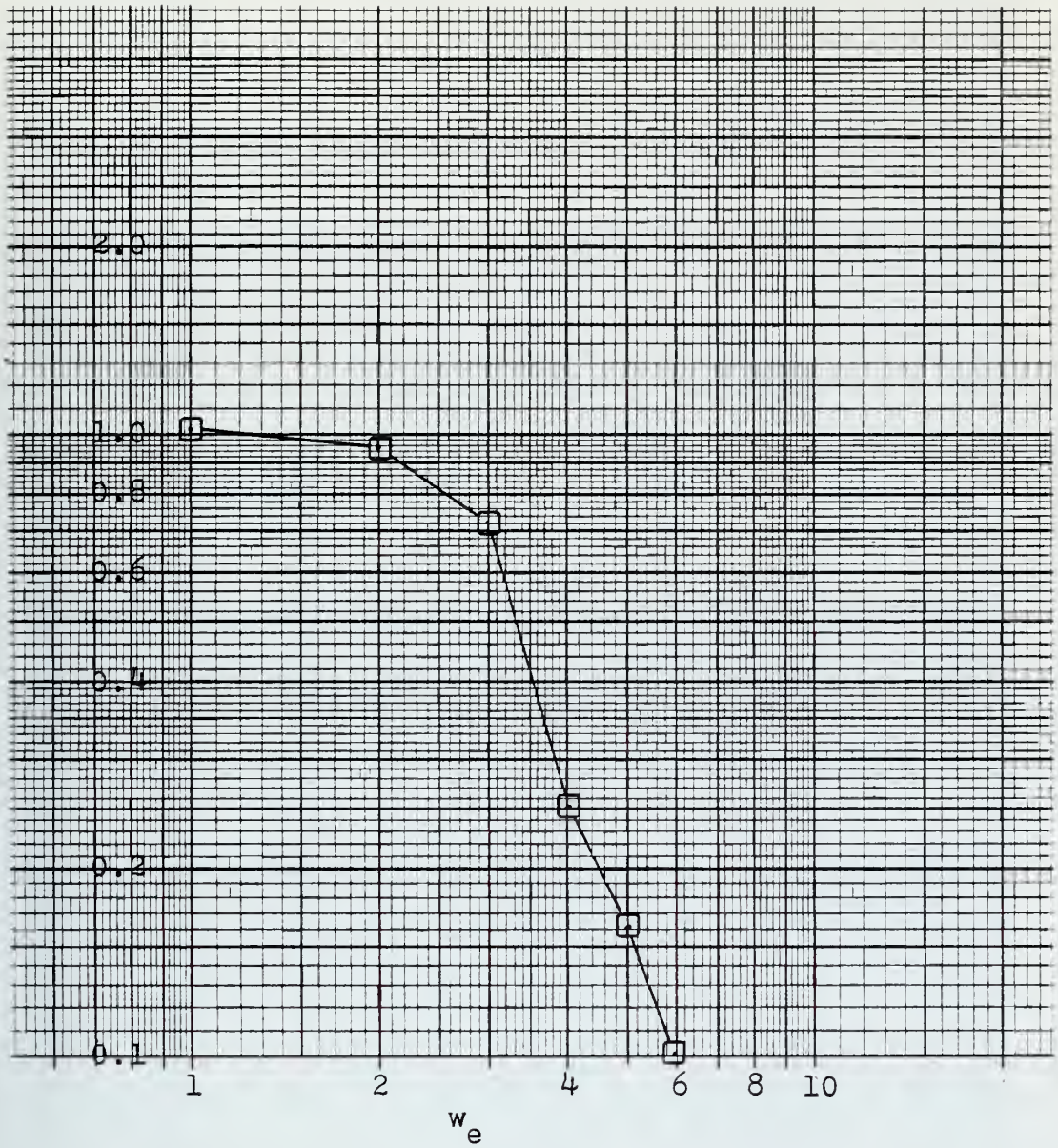

Figure 26. V=20 & 30 kts

Heave Frequency Response
Abeam Seas

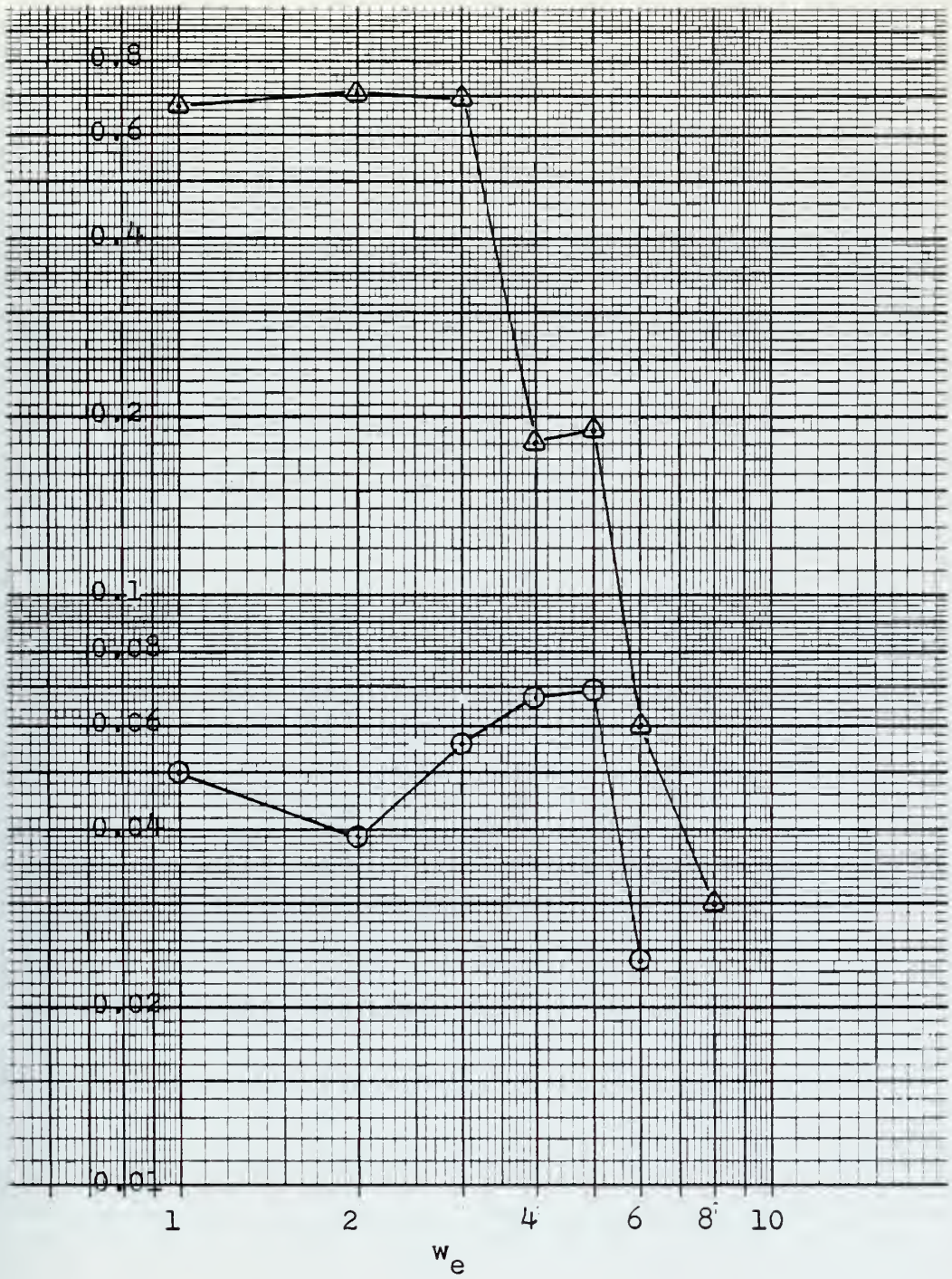

Figure 27. V=20 kts, A=0.2 ft,
Abeam Seas
⊙ = Pitch Frequency Response
△ = Roll Frequency Response

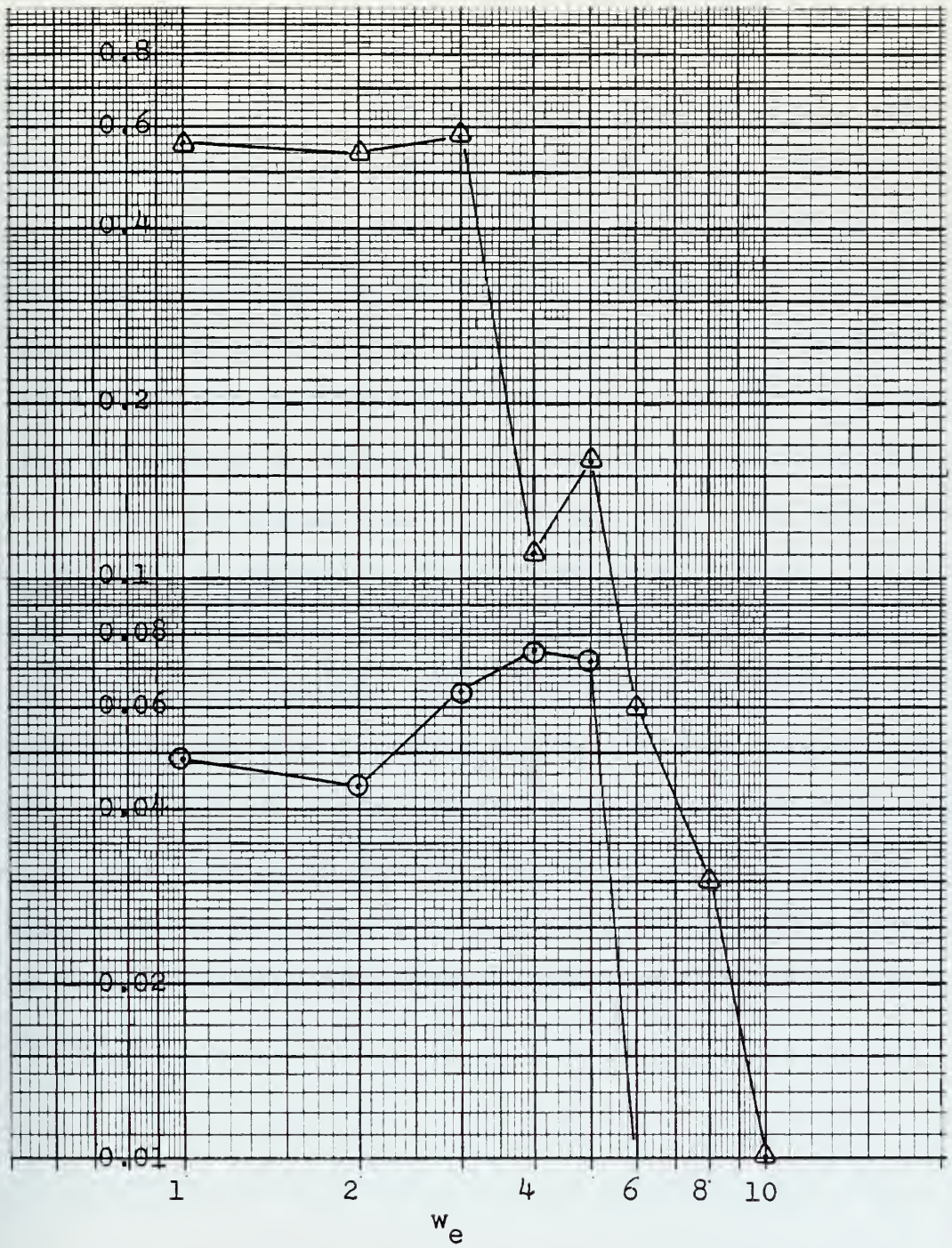

Figure 28. V=30 kts, A=0.2 ft,
Abeam Seas
⊙ = Pitch Frequency Response
△ = Roll Frequency Response

through 36 present this information as a function of encounter frequency, craft speed, wave height, and craft heading with respect to the waves. For both ahead and following seas the 20 and 30 knot runs show great similarity. At resonance there is a large increase in average pitch and draft along with a significant increase in the thrust necessary to counter the increased drag and maintain the desired speed. However the 10 knot runs are markedly different in that during resonance it was necessary to decrease the thrust to maintain the speed.

For the abeam seas conditions, the calm water thrust was adequate to maintain the desired craft speed. In all cases except one, the average draft and pitch remained at their calm water values. As noted in the procedures section steady-state yaw was a prerequisite for obtaining steady-state responses in heave, pitch, and roll. The peak-to-peak and average values of yaw at the end of 30 seconds run time without rudder control as well as the peak-to-peak value with rudder control are listed in Tables G-10 and G-11 of Appendix G.

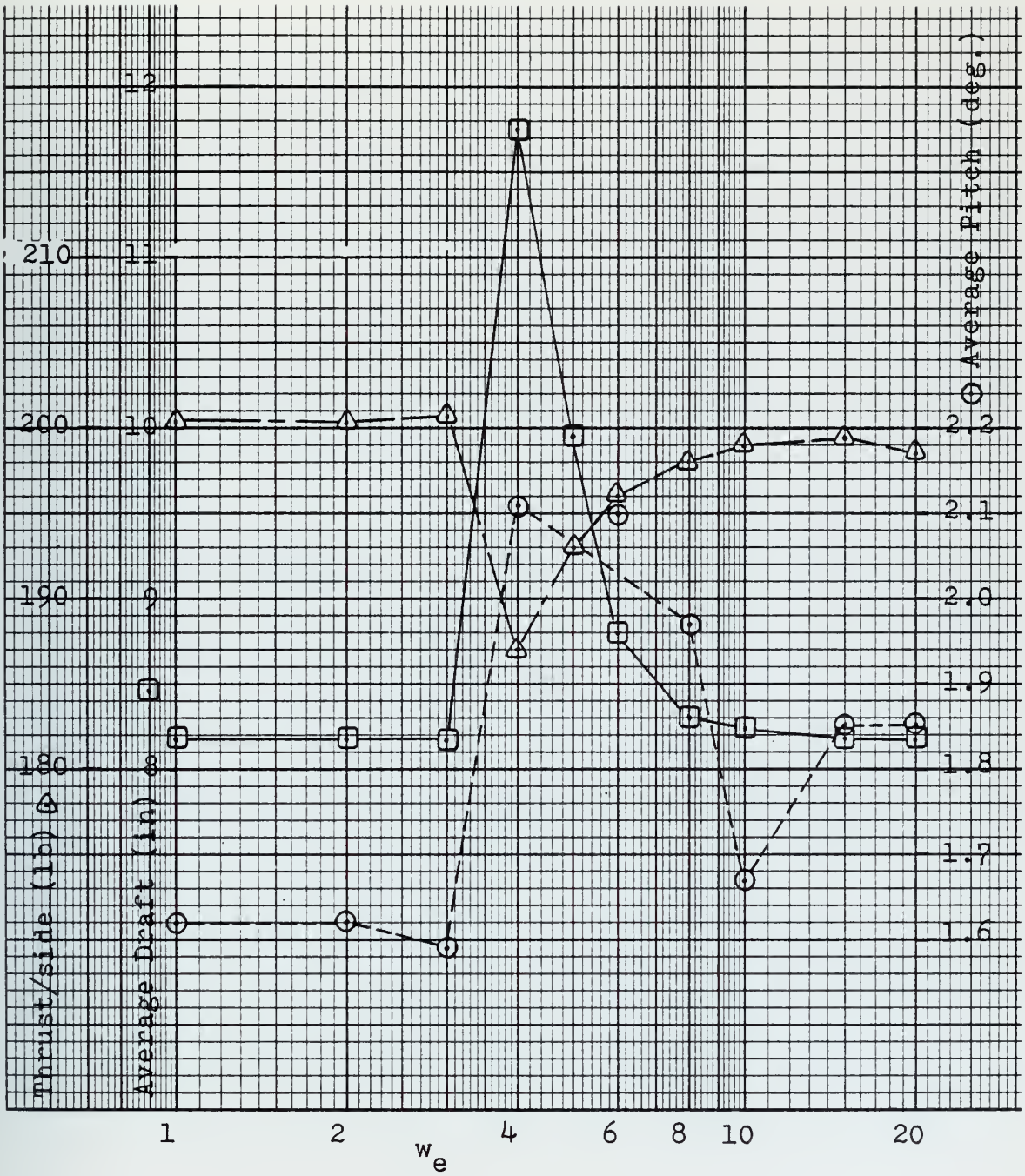

Figure 29. Operating Characteristics
V=10 kts, A=0.2 ft,
Ahead Seas

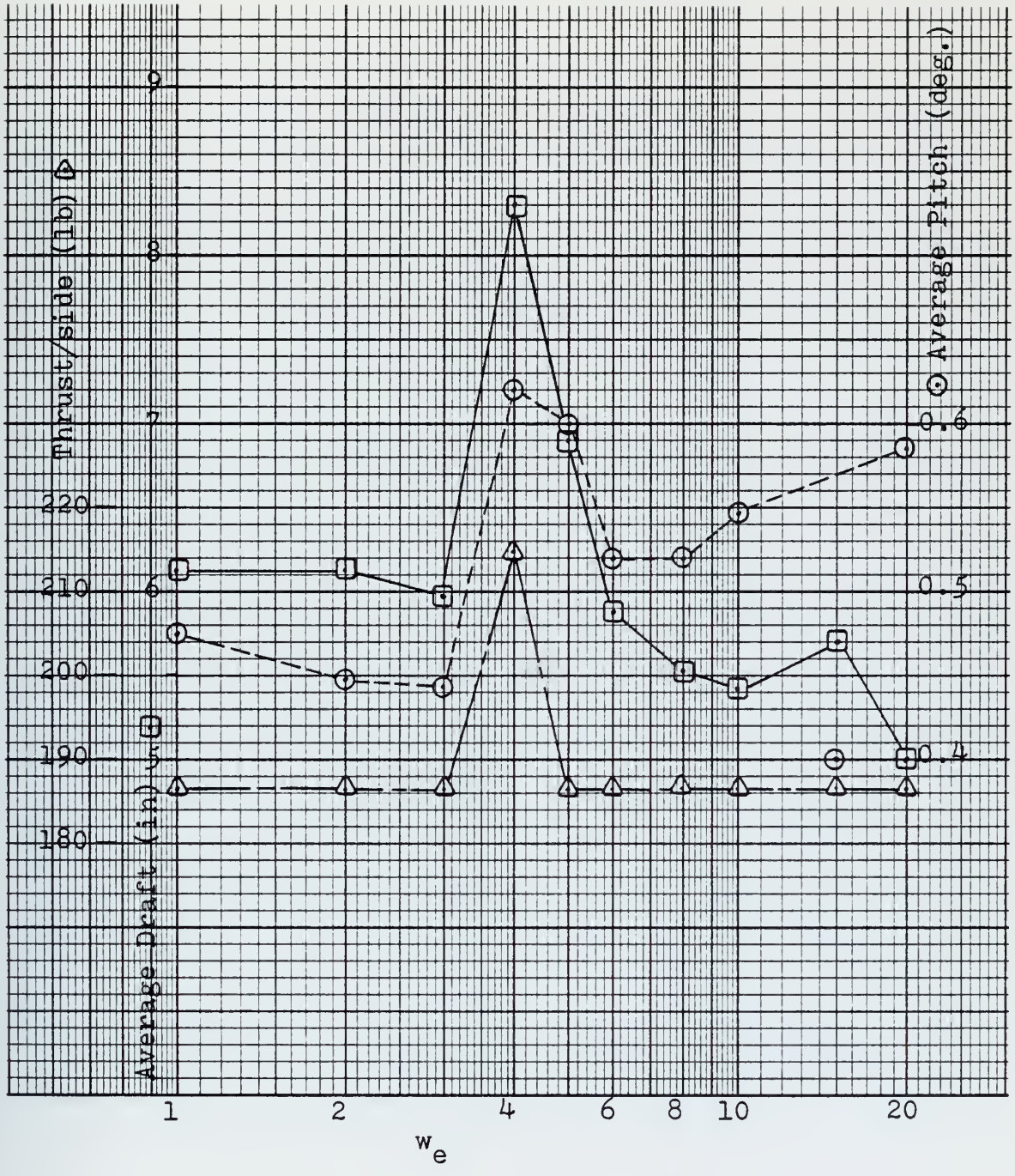

Figure 30. Operating Characteristics
V=20 kts, A=0.2 ft,
Ahead Seas

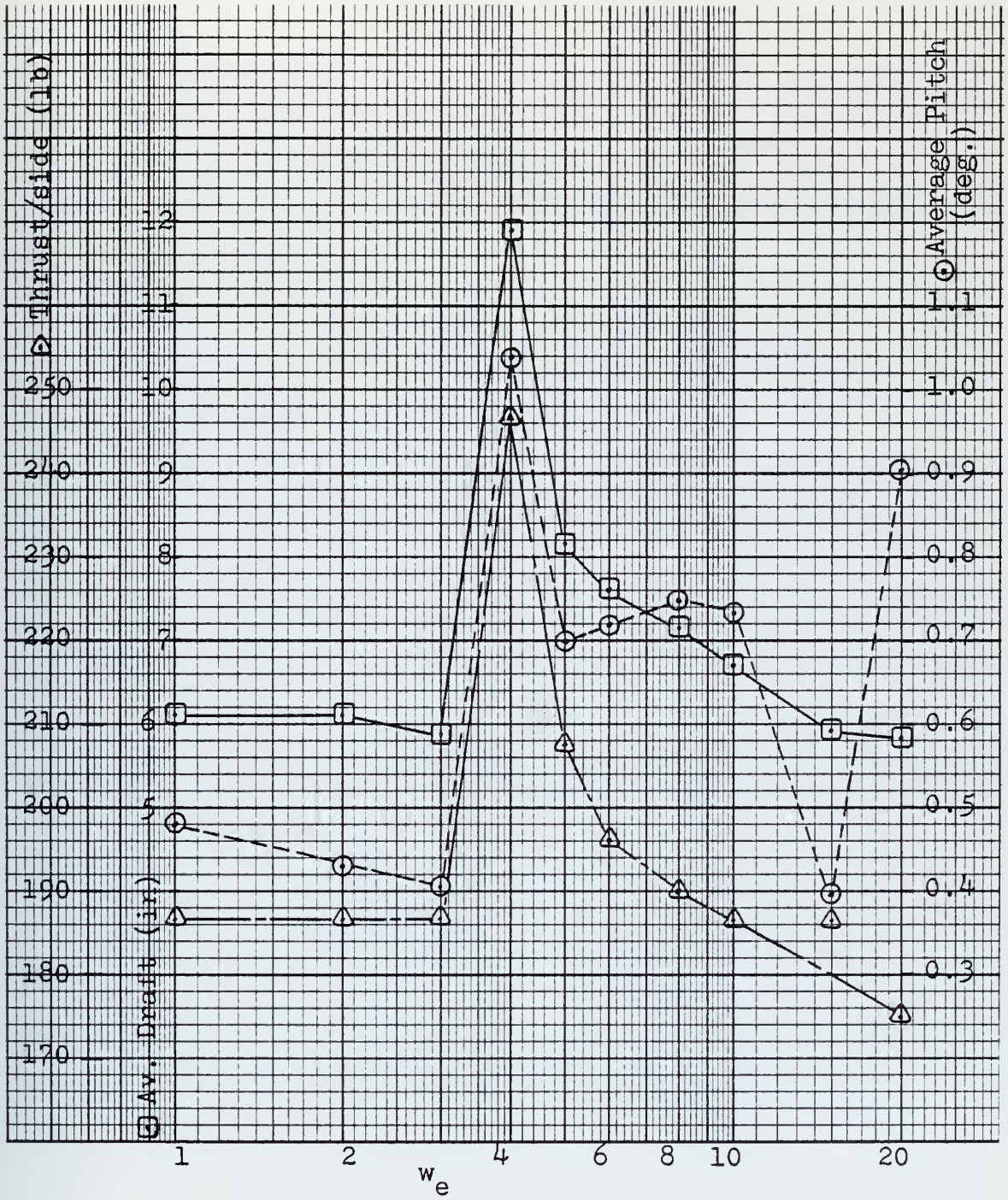

Figure 31. Operating Characteristics
V=20 kts, A=0.3 ft,
Ahead Seas

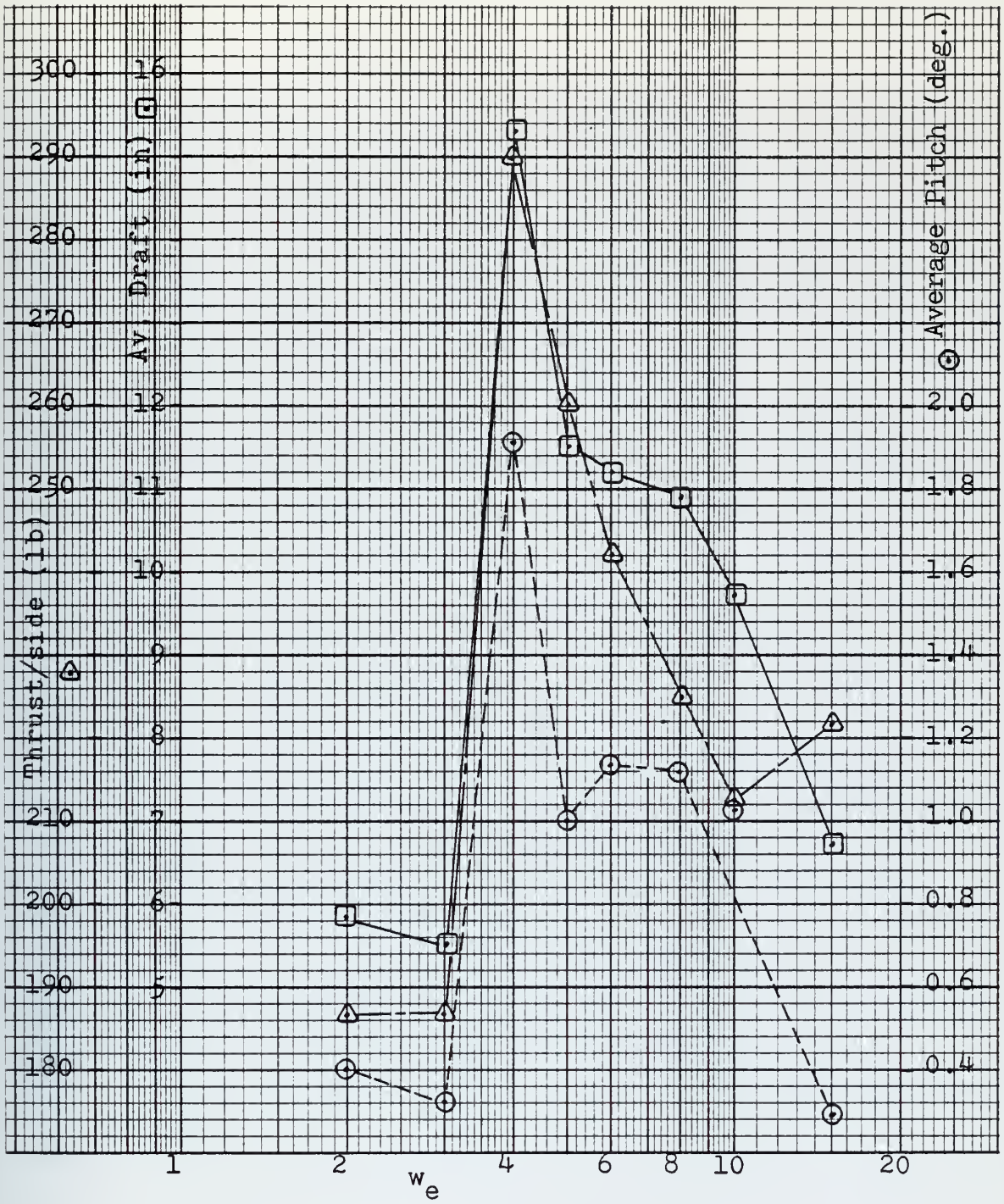

Figure 32. Operating Characteristics
V=20 kts, A=0.5 ft,
Ahead Seas

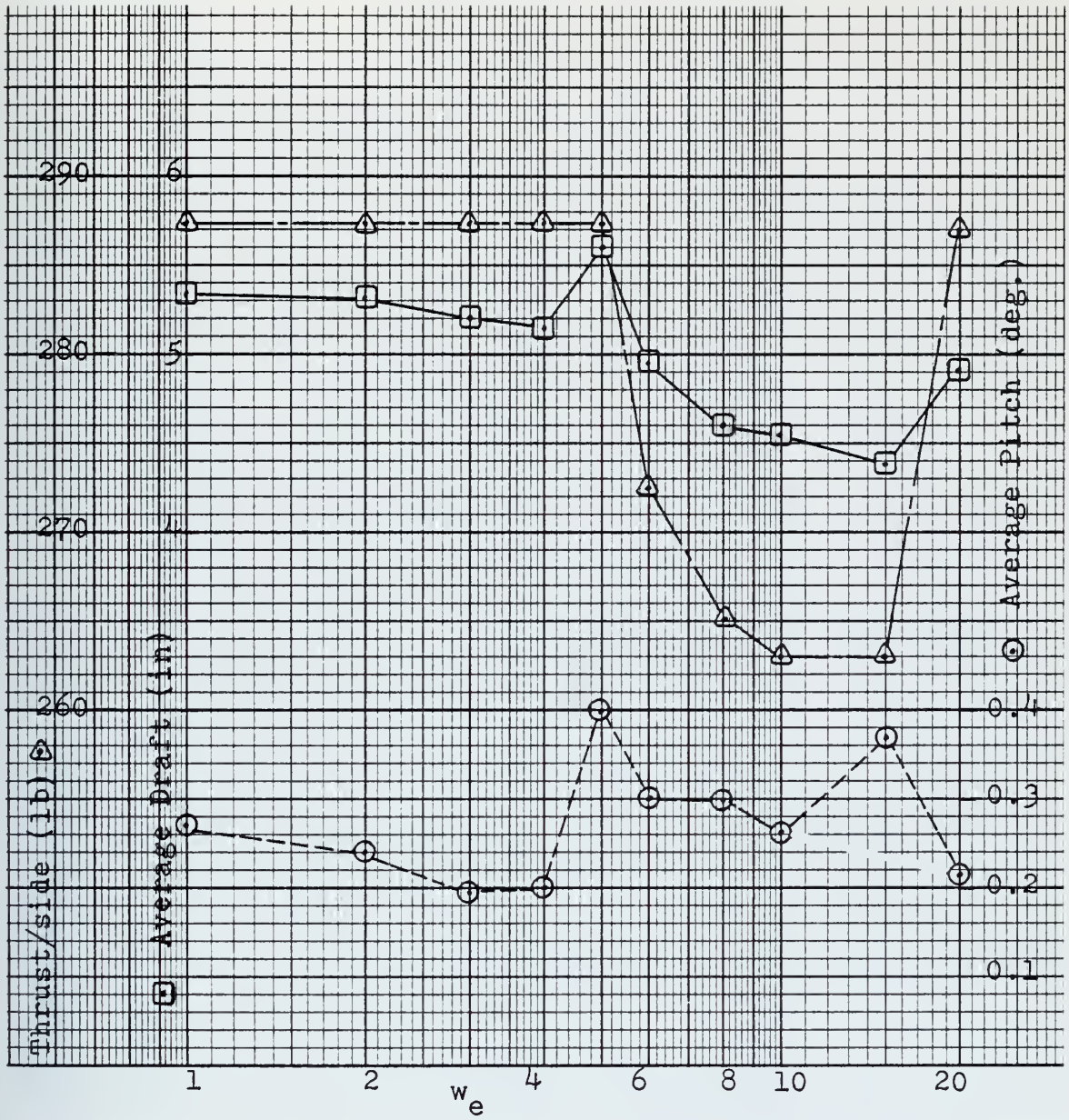

Figure 33. Operating Characteristics
V=30 kts, A=0.2 ft,
Ahead Seas

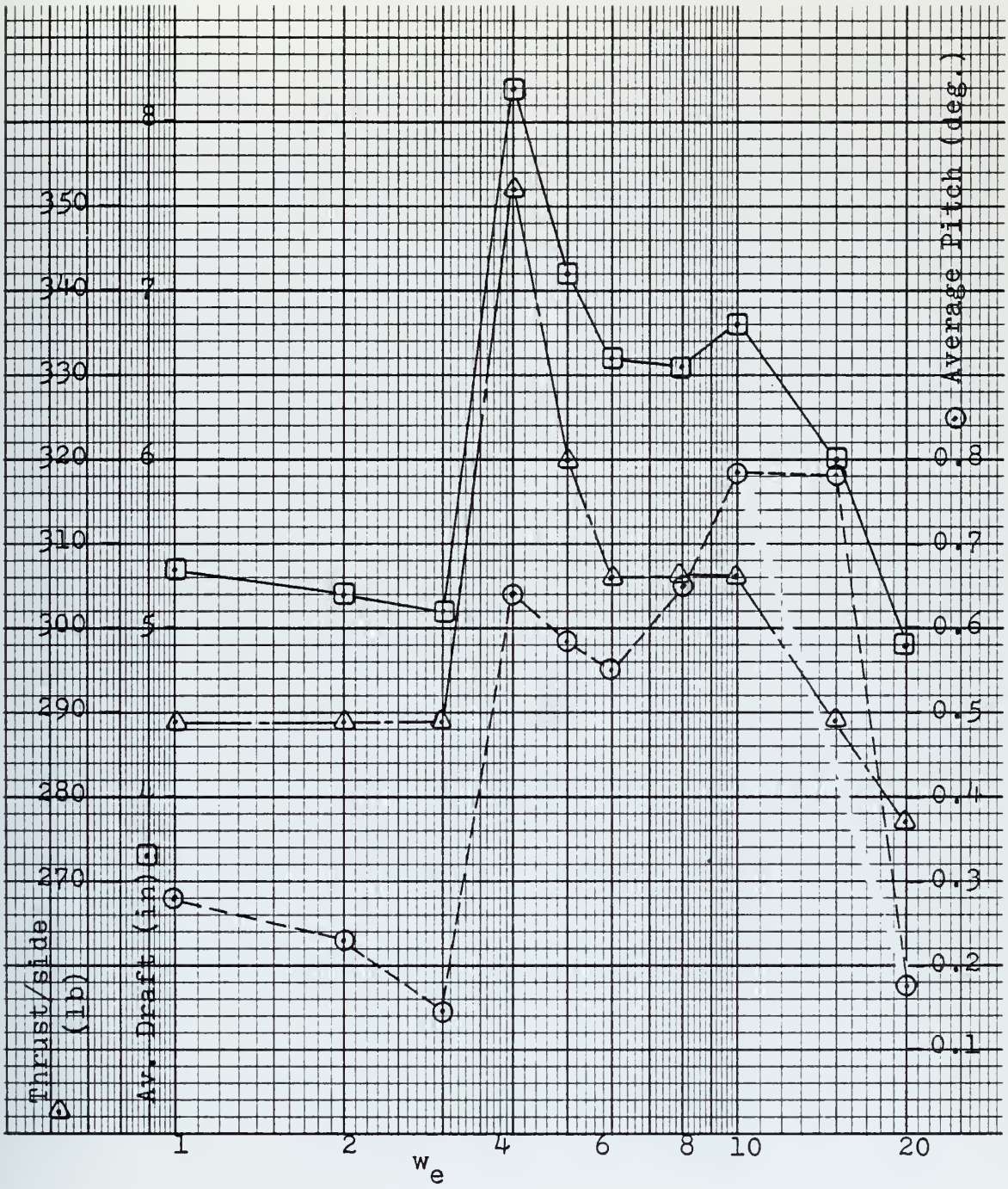

Figure 34. Operating Characteristics
V=30 kts, A=0.3 ft,
Ahead Seas

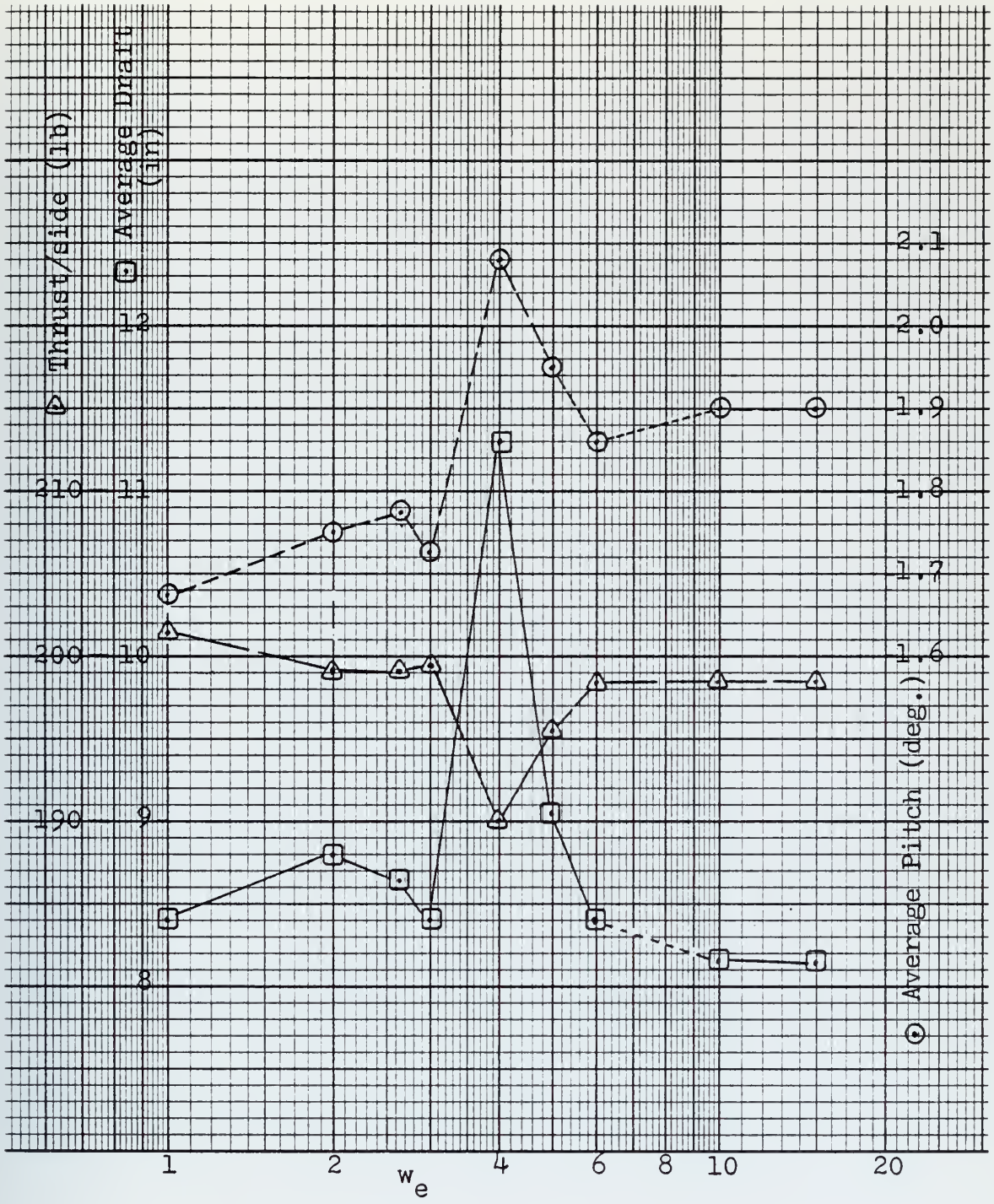

Figure 35. Operating Characteristics
V=10 kts, A=0.2 ft,
Following Seas

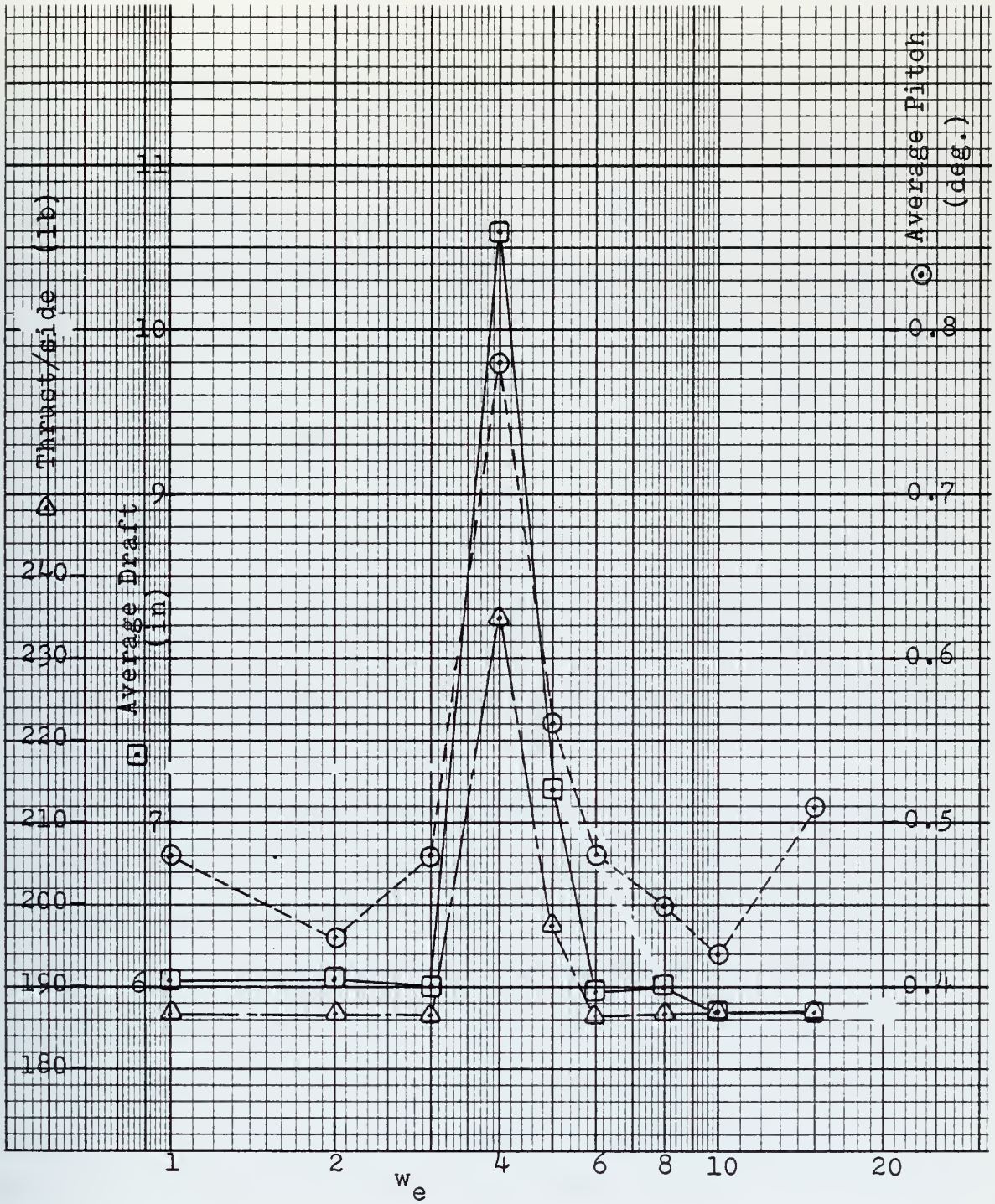

Figure 36. Operating Characteristics
V=20 kts, A=0.2 ft,
Following Seas

V. IRREGULAR SEA RESPONSE CHARACTERISTICS

A vessel's behavior in regular waves, as was obtained for the digital XR-3 in chapter IV, is of fundamental importance, for if the vessel can be described by linear responses, its motion in an irregular seaway can be described as the superposition of the responses of the vessel to all the wave components of the seaway, i.e.,

$$Y(w) = X(w) \cdot H(w)$$

To check the validity of the ahead sea frequency response characteristics obtained for the XR-3 digital model in regular seas, the program's ability to simulate the craft's motion in irregular seas was used.

The irregular seas were constructed using wave option 3 in which given the $\bar{H}_{1/3}$ and the range of significant periods the component wave frequencies and amplitudes are calculated by the program using the Pierson-Moskowitz spectrum. Each irregular sea generated was composed of ten wave components.

The significant wave heights and range of significant wave periods for various sea conditions were obtained from data compiled by the David Taylor Model Basin, a portion of which is listed in Table II. The associated spectrums were plotted in Figure 2. Using the procedures developed for ahead sea runs in regular waves, simulations were conducted for the conditions listed in Table III. It was found that in sea

TABLE II

Significant Wave Heights and Wave Periods

Sea State	Wing Velocity (knots)	$\overline{H}_{1/3}$ (ft.)	$\overline{H}_{1/10}$ (ft.)	Significant Range of Periods (sec)
0	2	0.08	0.10	0-1.2
1	5	0.29	0.37	0.4-2.8
1	8.5	1.0	1.2	0.8-5.0
2	10	1.4	1.8	1.0-6.0
2	12	2.2	2.8	1.0-7.0
2	13.5	2.9	3.7	1.4-7.6

TABLE III

Irregular Sea Simulation Conditions

Craft Speed (knots)	$\overline{H}_{1/3}$ (ft.)	Thrust per side (lb)
20	0.29	186.72
	1.0	210.0
	1.4	223.0
30	1.0	300.0
	1.4	310.0

states with significant wave heights greater than those listed in Table III there was nearly continuous contact with the top of the plenum chamber, a condition which is not accounted for in the program and therefore avoided. A typical example of the generated irregular wave as seen at the craft's center of gravity and the responses to the wave are shown in Figure 37-A through 37-E. Clearly apparent in the heave and pitch responses is the "low pass filtering" of the wave excitation's high frequency components which was the dominate characteristic of the heave and pitch regular sea frequency response functions.

The magnitude of the frequency response function is

$$H(w) = \frac{Y(w)}{X(w)}.$$

In order to determine the excitation and response spectrums, the discrete fourier transform (DFT) was taken of the wave excitation using an IBM 360 library subroutine as described in Appendix F.

To obtain an accurate representation of the spectrums with the DFT, several conditions had to be met. To prevent aliasing, the high-frequency components of the time function impersonating low frequency components, the sampling rate of the time response or excitation had to be greater than the Nyquist rate. A sampling interval of 0.03 seconds satisfied this condition. The frequency resolution of the DFT is $1/\tau$ where τ is the sample length. The longer the sample the greater the resolution. However this conflicted with the actual running of the program in which greater than 2.5 minutes

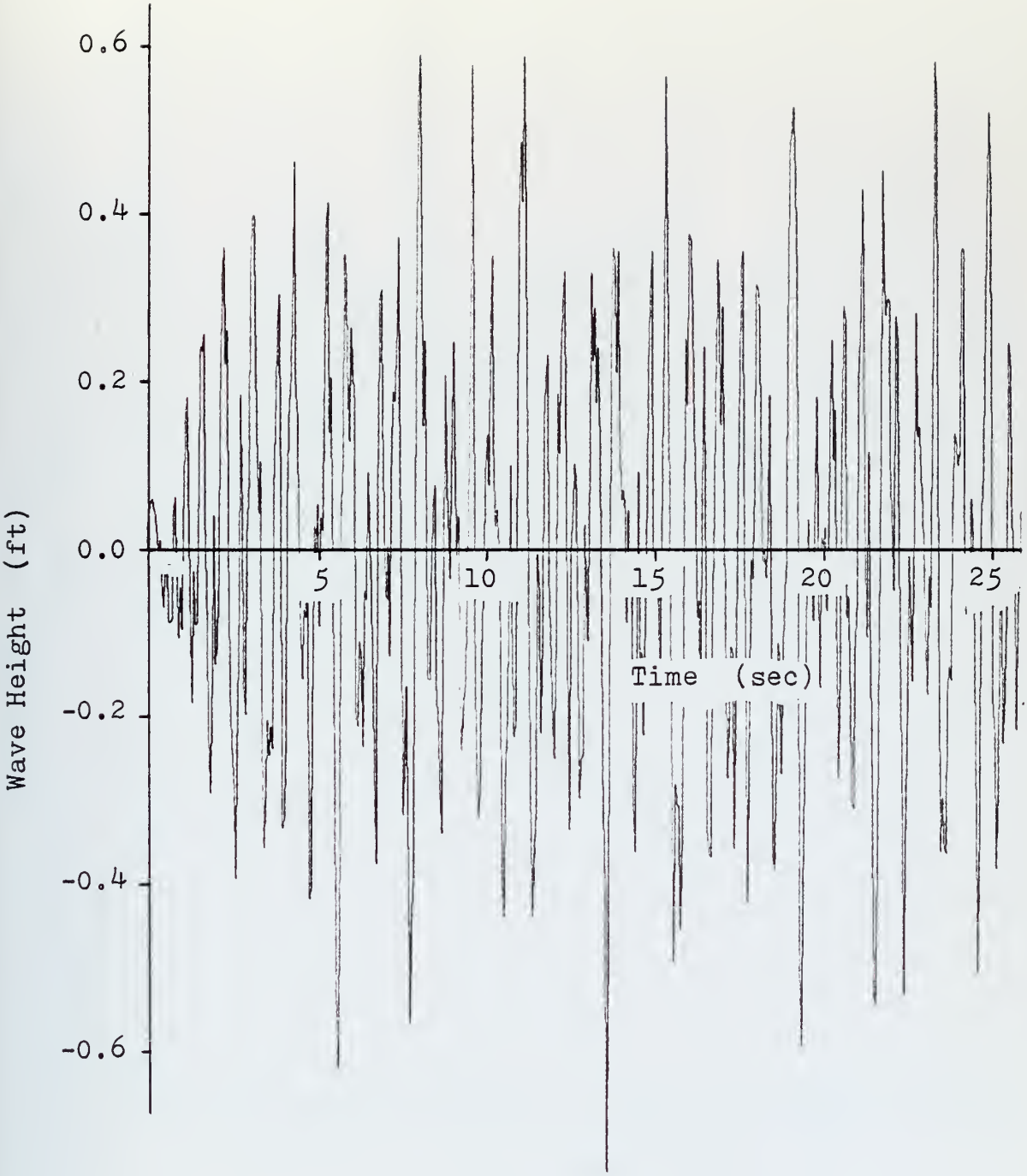

Figure 37-A. C.G. Wave Height vs. Time

V = 20 kts, $\bar{H}_{1/3}$ = 1.0 ft

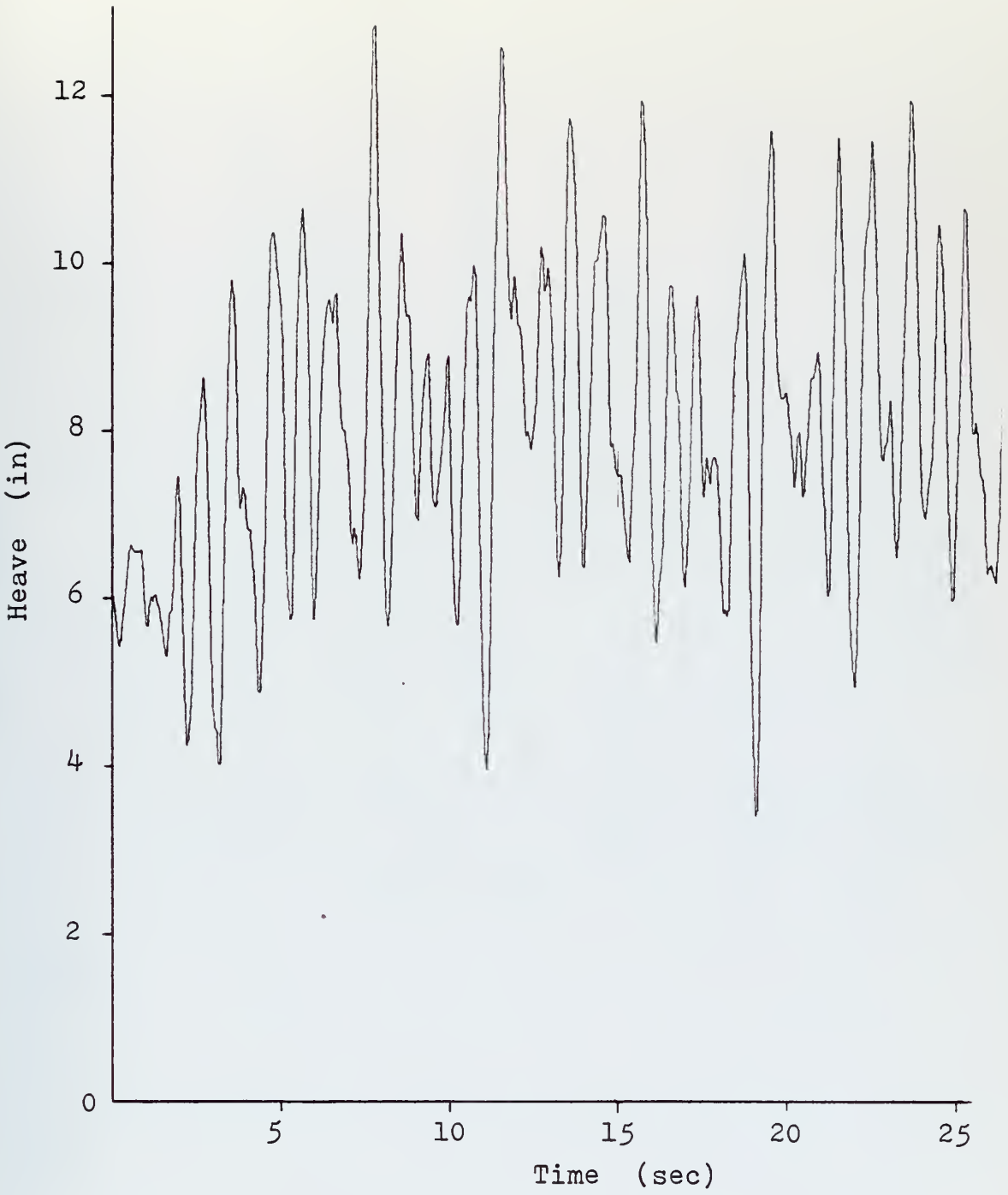

Figure 37-B. Heave vs. Time

V = 20 kts, $\bar{H}_{1/3}$ = 1.0 ft

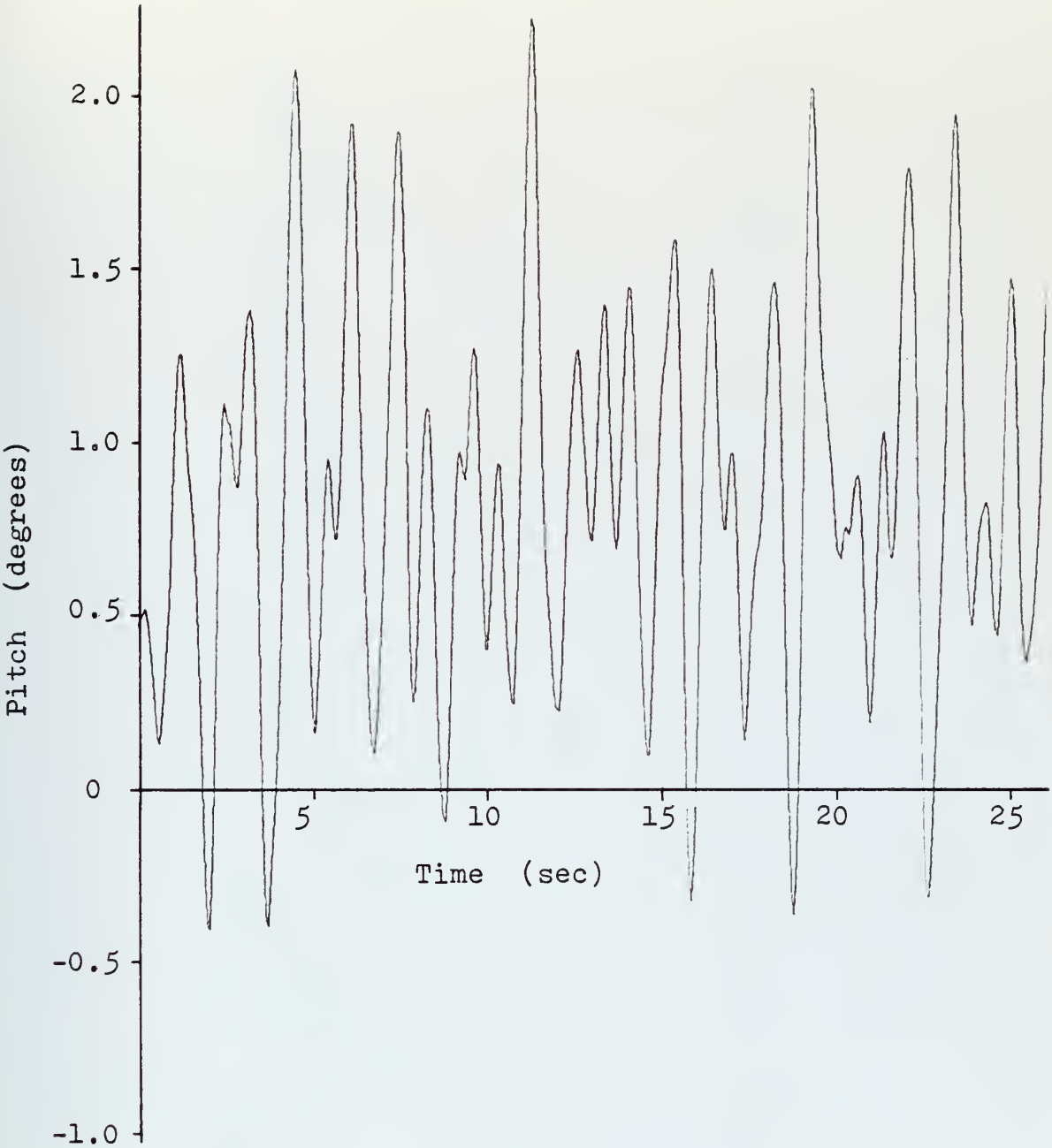

Figure 37-C. Pitch vs. Time

V = 20 kts, $\bar{H}_{1/3}$ = 1.0 ft

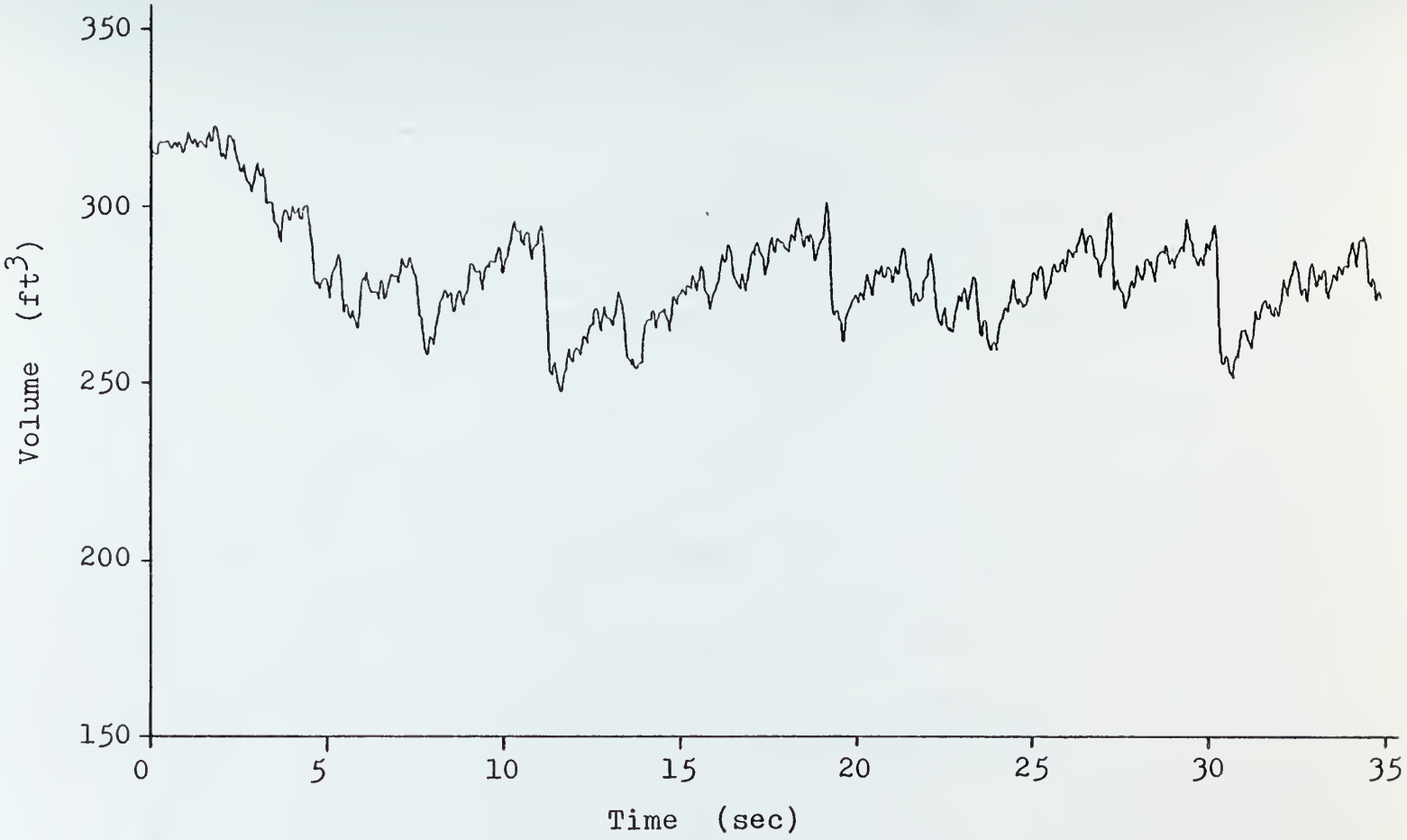

Figure 37-D. Plenum Volume vs. Time

V = 20 kts, $H_{1/3}$ = 1.0 ft

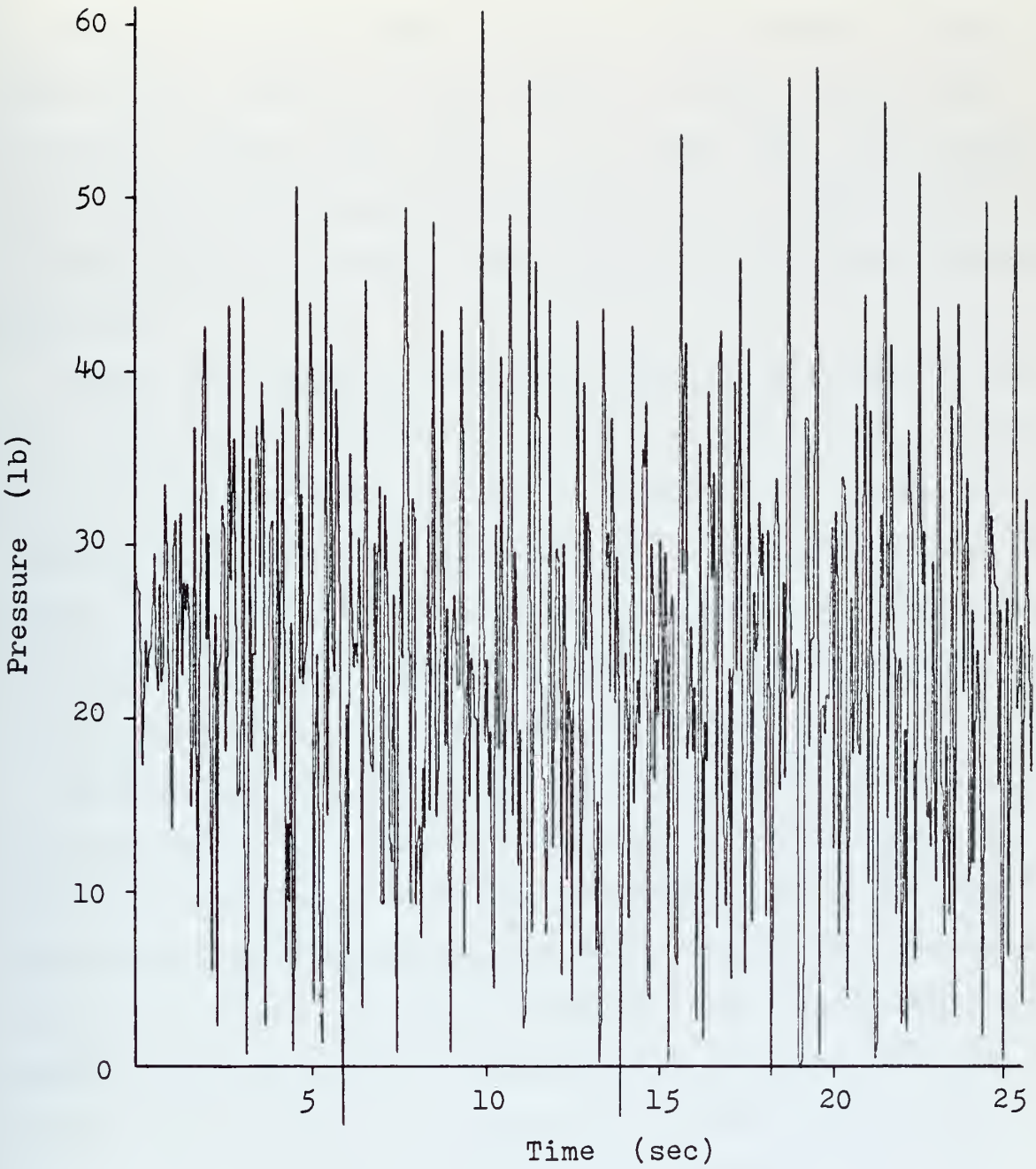

Figure 37-E. Plenum Pressure vs. Time

V = 20 kts, $\bar{H}_{1/3}$ = 1.0 ft

CPU time was required to simulate the craft for one second of run time in irregular seas. Finally, the bandwidth of the spectrum is a function of the number of sample points and the sample length [Ref. 12]. A 512 point DFT, which therefore produced 256 frequency components, and a sample length of approximately 16 seconds were found to produce good discrete spectrums.

Figure 38-A shows the discrete magnitude spectrum of the wave height at the center of gravity for V=20 kts, $\bar{H}_{1/3}$=1.0ft. Note that the spectrum produced is a function of encounter frequency since the data was taken while the craft was in motion. Also shown in the figure is the encounter frequencies and amplitudes of the components used in actually constructing the irregular wave. The two agree quite well.

Figures 38-B and 38-C present the magnitude spectrum of the heave and pitch responses to the above wave excitation, again as a function of encounter frequency. The "low pass" characteristics of the heave and pitch regular sea frequency response functions are clearly evident in the spectrums also. However also noted are the components at frequencies below w_e=3 for which there is no excitation. These values were ignored. From the wave spectra data, the frequencies and amplitudes of the peaks were obtained. The amplitudes of the heave spectra were also obtained at the same frequencies and the ratio of the two were calculated (see Table G-12, G-13, and G-14) and are plotted in Figure 38-D. As a comparison

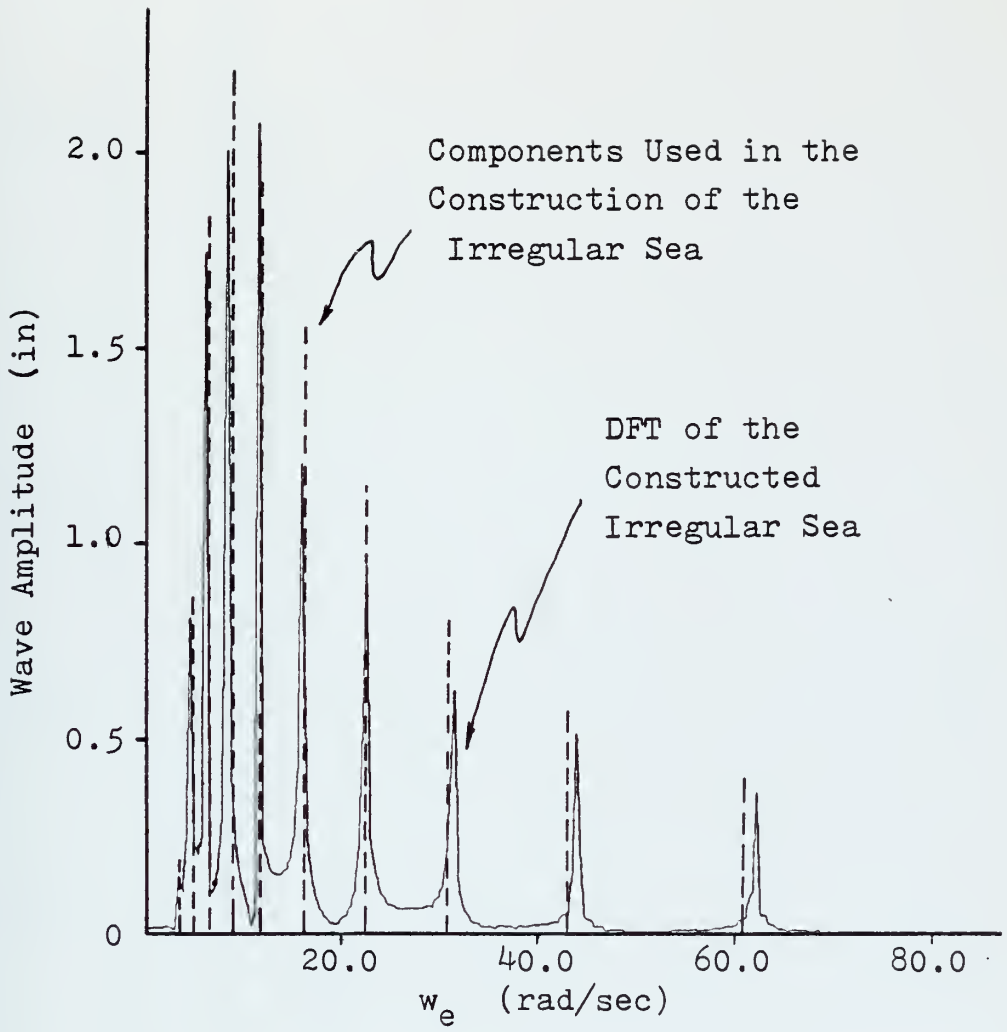

Figure 38-A. C.G. Wave Height Spectrum
V=20 kts, $\bar{H}_{1/3}$ = 1.0 ft

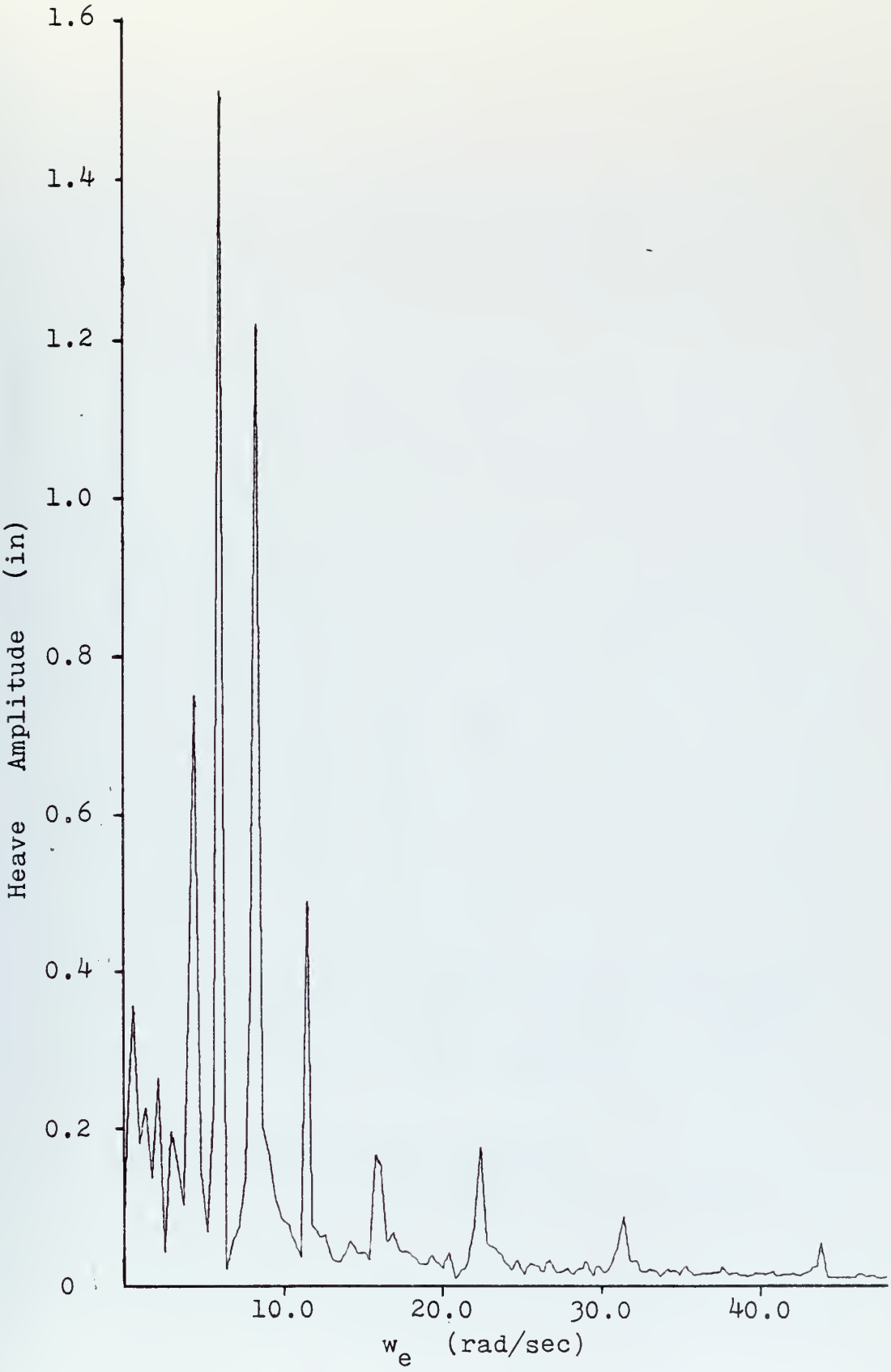

Figure 38-B. Heave Spectrum
V = 20 kts, $\bar{H}_{1/3}$ = 1.0 ft

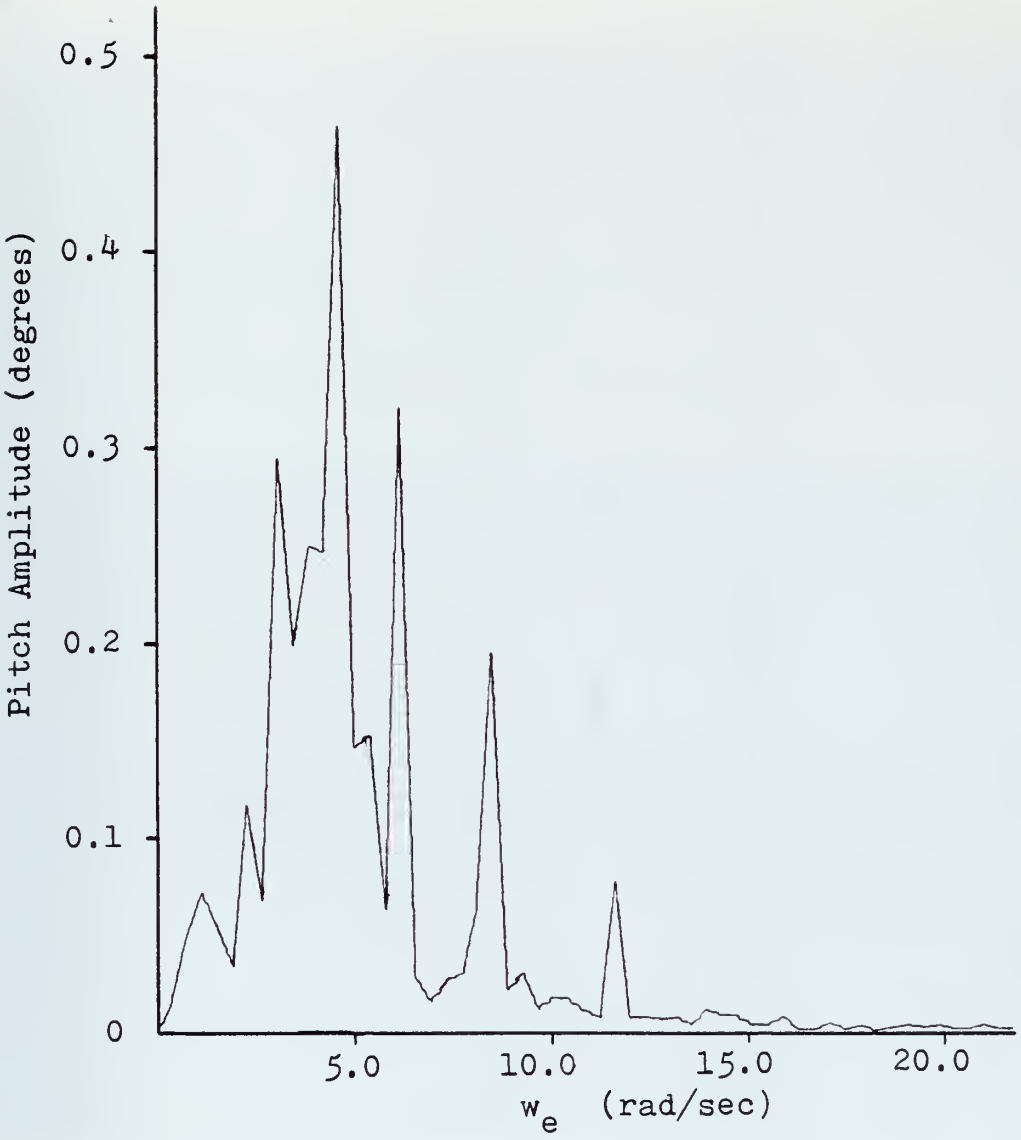

Figure 38-C. Pitch Spectrum
V = 20 kts, $\bar{H}_{1/3}$ = 1.0 ft

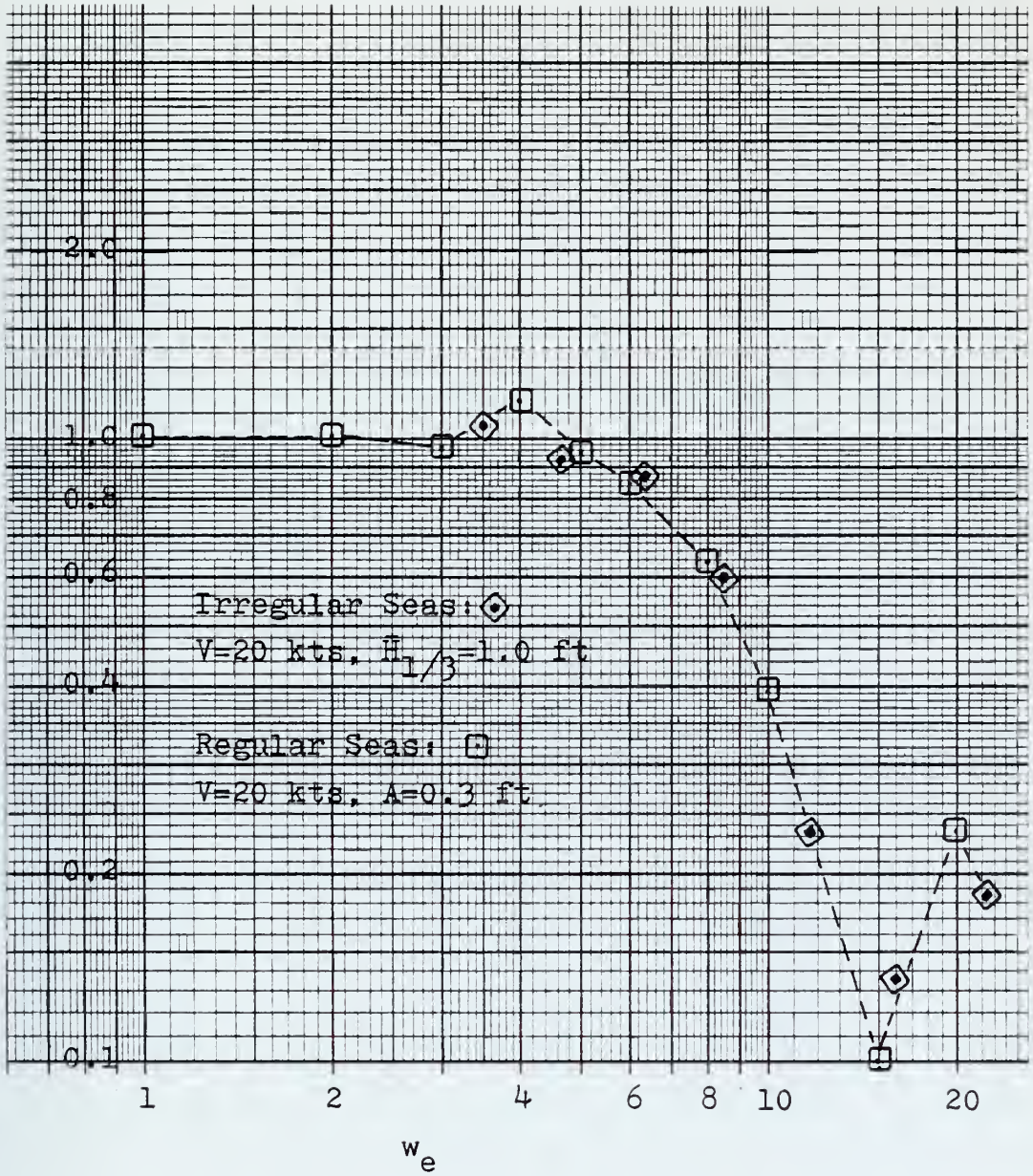

Figure 38-D. Heave Frequency Response

V=20 kts, $\bar{H}_{1/3}$=1.0 ft

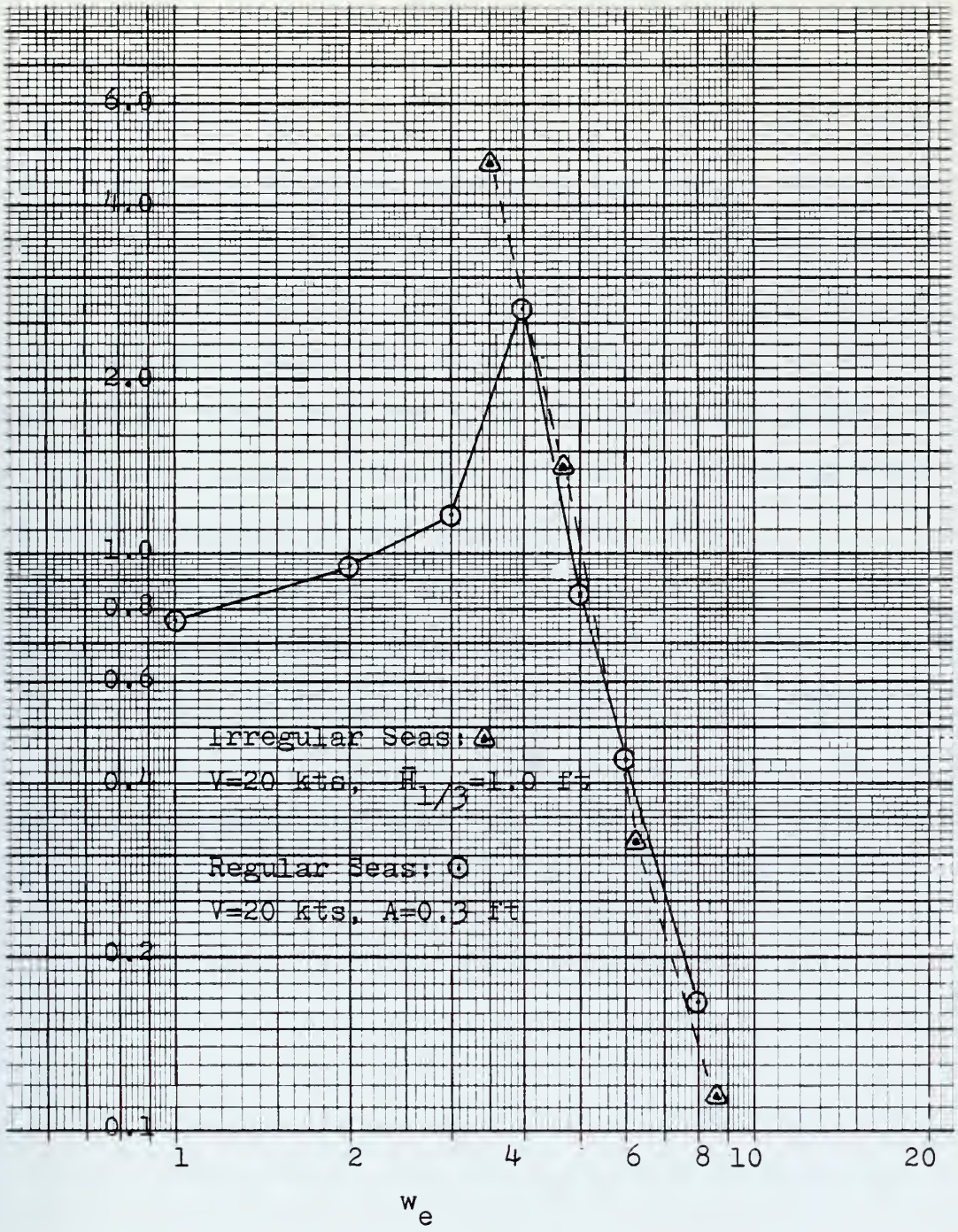

Figure 38-E. Pitch Frequency Response

V=20 kts, $\bar{H}_{1/3}$=1.0 ft

with the heave frequency response resulting from regular seas, the response for V=20, A=0.3 ft. is also plotted.

To determine the irregular sea pitch frequency response it was necessary to first calculate the actual wave frequency from the encounter frequency and then the maximum wave slope for each wave frequency. The ratio of the pitch amplitude to the maximum wave slope was then determined and is plotted in Figure 38-E. Note that for both the heave and pitch irregular sea frequency response functions there is close agreement with those obtained in the regular seas runs.

The spectrums of wave amplitude and pitch and heave responses for two other combinations of sea state and craft speed are shown in Figures 39 through 40. Also presented are the associated frequency response functions. As can be seen, the frequency response functions for the irregular sea runs agree well with the regular sea responses.

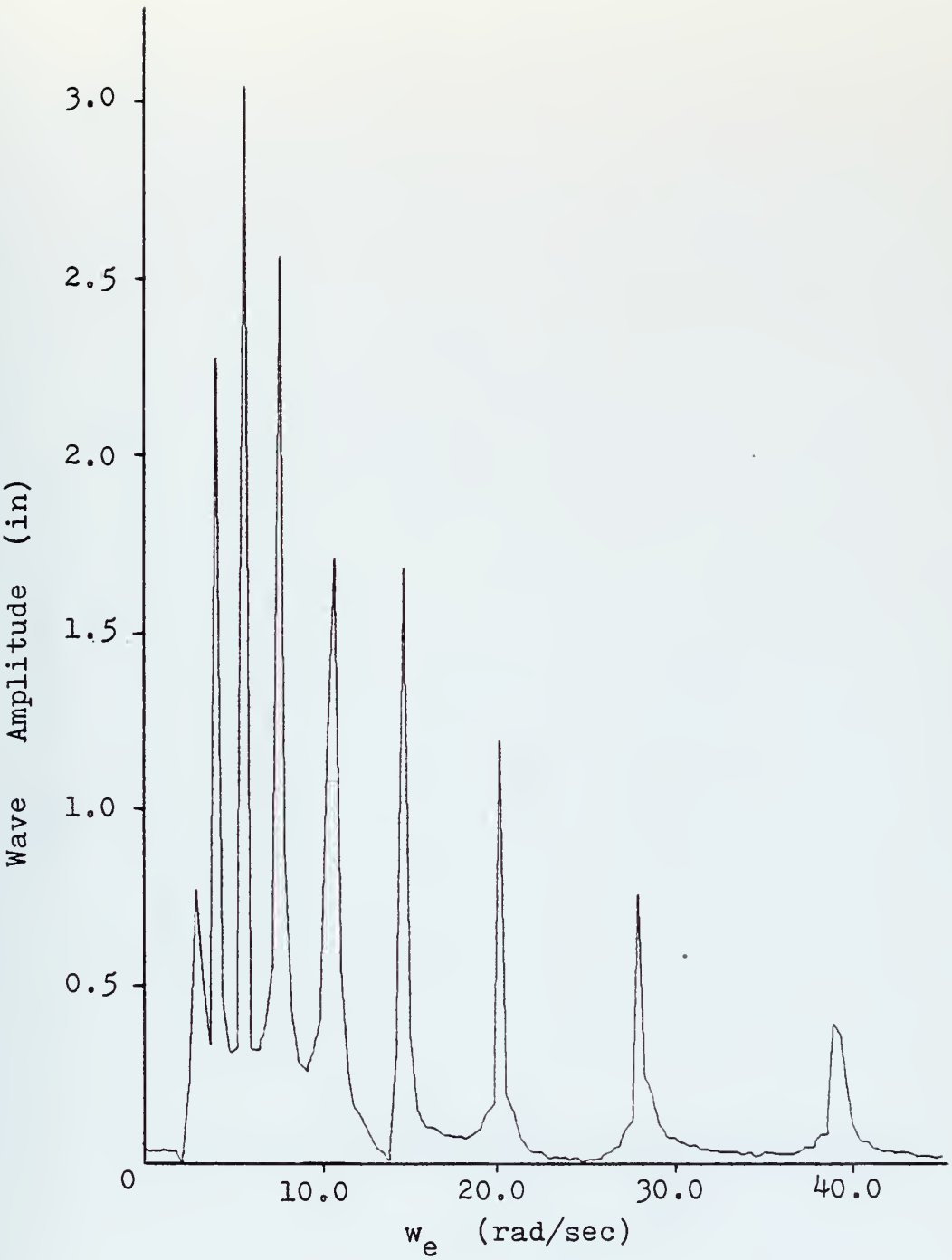

Figure 39-A. C.G. Wave Height Spectrum
V = 20 kts, $\bar{H}_{1/3}$ = 1.4 ft

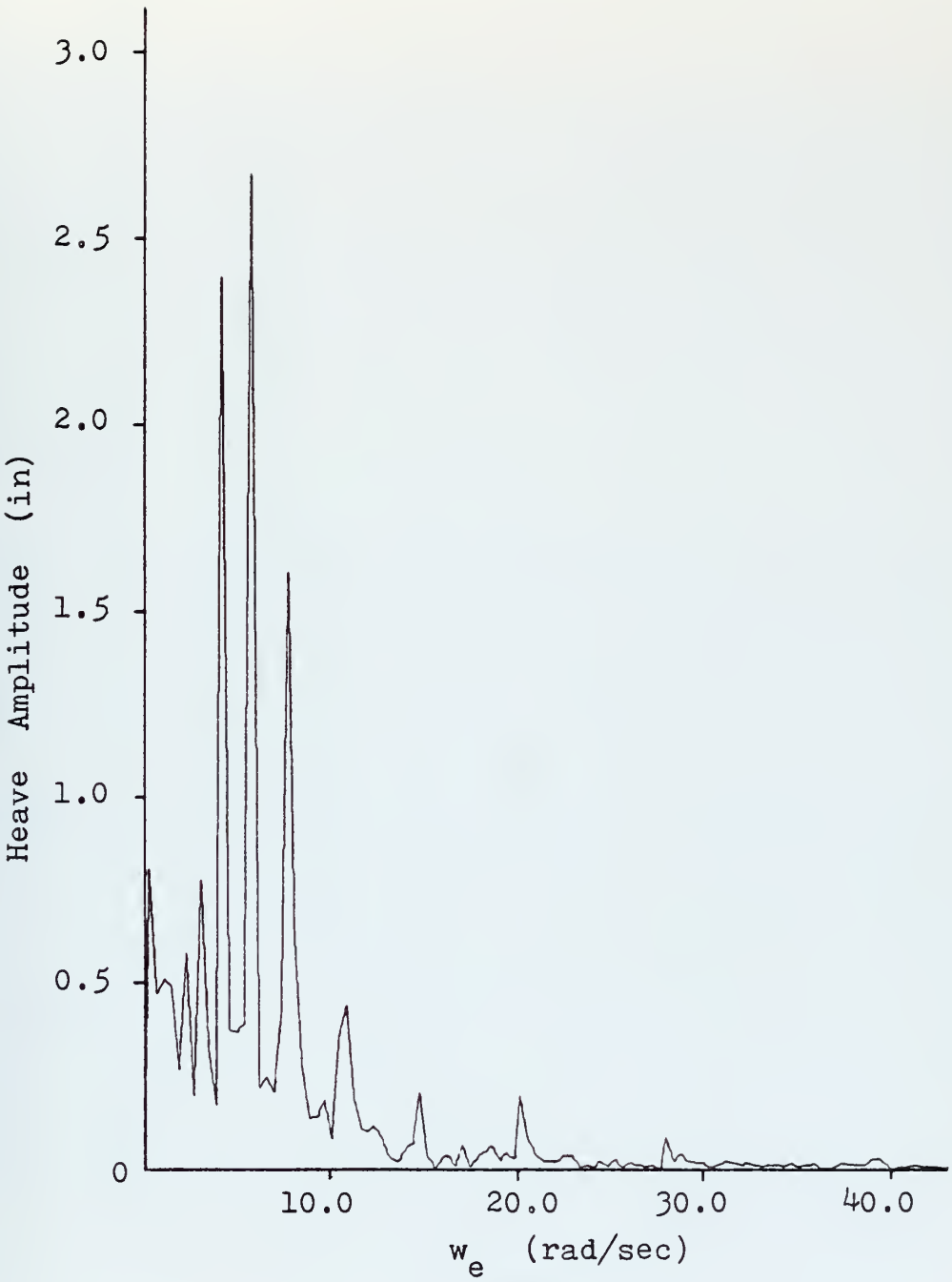

Figure 39-B. Heave Spectrum
V = 20 kts, $\bar{H}_{1/3}$ = 1.4 ft

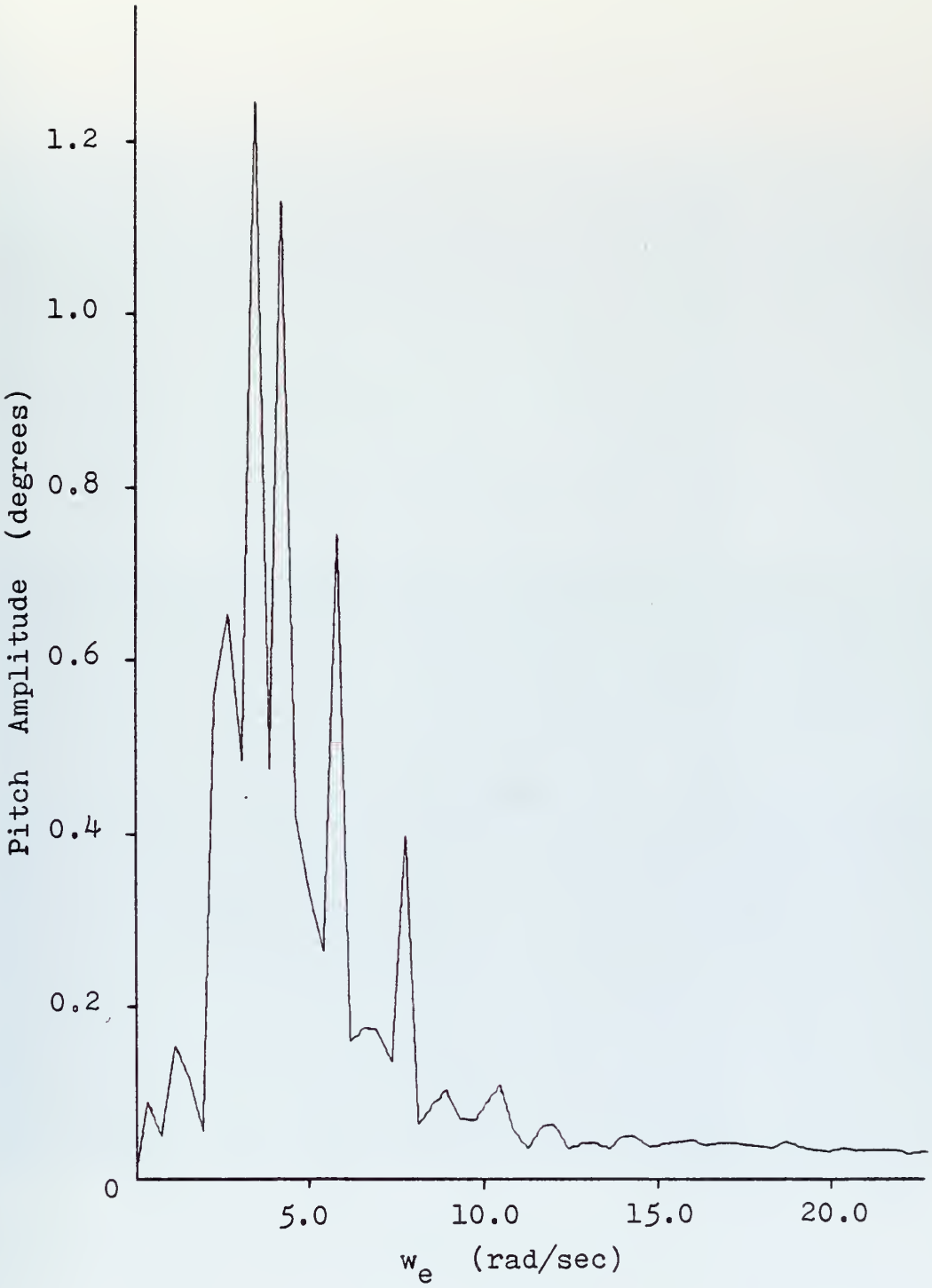

Figure 39-C. Pitch Spectrum
V = 20 kts, $\bar{H}_{1/3}$ = 1.4 ft

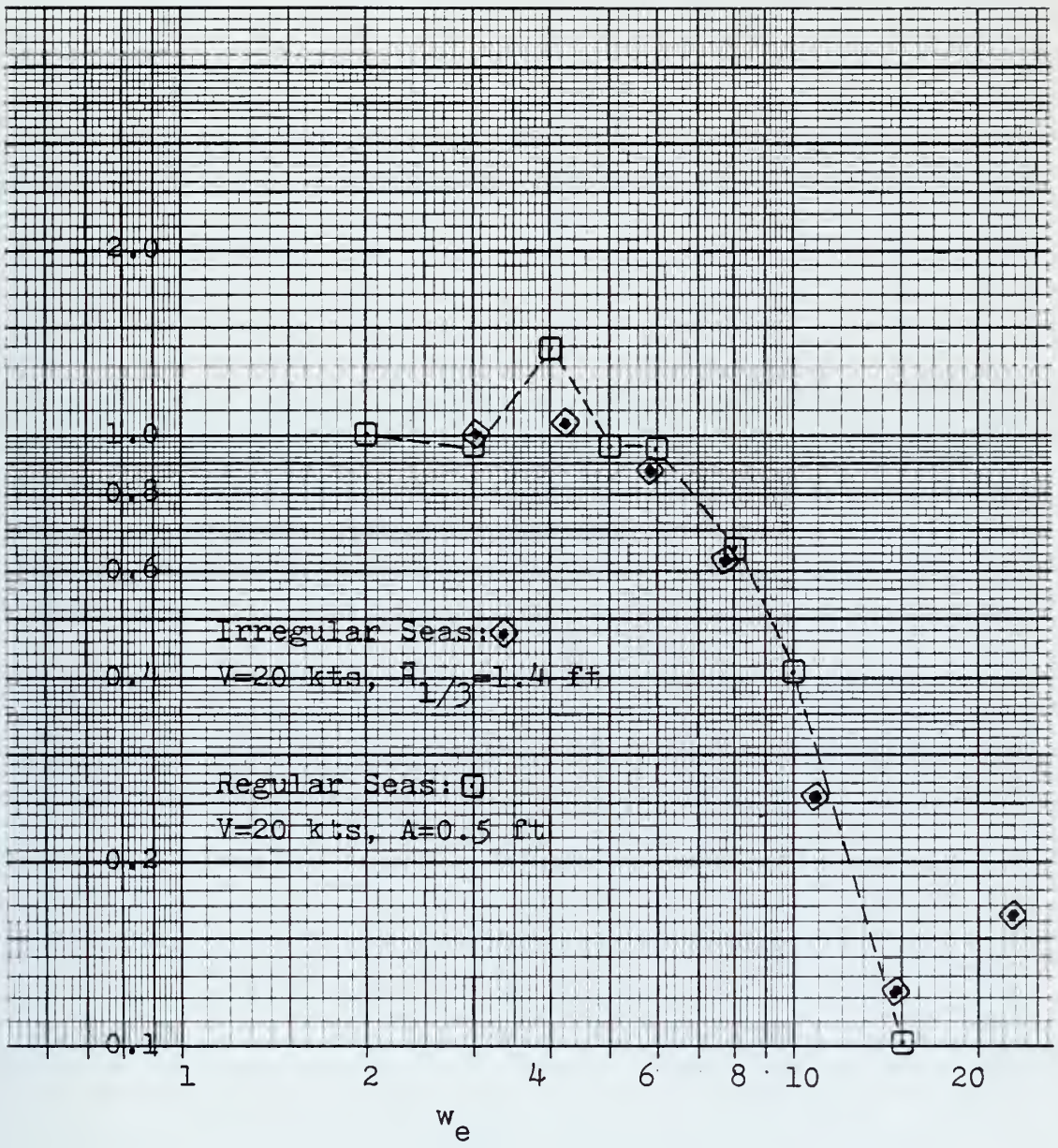

Figure 39-D. Heave Frequency Response

V=20 kts, $\bar{H}_{1/3}$=1.4 ft

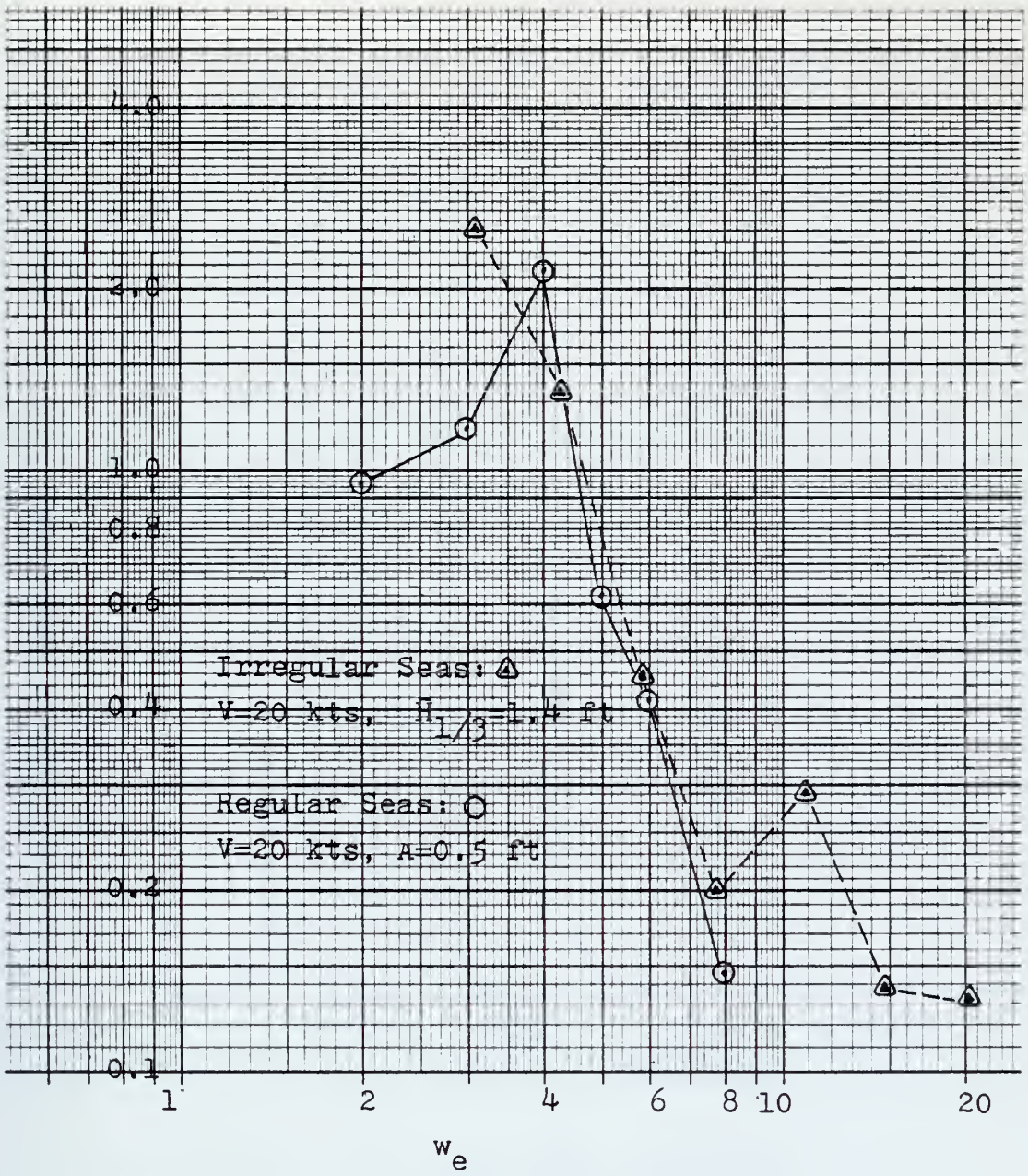

Figure 39-E. Pitch Frequency Response

V=20 kts, $\bar{H}_{1/3}$=1.4 ft

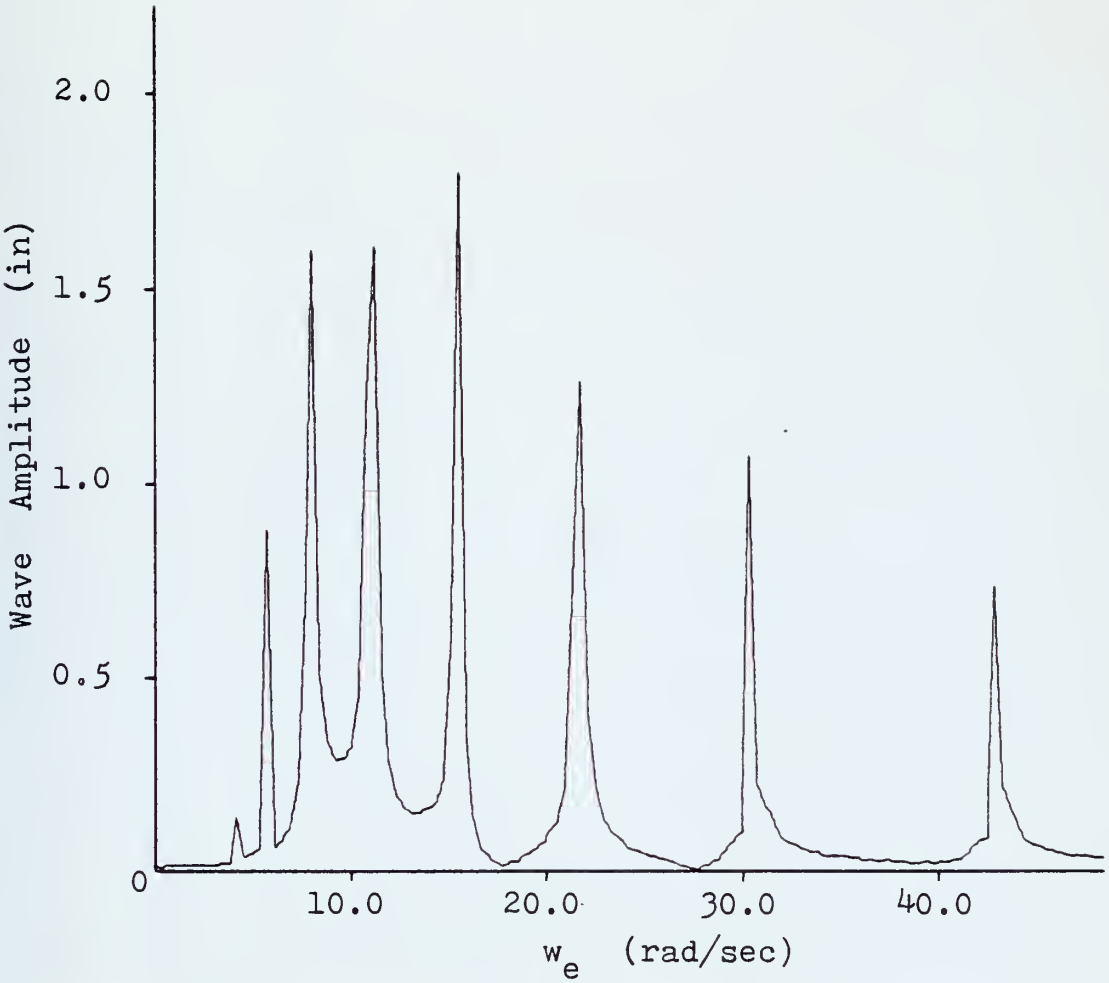

Figure 40-A. C.G. Wave Height Spectrum
V = 30 kts, $\bar{H}_{1/3}$ = 1.0 ft

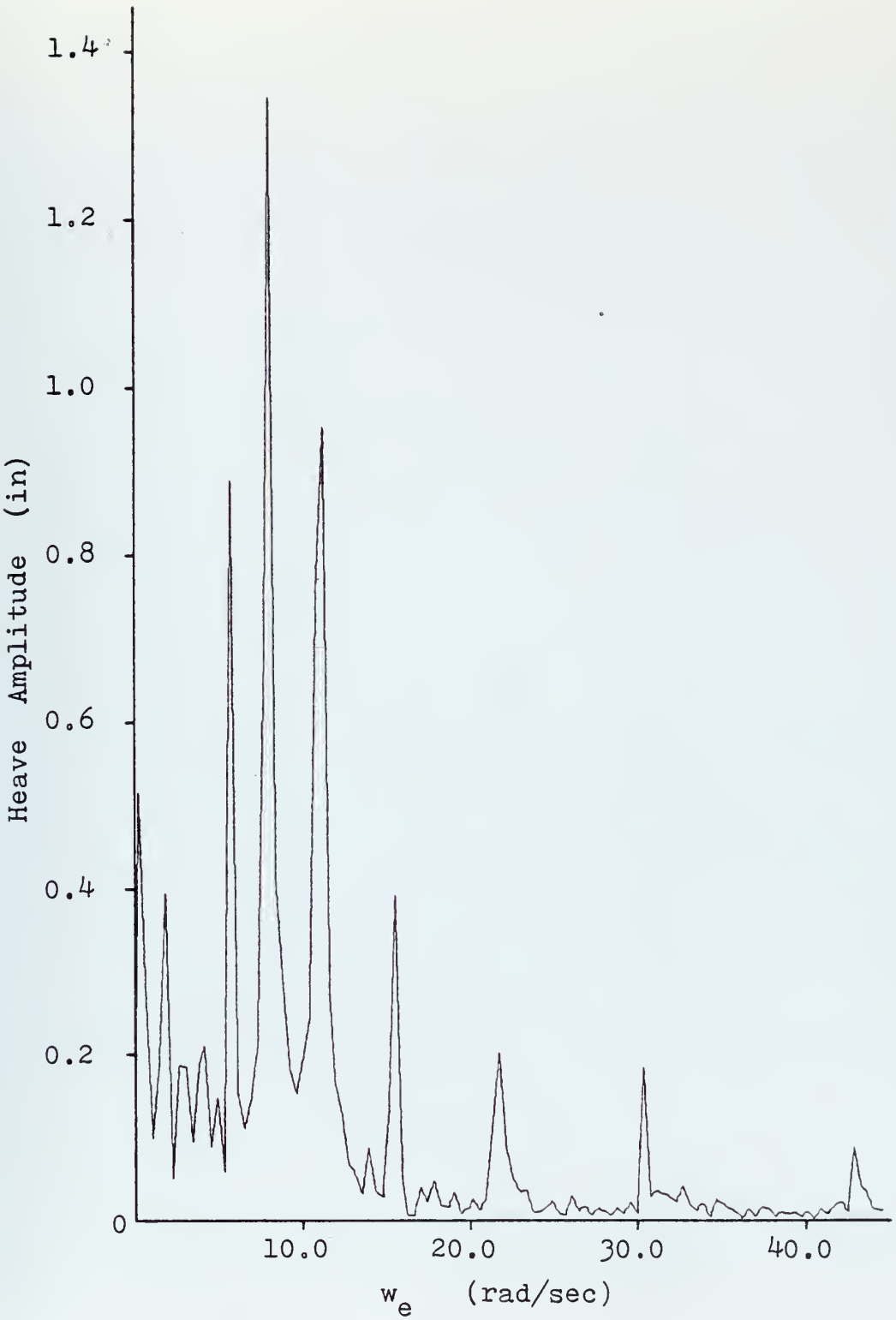

Figure 40-B. Heave Spectrum
V = 30 kts, $\bar{H}_{1/3}$ = 1.0 ft

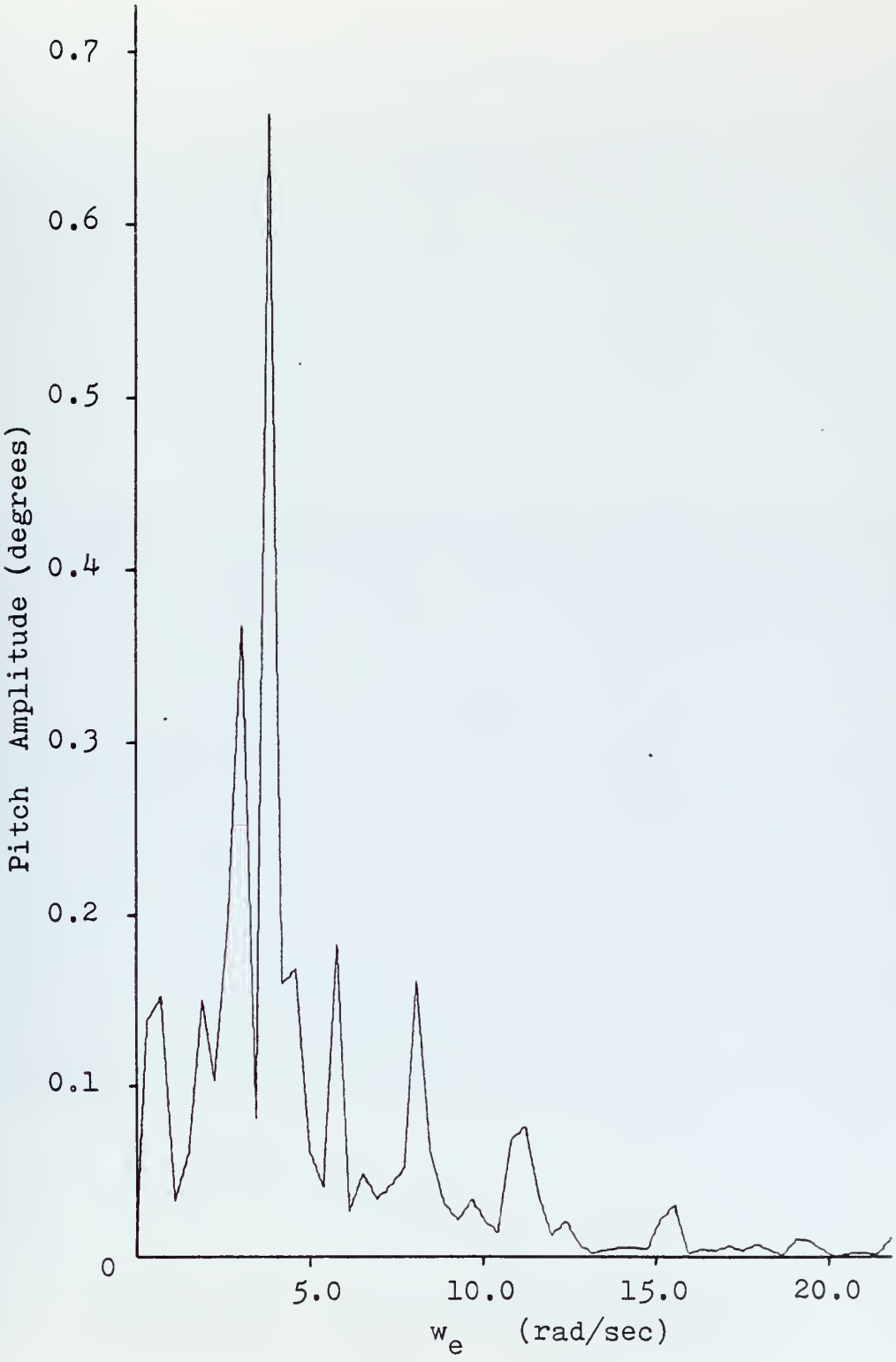

Figure 40-C. Pitch Spectrum
V = 30 kts, $\bar{H}_{1/3}$ = 1.0 ft

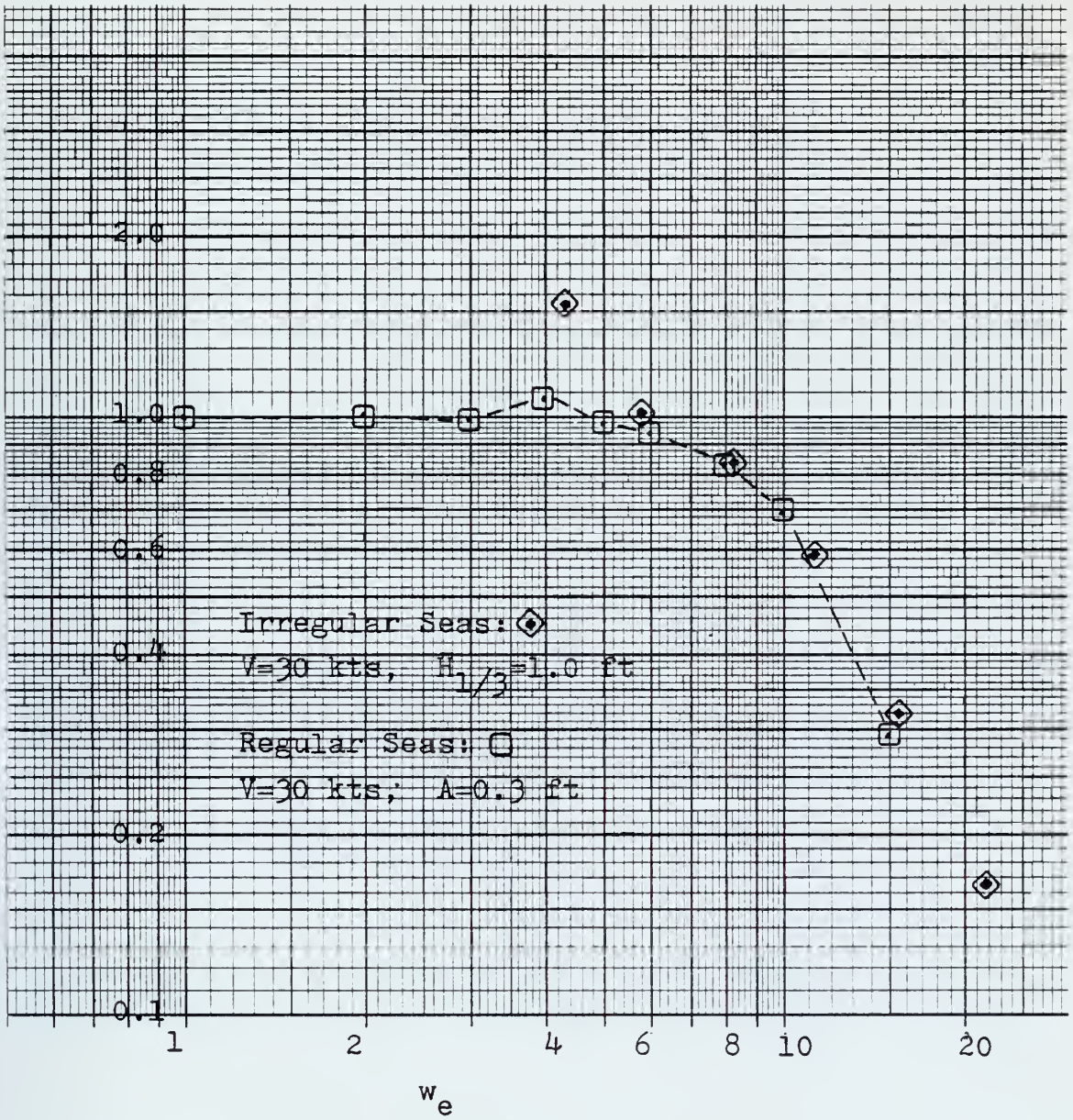

Figure 40-D. Heave Frequency Response

V=30 kts, $\bar{H}_{1/3}$=1.0 ft

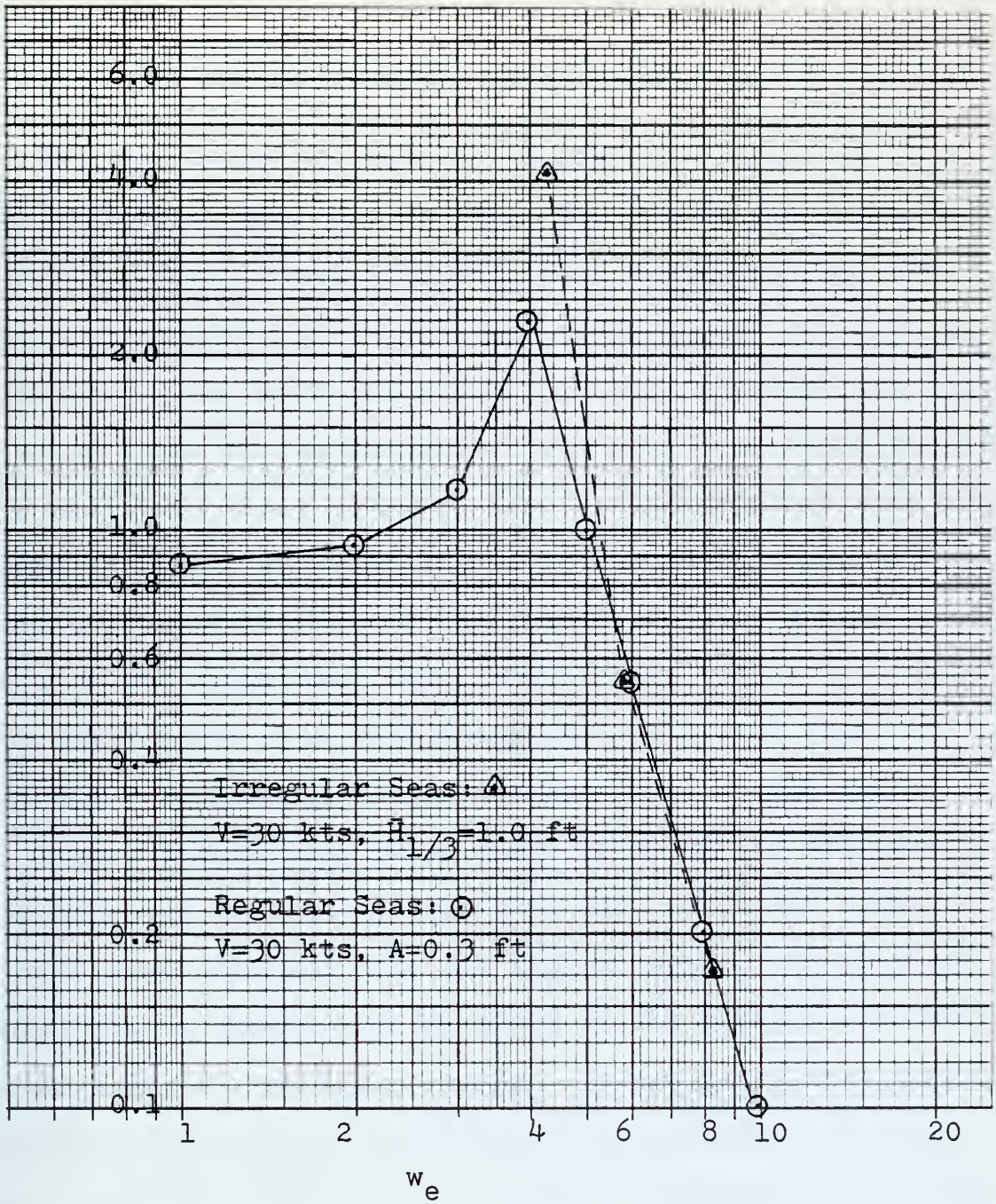

Figure 40-E. Pitch Frequency Response

V=30 kts, $\bar{H}_{1/3}$=1.0 ft

VI. CONCLUSIONS AND RECOMMENDATIONS

The XR-3 Loads and Motions Program was subjected to a wide variety of wave conditions. The conditions necessary to obtain steady-state operation were determined and the frequency response functions for heave, pitch, and roll were developed. The heave and pitch frequency response functions obtained from the regular ahead seas runs were found to compare well with those obtained from irregular ahead seas by use of the DFT. In general the nonlinearities inherent in a six degree-of-freedom model were found to be minimal and exist at the lower encounter frequencies. It is believed that the results from this study provide a good baseline with which to compare future modifications to the model.

A most interesting study would be to obtain frequency response data from the actual XR-3 test craft and compare it with that obtained from the digital model. It is recommended that a closer look be given to the model's simulation of the craft at the lower speeds. It was noted that during resonance at 10 knots, as the craft sank deeper actually less thrust was required to maintain the desired speed than at the other encounter frequencies. There appears to be no plausible explanation for this.

Although the conditions under which gapping of the sidewalls occurred were determined no effort was made to determine the actual air flow rates out of the gaps or if indeed the

air loss was great and rapid enough to cause the loss in plenum pressure noted and therefore the settling of the craft deeper into the water. Finally, although not analyzed or presented in this study, data was obtained and is available on the vertical accelerations of the center of gravity for the majority of the steady-state runs. Analysis of this data could be of use in defining the habitability zones for the simulated XR-3.

APPENDIX A

Encounter Frequency

The frequency of excitation is commonly given in terms of the encounter frequency, the frequency actually "seen" by the vessel. Due to the forward speed of the craft, the frequency of encounter with the waves is increased or decreased depending on the relative direction between the vessel's course and the direction of propagation of the surface wave. The encounter frequency is given by:

$$w_e = \frac{2\pi}{\lambda} (C - V \cos\beta) \text{ (rad/sec)} \qquad \text{(A-1)}$$

where λ = wave length (ft)

C = wave velocity (ft/sec)

V = craft velocity (ft/sec)

β = the angle between the craft's course and the direction of propagation of the wave.

Given that the wave velocity, $C = (\frac{g\lambda}{2\pi})^{\frac{1}{2}}$, and the wavelength, $\lambda = \frac{2\pi g}{w^2}$ where w is the wave frequency, by substitution into A-1 it can be shown that:

$$w_e = w - w^2 \cdot \frac{V \cos\beta}{g}. \qquad \text{(A-2)}$$

For a vessel heading into the waves, $\beta = 180^\circ$ and

$$w_e = \frac{2\pi}{\lambda} (C + V). \qquad \text{(A-3)}$$

For this study it was desired to simulate regular waves that produced integer values of w_e between 1 rad/sec and 20 rad/sec for a given value of vessel velocity. The application of the quadratic formula to equation A-2 yields

$$w = \frac{1 - \sqrt{1 + (4Vw_e)/g}}{-2\frac{V}{g}} \qquad \text{(A-4)}$$

for $\beta = 180^{\circ}$.

This relationship is plotted in Figure A-1.

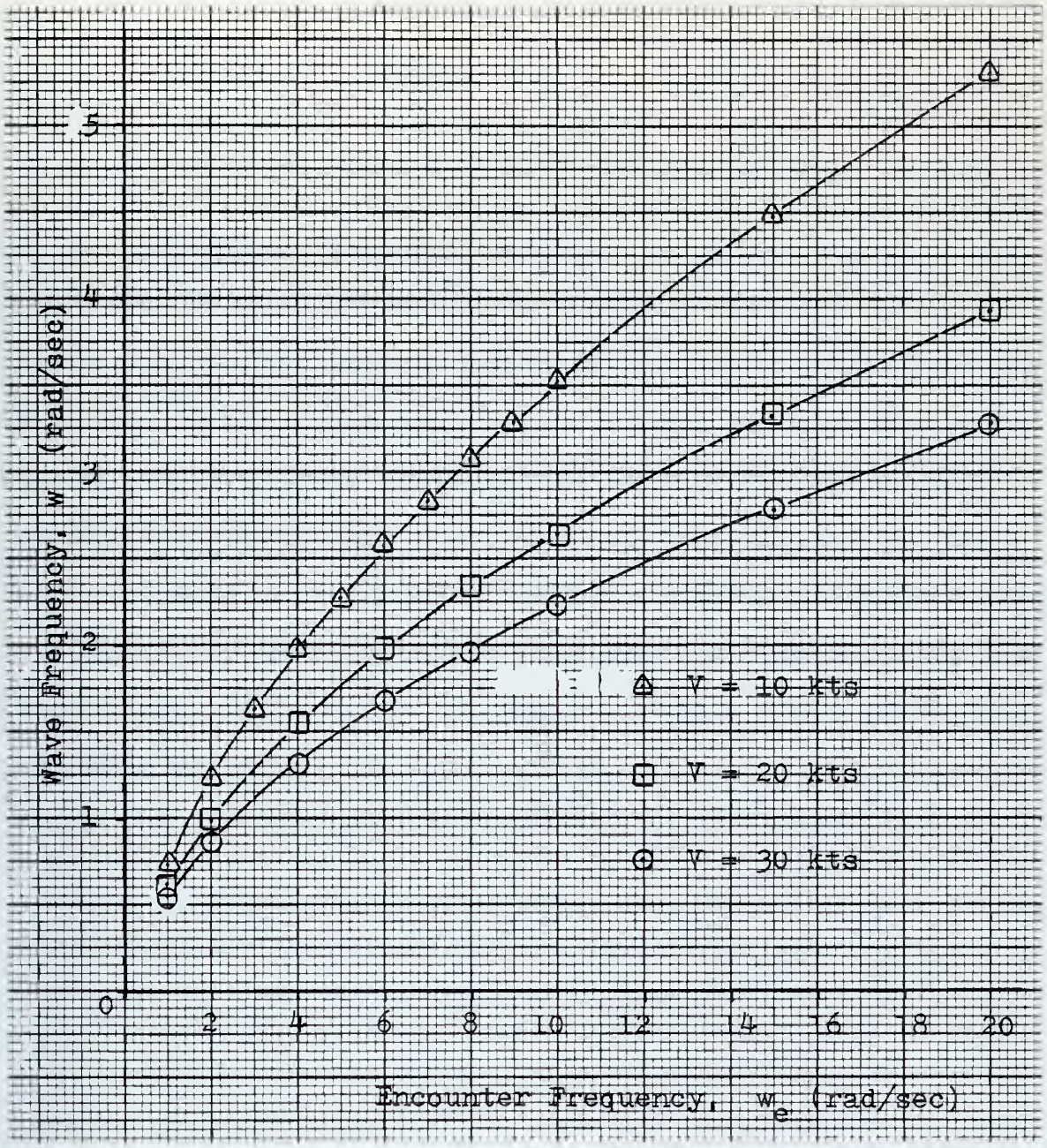

Figure A-1. Wave Frequency vs. Encounter Frequency

APPENDIX B

Theoretical Frequency Response Functions

A theoretical frequency response model for the XR-3 was developed by the Aerojet-General Corp. [Ref. 7] using a four degree-of-freedom representation of the craft with responses in heave, pitch, roll, and surge. It was assumed that the response motions were small enough so that deviation from the linear response was negligible for the motions in the vertical plane. The requency response characteristics obtained are reproduced in Figures B-1 thru B-3 and show not only the theoretical response but the results from $\frac{1}{2}$ scale model towing tests as well.

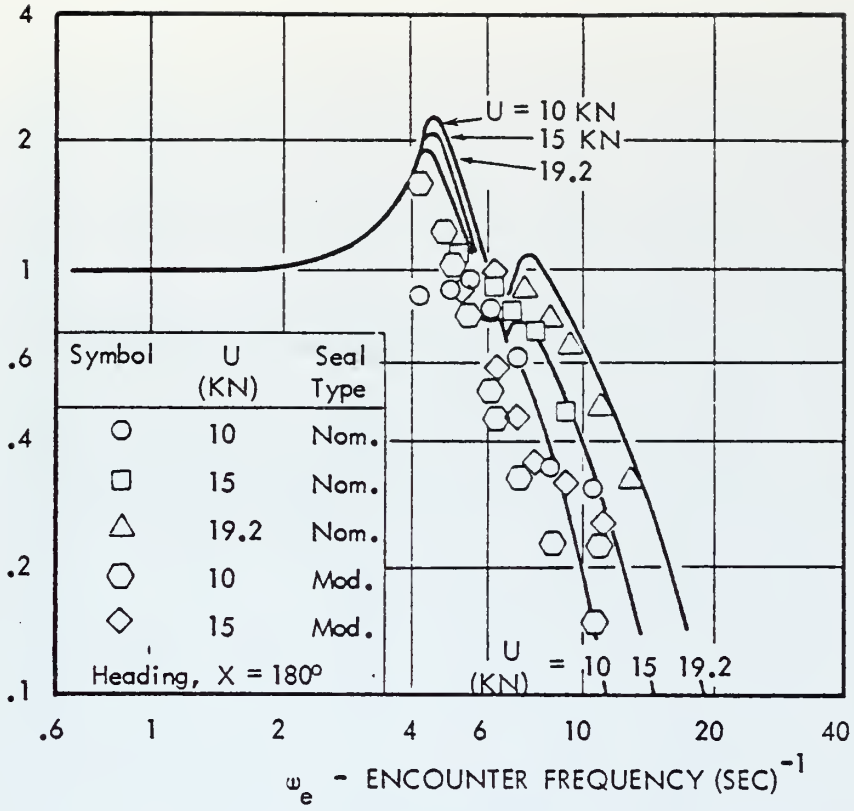

Figure B-1A. Heave Frequency Response, Ahead Seas

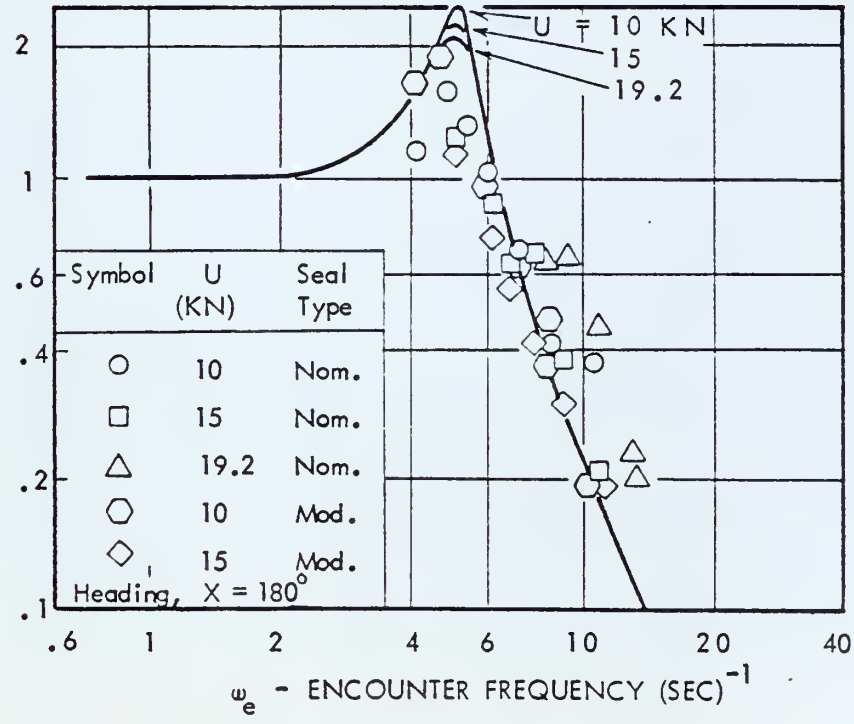

Figure B-1B. Pitch Frequency Response, Ahead Seas

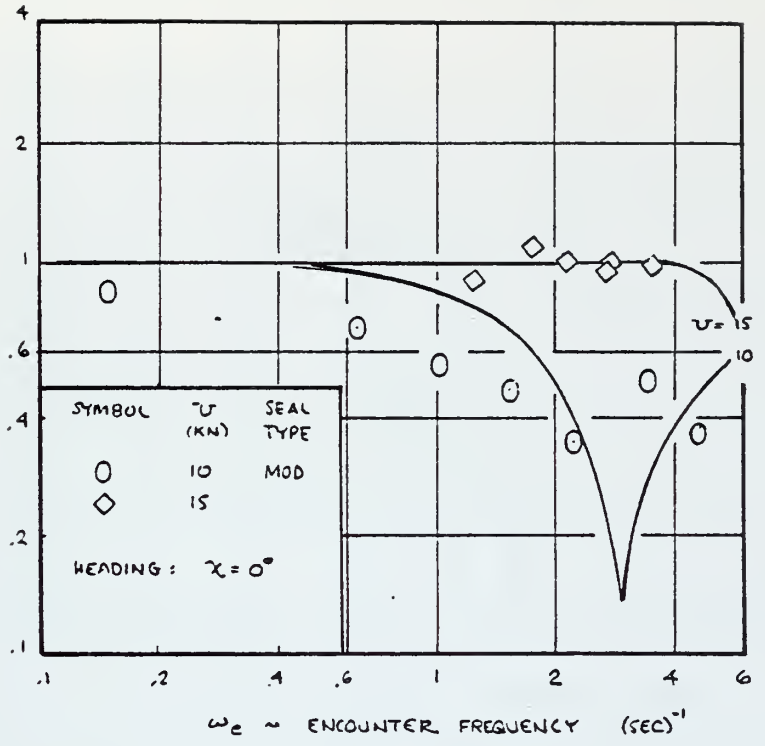

Figure B-2A. Heave Frequency Response, Following Seas

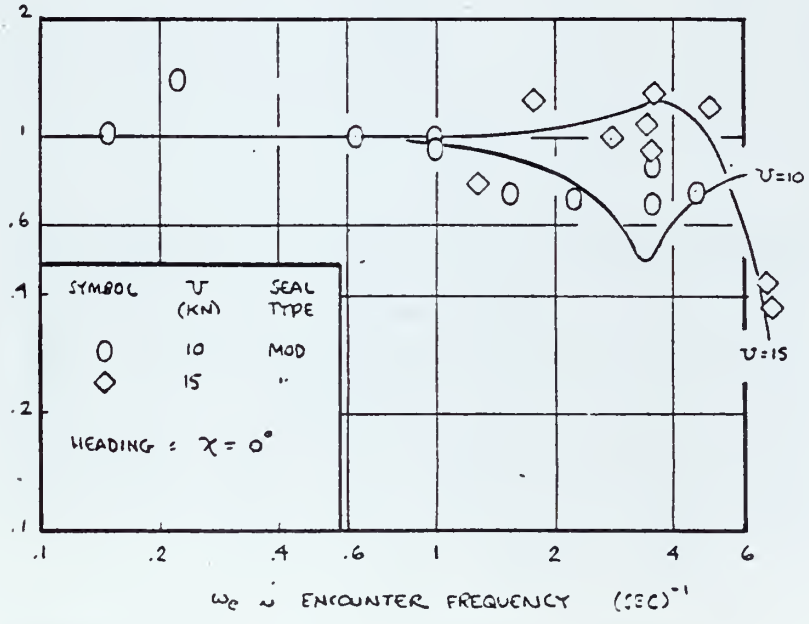

Figure B-2B. Pitch Frequency Response, Following Seas

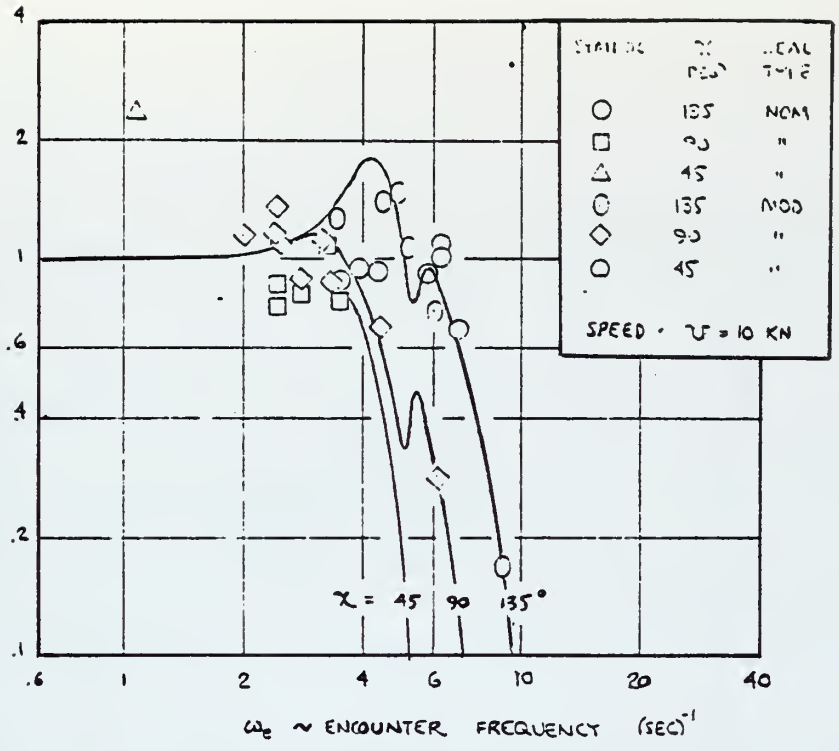

Figure B-3A. Heave Frequency Response, Oblique Seas

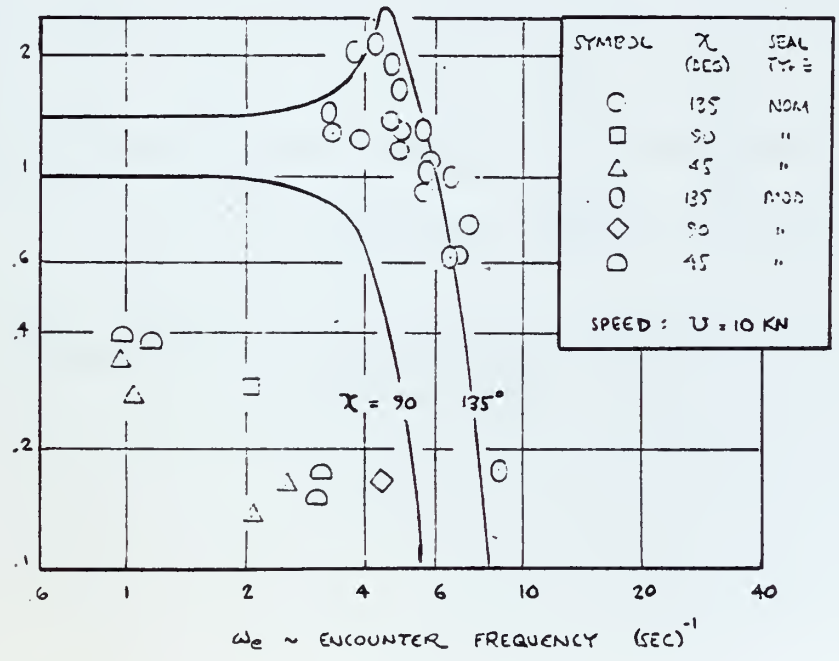

Figure B-3B. Pitch Frequency Response, Oblique Seas

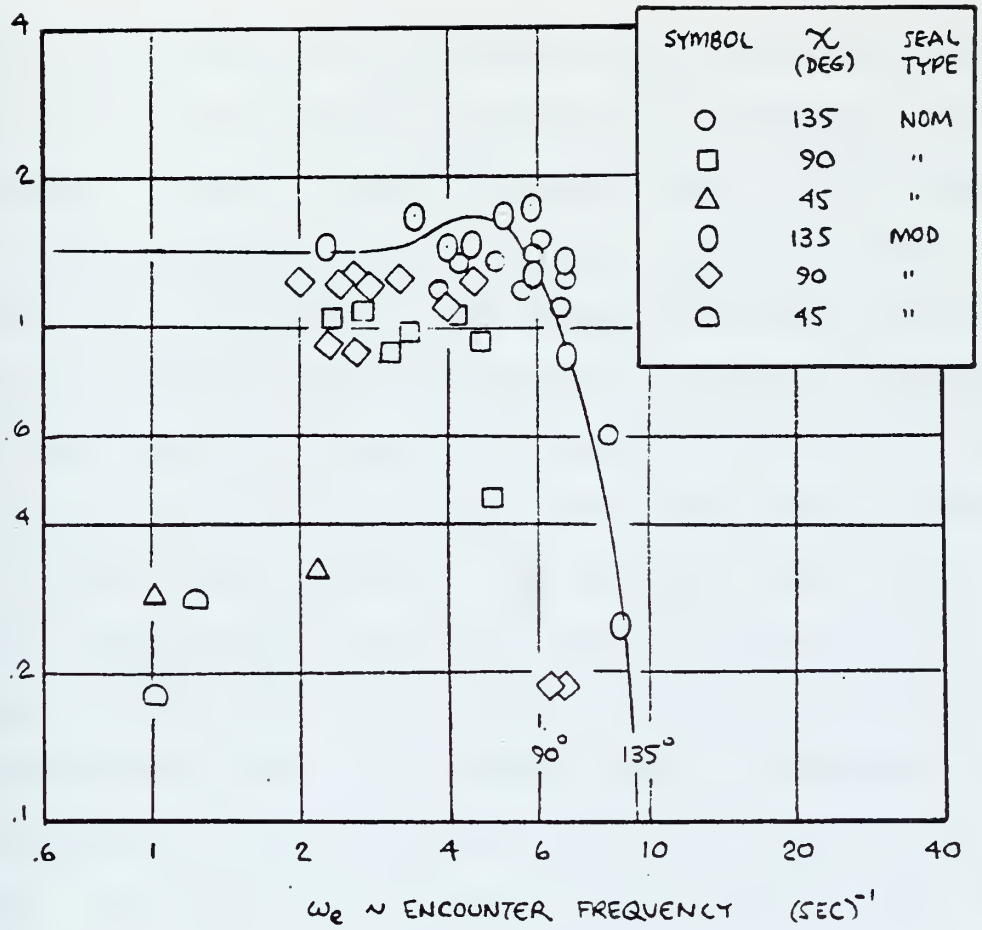

Figure B-3C. Roll Frequency Response, Oblique Seas

APPENDIX C

Initial Conditions

Prior to running the computer model with simulated wave conditions the "calm water" initial conditions had to be determined. Previous work by Forbes [Ref. 4] and Menzel [Ref. 5] had shown that the initial conditions used in the program had to be close to the steady state operating values. Failure to ensure this would result in either an imbalance in the forces generated within the program and cause the program to stop due to an improper integration step size or transients that obscured the response of the variable under study.

The steady state conditions found by Menzel for his Program 3 [Table XVI, Ref, 5] were used as the initial input to the computer model. The program was run using the constant speed option for forty seconds simulation time at nine different speeds. The steady state value of pitch angle, draft, plenum pressure, and thrust were determined for each speed. These values were then used as the initial conditions for a second set of constant speed runs to verify that the steady state values produced no transients when used as initial conditions. A third set of runs with the constant thrust option in use was performed to verify that the speed was maintained at its desired value.

The "calm water" steady state values determined by the above procedure and used throughout this study as initial conditions are listed in Table C-1 and plotted in Figure C-1.

TABLE C-1

Calm Water Initial Conditions

Speed (knots)	Pitch Angle (deg)	Draft (in)	Plenum Pressure (psf)	Thrust per side (lb)
10.0	1.62	8.17	23.93	200.31
12.5	1.11	7.03	24.84	174.71
15.0	0.84	6.74	24.84	167.85
17.5	0.63	6.41	24.84	173.23
20.0	0.48	6.12	24.84	186.72
22.5	0.36	5.87	24.84	205.77
25.0	0.29	5.66	24.84	229.31
27.5	0.25	5.48	24.84	256.65
30.0	0.26	5.34	24.84	287.22

Figure C-1: Initial Conditions vs. Speed
Speed (kts)
10
20
30
Pitch (degrees)
Thrust/side (lb)
Plenum Pressure (psi)
Dmeas (inches)

APPENDIX D

Craft Parameters

The following craft parameters were used throughout this study. The parameters are listed by Input Blocks. Also listed are the associated variable names as used in the program.

Integrator Tolerances: Block 1

Number of Integrators Used: 10

Runga-Kutta Variable Step Sized Used

Initial Step Sizes: $1x10^{-4}$, $2x10^{-4}$, $1x10^{-5}$, $1x10^{-7}$, $1x10^{-4}$, $1x10^{-6}$, $1x10^{-9}$, $1x10^{-9}$, $1x10^{-4}$, $1x10^{-4}$

Masses and Inertias: Block 2

Weight: 6050 lb WEIGHT

Longitudinal Center of Gravity: 10.05 ft forward of transom, XS

Vertical Center of Gravity: 2.54 ft above keel, ZS

I_{xx}, Mass Moment of Inertia About X axis: 2870.0 slug-ft^2 AIXX

I_{yy}, Mass Moment of Inertia About Y axis: 9320.0 slug-ft^2, AIYY

I_{zz}, Mass Moment of Inertia About Z axis: 10,580.0 slug-ft^2, AIZZ

I_{xz}, Mass Moment of Inertia About XZ axis: -2800.0 slug-ft^2, AIXZ

Craft Geometry: Block 3

Total Craft Length: 24.7 ft, XLTOT

Number of Stations along Port and Starboard Sidewalls: 11

Number of Stations along Bow and Stern Seals: 5

Sidewal: Block 4

Y distance from centerline to sidewall: 5.37 ft, YSW

Average Wetted Length of Sidewall: 21.9 ft, XLSW

Leakage Orifice Coefficient of Sidewall: 0.7, CFSW

Cross-flow Drag Coefficient of Sidewall: 1.28, CDSW

Average Beam of Sidewall: 0.5 ft, AVBMSW

Stern Seal: Block 5

X corrdinate of Stern Seal Hinge: 3.97 ft forward of transom, XSSI

Z coordinate of Stern Seal Hinge: 1.875 ft above keel, ZSSI

Base leakage area: 3.87 ft^2, ALEAK

Seal Leakage Orifice Coefficient: 0.9, CFSS

Length of Rear Support Cable: 1.875 ft

Pressure Differential Between Stern Seal and Plenum Chamber: 1 psf, DPSS

Length of Leading Edge of Seal: 4.06 ft, XLF

Bow Seal: Block 6

X coordinate of Bow Seal Hinge: 23.44 ft forward of transom, XBSI

Seal Leakage Orifice Coefficient: 0.9, CFBS

Pressure Differential between Bow Seal and Plenum Chamber: 1 psf, DPBS

Z coordinate of Bow Seal Hinge: 1.875 ft above keel, ZBSI

Length of Rear Support Cable: 1.875 ft

Length of Leading Edge of Seal: 4.06 ft, XBF

Base Leakage Area: 0.08 ft^2, BLEAK

Length of Middle Support Cable: 1.875 ft

Plenum: Block 7

Plenum Length at Water Surface: 20.0 ft, XLBW

Plenum Width at Water Surface: 10.0 ft, XBBW

X coordinate of Pressure Wave Pivot Point: 17.2 ft forward of transom, XPMV

Plenum Length at Deck: 20.0 ft, XL

X coordinate of Center of Pressure: 10.4 ft forward of transom, XCPO

Plenum Average Height: 1.915 ft, BUBHGT

Froude Number: 0.556, FNCRIT

Propulsion Geometry: Block 8

X coordinate of Propeller Center: -1.275 ft forward of transom, XPO

Y distance from centerline to propeller center: 5.55 ft, YPO

Z coordinate of propeller: -0.604 ft above keel, ZPO

Rudder Geometry: Block 9

X coordinate of Centroid of Rudder, -1.125 ft forward of transom, XRO

Y distance from Centerline to Rudder Centroid: 5.55 ft, YR

Z coordinate of Centroid of Rudder: -0.208 ft above keel, ZRO

Rudder Span: 1.21 ft, RSPAN

Rudder Aspect Ratio: 2.15, RASPR

Rudder Area: 0.68 ft^2, RAREA

Average Thickness Ratio of Rudder Section: 0.167, RTC

Aerodynamics: Block 10

Reference Length: 20.0 ft, XLAERO

Reference Width: 10.0 ft, BEAM

Thrust: Block 16

Starboard and Port Side Thrust Coefficients: 0.01, STHS and STHP

APPENDIX E

Gapping

Subroutine SIDEWL calculates the forces and moments acting on the craft due to the sidewalls as well as the leakage flow rates associated with any gaps which open under the sidewalls due either to craft motion or waves. A print switch option allows printing the sidewall gaps, imersion depths, and total forces and moments at each integration step. For purposes of this study in which 35 second runs were normally conducted the printed output of this print option was excessive since all the above quantities are printed each integration step. Since it was desired to know only if a gap occurred, its location along the sidewall, and the magnitude, a simple program addition was made to SIDEWL as follows.

```
C       GAP OR WETTED DRAFT CALCULATION                    SDWL0460
C                                                          SDWL0470
      → GAPT=0.0
        DO 10 J=1,2                                        SDWL0480
           .
           .
           .
      7 GAP(J,K)=-DDIN*(1.-(DSW(J,K))/PBHEAD               SDWL0630
      → GAPT=GAPT+GAP(J,K)
        GO TO 10                                           SDWL0640
      8 GAP(J,K)=0.0                                       SDWL0650
     10 CONTINUE                                           SDWL0660
        IF(GAPT.EQ.0.0) GO TO 12
        WRITE (6,11)VAL(1),((GAP(I,J),J=1,11),
       1I=1,1) ,GAPT,((GAP(I,J),J=1,11,I=2,2)
   →   11 FORMAT('(T)',F10.5,11(F8.5),/,
       2'(G)',FL0.5,11(F8.5))
```

```
C
C       LEAKAGE AREA                                    SDWL0670
                                                        SDWL0680
  →12 ALSW=0.0
```

Gapping was found to occur under the sidewall station 1 for the following conditions:

V = 10 knots, A = 0.2 ft

w_e= 4

V = 20 knots, A = 0.2 ft

w_e=4.5

A = 0.3 ft

w_e=4, 5, 6, 8, 20

A = 0.5 ft

w_e= 4, 5, 6, 8, 10

V = 30 knots, A = 0.2 ft

w_e= 4, 5, 6, 8, 10

A = 0.3 ft

w_e= 4, 5, 6, 8, 10, 15

Gapping was found under station 2 for the following conditions:

V = 20 knots, A = 0.5 ft

w_e= 5, 6, 8, 10

V = 30 knots, A = 0.3 ft

w_e= 5, 6, 10, 15

Gapping was noted at additional stations for V=20 knots, A = 0.5 ft. No gapping was noted during steady-state operation in abeam seas, however it was noted under the most forward station in following sea runs at V=10, w_e=4 and at station 2 at V=20, w_e=4.

APPENDIX F

A DFT Program

The IBM 360 library subroutine HARM which performs discrete complex fourier transforms on a complex three dimensional array, was used to take the DFT of the wave excitation and the heave and pitch time responses from ahead irregular seas in order to determine the frequency response functions. Once the complex fourier transform of the excitation and responses was determined, the magnitude of the spectrum was computed and plotted using the library subroutine DRAWP. The program is listed on the following pages.

```
      DIMENSION W(600),Z(600),P(600)
      DIMENSION FV(514)
      DIMENSION S(1012),INV(1012),M(3)
      DIMENSION TIME(600),WH(600),ZD(600),PA(600)
      COMPLEX*8 A(1024,1,1)
      INTEGER*4 ITB(12)/12*0/
      REAL*4    RTB(28)/28*0.0/
C
C
C     READ IN THE POWER OF TWO (DETERMINES THE NUMBER
C     OF DATA POINTS)  SAMPLE LENGTH, AND SAMPLING
C     INTERVAL
C
C
      READ(5,5)KK,T,DT
    5 FORMAT(I5,F10.4,F10.4)
      PI=3.14159
      N1=2**KK
      N2=1
      N3=1
      NF=N1/2
C
C     READ IN TIME, WAVE HEIGHT, HEAVE, AND PITCH DATA
C
      DO 10 K=1,N1
      READ(5,6)TIME(K),WH(K),ZD(K),PA(K)
    6 FORMAT(4F16.4)
   10 CONTINUE
      M(1)=KK
      M(2)=0
      M(3)=0
C
C     CALCULATE THE FUNDAMENTAL FREQUENCY AND THE
C     FREQUENCY COMPONENTS
C
      FUND=(2.0*PI)/T
      FV(1)=0.0
      DO 20 J=2,NF
      FV(J)=FV(J-1)+FUND
   20 CONTINUE
C
C     SET THE COMPLEX A MATRIX TO ZERO
C
      DO 2 I1=1,N1
      DO 2 I2=1,N2
      DO 2 I3=1,N3
    2 A(I1,I2,I3)=(0.0,0.0)
C
C     TRANSFER THE WAVEHEIGHT DATA TO THE COMPLEX A MATRIX
C
      DO 3 I1=1,N1
      DO 3 I2=1,N2
      DO 3 I3=1,N3
      A(I1,1,1)=WH(I1)
    3 CONTINUE
C
C     COMPUTE THE DISCRETE FOURIER TRANSFORM OF THE
C     WAVE HEIGHT DATA
C
      CALL HARM(A,M,INV,S,-1,IFERR)
C
```

```
C
C     CALCULATE THE MAGNITUDE OF THE FOURIER COMPONENTS
C     AND CONVERT THE RESULTS TO INCHES
C
      DO 30 I1=1,NH
   30 W(I1)=CABS(A(I1,1,1))*24.0
C
C     CLEAR THE A MATRIX
C
      DO 4 I1=1,N1
      DO 4 I2=1,N2
      DO 4 I3=1,N3
    4 A(I1,I2,I3)=(0.0,0.0)
C
C     COMPUTE THE DFT OF THE HEAVE DATA AND THE MAGNITUDES
C     OF THE FOURIER COMPONENTS
C
      DO 7 I1=1,N1
      DO 7 I2=1,N2
      DO 7 I3=1,N3
      A(I1,1,1)=ZD(I1)
    7 CONTINUE
      CALL HARM(A,M,INV,S,-1,IFERR)
      DO 50 I=1,NH
   50 Z(I)=2.0*CABS(A(I,1,1))
C
C     THE DC VALUE OF HEAVE  (THE AVERAGE DRAFT) IS
C     STORED AND LATER PRINTED.  IT IS NOT PLOTTED
C
      ZAVG=Z(1)
      Z(1)=0.0
C
C     COMPUTE THE DFT OF THE PITCH ANGLE DATA AND THE
C     MAGNITUDES OF THE FOURIER COMPONENTS
C
      DO 8 I1=1,N1
      DO 8 I2=1,N2
      DO 8 I3=1,N3
    8 A(I1,I2,I3)=(0.0,0.0)
      DO 9 I1=1,N1
      DO 9 I2=1,N2
      DO 9 I3=1,N3
      A(I1,1,1)=PA(I1)
    9 CONTINUE
      CALL HARM(A,M,INV,S,-1,IFERR)
      DO 55 J=1,NH
   55 P(J)=2.0*CABS(A(J,1,1))
C
C     STORE THE DC VALUE OF PITCH FOR LATER OUTPUT.  IT
C     IS NOT PLOTTED
C
      PAVG=P(1)
      P(1)=0.0
      WRITE(6,60) T,DT,N1,FUND,ZAVG,PAVG
   60 FORMAT(//,' SAMPLE TIME = ',F7.4,' SECONDS'//,' SAMP
     &LE INTERVAL = ',F6.4,' SECONDS'//,' NUMBER OF SAMPL
     &ES = ',I4//,' FUNDAMENTAL FREQUENCY = ',F6.4,' RPS'
     &//,' ZAVG = ',F7.4//,' PAVG = ',F7.4)
C
C     PLOT THE SPECTRUMS
C
```

```
ITE(12)=1
ITE(3)=5
RTE(1)=20.0
RTE(2)=0.5
CALL DRAWP (NH,FV,W,ITB,RTB)
RTE(1)=10.0
RTE(2)=0.2
CALL DRAWP (NH,FV,Z,ITB,RTB)
RTE(1)=5.0
RTE(2)=0.1
CALL DRAWP (NH,FV,P,ITB,RTB)
STOP
END
```

APPENDIX G

Data Tables

The frequency response and operating characteristics data presented graphically in the text are listed in Tables G-1 through G-14. The undefined headings and symbols are:

Ratio 1	the ratio of the peak-to-peak heave to the peak-to-peak wave height
Ratio 2	the ratio of the peak-to-peak pitch amplitude to twice the maximum wave slope
Ratio 3	the ratio of the peak-to-peak roll amplitude to twice the maximum wave slope
λ	wavelength (ft)
L	plenum chamber length, 20 ft.
*	water contact with the top of the plenum chamber occurred during steady-state operation
Z	calm water draft (in)
θ	calm water pitch (degrees)
T	calm water thrust used per side (lb)
V	craft velocity (knots)
A	wave amplitude (ft)
β	angle between the craft and wave headings

Encounter Frequency, w_e (rad/sec)	Peak-to-Peak Heave Amplitude (in)	Ratio 1	Average Draft (in)	Maximum Wave Slope (Degrees)	Peak-to-Peak Pitch Amplitude (Degrees)	Ratio 2	Average Pitch (Degrees)	Thrust used per side (lb)	Wavelength (ft)	λ/L
1	4.8	1	8.17	0.187	0.26	0.695	1.62	200.3	384.5	19.227
2	4.76	0.991	8.17	0.530	0.925	0.872	1.62	200.3	135.8	6.79
3	4.4	0.916	8.17	0.936	2.4	1.28	1.59	200.6	76.92	3.84
4*	5.5	1.14	11.75	1.380	5.2	1.88	2.1	187.0	52.18	2.60
5	3.84	0.8	9.96	1.848	2.7	0.73	2.0	193.0	38.95	1.94
6	2.4	0.5	8.8	2.334	1.65	0.353	1.97	196.0	30.84	1.54
8	0.44	0.09	8.3	3.351	2.85	0.425	1.67	198.0	21.48	1.07
10	0.84	0.175	8.24	4.404	0.225	0.051	1.85	199.0	16.35	0.81
15	0.2	0.041	8.17	7.143	0.1		1.85	199.5	10.03	0.50
20	0.3	0,062	8.17					198.5	7.21	0.360

V = 10 kts $\quad \beta = 180^\circ \quad$ Z = 8.17

TABLE G-1 $\quad$ A = 0.2 ft $\quad \theta = 1.62$

Encounter Frequency, w_e (rad/sec)	Peak-to-Peak Heave Amplitude (in)	Ratio 1	Average Draft (in)	Maximum Wave Slope (Degrees)	Peak-to-Peak Pitch Amplitude (Degrees)	Ratio 2	Average Pitch (Degrees)	Thrust used per side (lb)	Wavelength (ft)	λ/L
1	2.46	1.0	6.12	0.066	0.108	.818	.48	186.72	543.2	27.16
2	2.46	1.0	6.12	0.172	0.323	.938	.467	186.72	208.757	10.43
3	2.35	0.97	6.12	0.292	0.679	1.162	.468	186.72	123.70	6.185
4	2.18	0.9	6.06	0.419	1.35	1.610	.46	186.72	86.01	4.30
5	2.25	0.937	5.95	0.550	2.025	1.840	.48	186.72	65.40	3.27
6	2.09	0.87	5.93	0.686	1.24	0.903	.48	186.72	52.5	2.625
8	1.55	0.64	5.85	0.964	0.6	0.311	.46	186.72	37.36	1.868
10	0.95	0.39	5.9	1.248	0.368	0.14	.48	186.72	28.84	1.442
15	0.27	.11	6.0	1.980	0.1	0.025	.435	186.72	18.18	0.909
20	0.5	.20	5.5	2.730	0.08	0.014	.388	186.72	13.18	0.659

TABLE G-2

V = 20 kts
A = 0.1 ft
β = 180°
Z = 6.12
θ = 0.48

Encounter Frequency, ω_e (rad/sec)	Peak-to-Peak Heave Amplitude (in)	Ratio 1	Average Draft (in)	Maximum Wave Slope (Degrees)	Peak-to-Peak Pitch Amplitude (Degrees)	Ratio 2	Average Pitch (Degrees)	Thrust used per side (lb)	Wavelength (ft)	λ/L
1	4.9	1.02	6.12	0.133	.21	.789	.475	186.72	543.2	27.16
2	4.84	1.00	6.12	0.345	.653	.946	.448	186.72	208.75	10.43
3	4.64	0.96	5.98	0.584	1.36	1.16	.444	186.72	123.7	6.185
4	5.2	1.08	8.3	0.837	4.5	2.68	.62	215.0	86.01	4.30
5	4.6	0.95	6.9	1.101	2.625	1.19	.6	186.72	65.4	3.27
6	4.0	0.83	5.88	1.37	1.55	.56	.52	186.72	52.5	2.625
8	2.92	0.60	5.52	1.927	.77	.199	.52	186.72	37.36	1.868
10	1.85	0.38	5.42	2.496	.45	0.09	.548	186.72	28.84	1.442
15	0.5	0.104	5.7	3.959	.142	0.01	.4	186.72	18.18	0.909
20	1.1	0.22	5.0				.587	186.72	13.18	0.659

V = 20 kts
A = 0.2 ft
$\beta = 180^{\circ}$
Z = 6.12
θ = 0.48

TABLE G-3

Encounter Frequency, w_e (rad/sec)	Peak-to-Peak Heave Amplitude (in)	Ratio 1	Average Draft (in)	Maximum Wave Slope (Degrees)	Peak-to-Peak Pitch Amplitude (Degrees)	Ratio 2	Average Pitch (Degrees)	Thrust used per side (lb)	Wavelength (ft)	λ/L
1	7.3	1.01	6.12	0.199	0.305	.766	.48	186.72	543.2	27.16
2	7.3	1.01	6.12	0.517	0.984	.952	.43	186.72	208.75	10.43
3	7.0	0.97	5.88	0.875	2.05	1.17	.405	186.72	123.7	6.185
4	8.25	1.15	11.9	1.256	6.64	2.64	1.04	247.5	86.01	4.30
5	6.8	0.95	8.16	1.651	2.8	0.85	0.7	207.5	65.4	3.27
6	6.14	0.852	7.6	2.057	1.83	0.44	0.72	196.0	52.5	2.625
8	4.6	0.638	7.16	2.891	0.98	0.169	0.748	190.0	37.36	1.868
10	2.8	0.388	6.7	3.744	0.54	0.072	0.736	186.72	28.84	1.442
15	0.7	0.097	5.93	5.939	0.15		0.398	186.72	18.18	0.909
20	1.7	0.236	5.82	8.189			0.904	175.0	13.18	0.659

TABLE G-4

V = 20 Kts
A = 0.3 ft

$\beta = 180^{\circ}$

Z = 6.12
θ = 0.48

Encounter Frequency, ω_e (rad/sec)	Peak-to-Peak Heave Amplitude (in)	Ratio 1	Average Draft (in)	Maximum Wave Slope (Degrees)	Peak-to-Peak Pitch Amplitude (Degrees)	Ratio 2	Average Pitch (Degrees)	Thrust used per side (lb)	Wavelength (ft)	λ/L
2	12.1	1.008	5.8	0.862	1.675	0.971	0.4	186.72	208.757	10.43
3	11.6	0.96	5.52	1.459	3.5	1.19	0.325	186.72	123.70	6.185
4*	16.75	1.393	15.3	2.093	9.16	2.18	1.92	290.0	86.010	4.30
5	11.5	0.958	11.5	2.752	3.4	0.617	1.0	260.0	65.402	3.27
6	11.4	0.95	11.2	3.428	2.85	0.415	1.15	242.0	52.509	2.625
8	7.8	0.65	10.9	4.818	1.425	0.147	1.125	225.0	37.360	1.868
10	4.9	0.408	9.72	6.239	0.72	0.057	1.06	212.5	28.848	1.442
15	1.2	0.1	6.72	9.899	0.135	0.006	0.285	222.0	18.184	0.909

V = 20 kts β = 180° Z = 6.12

A = 0.5 ft θ = 0.48

TABLE G-5

Encounter Frequency, ω_e (rad/sec)	Peak-to-Peak Heave Amplitude (in)	Ratio 1	Average Draft (in)	Maximum Wave Slope (Degrees)	Peak-to-Peak Pitch Amplitude (Degrees)	Ratio 2	Average Pitch (Degrees)	Thrust used per side (lb)	Wavelength (ft)	λ/L
1	4.8	1.0	5.34	0.104	0.185	0.889	0.27	287.2	692.16	34.60
2	4.85	1.01	5.31	0.259	0.49	0.945	0.24	287.2	277.47	13.87
3	4.75	0.989	5.2	0.430	1.014	1.179	0.196	287.2	167.34	8.36
4	4.55	0.947	5.16	0.609	1.95	1.60	0.2	287.2	118.16	5.90
5	4.8	1.0	5.6	0.794	2.325	1.46	0.4	287.2	90.70	4.53
6	4.45	0.92	4.95	0.982	1.5	0.76	0.3	272.5	73.31	3.665
8	3.9	0.81	4.6	1.367	0.82	0.299	0.29	265.0	52.66	2.63
10	3.25	0.67	4.55	1.760	0.466	0.132	0.26	263.0	40.90	2.04
15	1.35	0.281	4.38				0.368	263.0	26.04	1.30
20	0.3	0.06	4.9				0.215	287.0	19.00	0.95

V = 30 kts
A = 0.2 ft
$\beta = 180^{\circ}$
Z = 5.34
θ = 0.26

TABLE G-6

Encounter Frequency, ω_e (rad/sec)	Peak-to-Peak Heave Amplitude (in)	Ratio 1	Average Draft (in)	Maximum Wave Slope (Degrees)	Peak-to-Peak Pitch Amplitude (Degrees)	Ratio 2	Average Pitch (Degrees)	Thrust used per side (lb)	Wavelength (ft)	λ/L
1	7.2	1.0	5.34	0.156	0.27	0.865	0.28	287.2	692.16	34.6
2	7.3	1.01	5.2	0.389	0.738	0.948	0.228	287.2	277.47	13.87
3	7.16	0.99	5.1	0.645	1.54	1.177	0.144	287.2	167.34	8.36
4	7.82	1.086	8.2	0.914	4.2	2.29	0.64	352.0	118.16	5.90
5	7.14	0.99	7.1	1.191	2.4	1.0	0.585	320.0	90.70	4.53
6	6.8	0.94	6.6	1.472	1.625	0.55	0.555	306.5	73.31	3.665
8	6.0	0.833	6.56	2.051	0.86	0.20	0.65	306.5	52.66	2.63
10	5.0	0.694	6.8	2.640	0.53	0.10	0.784	306.5	40.90	2.04
15	2.1	0.29	6.0	4.147	0.2		0.78	287.2	26.04	1.30
20	0.4	0.05	4.9	5.682	0.09		0.175	277.0	19.00	0.95

V = 30 kts
A = 0.3 ft
$\beta = 180^{\circ}$
Z = 5.34
θ = 0.26

TABLE G-7

Encounter Frequency, ω_e (rad/sec)	Peak-to-Peak Heave Amplitude (in)	Ratio 1	Average Draft (in)	Maximum Wave Slope (Degrees)	Peak-to-Peak Pitch Amplitude (Degrees)	Ratio 2	Average Pitch (Degrees)	Thrust used per side (lb)	Wavelength (ft)	λ/L
0.6	4.6	0.958	6.12	0.669	0.99	0.739	0.48	186.72	107.69	5.38
1	4.4	0.916	6.04	0.912	1.38	0.756	0.48	186.72	78.95	3.94
2	3.84	0.8	6.05	1.354	2.15	0.793	0.43	186.72	53.15	2.65
3	3.0	0.625	6.00	1.803	3.06	0.848	0.48	186.72	39.34	1.99
4	3.6	0.75	10.6	2.226	5.5	1.435	0.78	235.0	32.34	1.617
5	2.0	0.416	7.2	2.635	2.65	0.502	0.56	197.5	27.32	1.366
6	0.92	0.191	5.98	3.037	1.5	0.246	0.48	186.72	23.70	1.185
8	0.4	0.083	6.0	3.832	0.55	0.071	0.45	186.72	18.78	0.939
10	1.1	0.229	5.85	4.616	0.3	0.032	0.42	186.72	15.59	0.779
15	0.4	0.083	5.85	6.586	0.2	0.015	0.51	186.72	10.93	0.546

V = 20 kts Z = 6.12
A = 0.2 ft $\beta = 0^o$ $\theta = 0.48$

TABLE G-8

Encounter Frequency, ω_e (rad/sec)	Peak-to-Peak Heave Amplitude (in)	Ratio 1	Average Draft (in)	Maximum Wave Slope (Degrees)	Peak-to-Peak Pitch Amplitude (Degrees)	Ratio 2	Average Pitch (Degrees)	Thrust used per side (lb)	Wavelength (ft)	λ/L
0.6	1.0	0.208	8.6	2.03	1.82	0.448	1.62	203.0	35.38	1.76
1	1.0	0.208	8.4	2.50	1.81	0.361	1.675	201.5	28.78	1.43
2	0.96	0.2	8.8	3.53	1.54	0.217	1.75	199.0	20.37	1.01
2.66	1.0	0.208	8.64	4.11	1.55	0.188	1.775	199.0	17.48	0.87
3	1.12	0.233	8.4	4.48	1.65	0.183	1.725	199.5	16.03	0.80
4	2.66	0.554	11.3	5.41	4.9	0.452	2.08	190.0	13.28	0.66
5	1.2	0.25	9.04	6.28	2.4	0.190	1.95	195.5	11.45	0.57
6	0.46	0.09	8.4	7.14	1.275	0.089	1.86	198.5	10.07	0.50
8	--	--	--	--	--	--	--	--	8.18	0.40
10	0.34	0.07	8.17	10.54	0.35	0.016	1.9	198.5	6.83	0.34
15	0.2	0.04	8.17	14.59	0.14		1.9	198.5	4.93	0.24

V = 10 kts $\beta = 0^{\circ}$ Z = 8.17

A = 0.2 ft $\theta = 1.62$

TABLE G-9

Encounter Frequency, w_e (rad/sec)	Peak-to-Peak Heave Amplitude (in)	Ratio 1	Maximum Wave Slope (Degrees)	Peak-to-Peak Pitch Amplitude (Degrees)	Ratio 2	Peak-to-Peak Roll Amplitude (Degrees)	Ratio 3	Peak-to-Peak Yaw Amplitude (Degrees)	Average Yaw (Degrees)
1	4.9	1.02	0.356	0.04	0.05	0.47	0.67		
2	4.6	0.95	1.425	0.11	0.038	2.02	0.71	0.93	-0.44
3	3.5	0.72	3.206	0.36	0.056	4.45	0.69	1.8	-2.5
4	1.2	0.25	5.69	0.77	0.067	2.1	0.18	0.48	-0.24
5	0.8	0.16	8.90	1.24	0.069	3.5	0.19	1.3	0.60
6	0.5	0.10	12.82	0.63	0.024	1.6	0.06	0.4	0.33
8	0.25	0.05	22.79	0.10	0.002	1.4	0.03	0.36	-0.86
10	0.1	0.02	35.62	0.09		1.3		0.28	-0.395

TABLE G-10 V = 20 kts A = 0.2 ft $\beta = 90^{\circ}$ T = 186.72 lbs

NOTE: Peak-to-Peak and Average Yaw measured at the end of 30 second run without rudder input.

Encounter Frequency, w_e (rad/sec)	Peak-to-Peak Heave Amplitude (in)	Ratio 1	Maximum Wave Slope (Degrees)	Peak-to-Peak Pitch Amplitude (Degrees)	Ratio 2	Peak-to-Peak Roll Amplitude (Degrees)	Ratio 3	Peak-to-Peak Yaw Amplitude (Degrees)	Average Yaw (Degrees)
1	4.85	1.01	0.356	0.035	0.049	0.4	0.56	0.26	0.29
2	4.6	0.95	1.425	0.127	0.044	1.56	0.54	0.80	-0.036
3	3.4	0.70	3.206	0.41	0.064	3.75	0.58	1.67	-0.825
4	1.2	0.25	5.699	0.86	0.075	1.35	0.11	0.30	-0.023
5	0.8	0.16	8.905	1.30	0.072	2.95	0.16	1.14	-0.072
6	0.5	0.10	12.823	0.24	0.009	1.54	0.06	0.51	+0.72
8	0.25	0.05	22.797	0.135	0.002	1.4	0.03	0.40	-0.73
10	0.1	0.02	35.621	0.055		1.06	0.01	0.29	-0.51

TABLE G-11

V = 30 kts $\beta = 90^{\circ}$

A = 0.2 ft T = 287.2 lbs

NOTE: Peak-to-Peak and Average Yaw measured at the end of 30 second run without rudder input.

Encounter Frequency, ω_e (rad/sec) (from DFT)	Wave Amplitude (in)	Heave Amplitude (in)	Ratio	Calculated Wave Frequency (rad/sec)	Maximum Wave Slope (Degrees)	Pitch Amplitude (Degrees)	Ratio
3.512	0.147	0.154	1.049	1.395	0.042	0.1975	4.76
4.683	0.805	0.746	0.926	1.66	0.329	0.4636	1.40
6.244	1.740	1.510	0.867	1.98	1.012	0.3198	0.316
8.586	2.001	1.216	0.607	2.39	1.696	0.1943	0.114
11.71	2.072	0.486	0.234	2.80	2.41	0.0776	0.03
16.0	1.202	0.164	0.136	3.40	2.068		
22.6	0.942	0.174	0.185	4.12	2.374		

TABLE G-12 V = 20 kts $\bar{H}_{1/3}$ = 1.0 ft

Encounter Frequency, w_e (rad/sec) (from DFT)	Wave Amplitude (in)	Heave Amplitude (in)	Ratio	Calculated Wave Frequency (rad/sec)	Maximum Wave Slope (Degrees)	Pitch Amplitude (Degrees)	Ratio
3.122	0.77	0.77	1.0	1.296	0.192	0.483	2.5
4.29	2.27	2.39	1.05	1.579	0.84	1.129	1.34
5.85	3.044	2.669	0.876	1.905	1.639	0.745	0.45
7.8	2.562	1.602	0.625	2.258	1.93	0.396	0.20
10.93	1.713	0.442	0.258	2.745	1.91	0.555	0.29
14.83	1.688	0.208	0.1232	3.26	2.66	0.371	0.139
20.29	1.197	0.197	0.164	3.88	2.67	0.350	0.131

TABLE G-13 V = 20 kts $\bar{H}_{1/3}$ = 1.4 ft

Encounter Frequency, w_e (rad/sec) (from DFT)	Wave Amplitude (in)	Heave Amplitude (in)	Ratio	Calculated Wave Frequency (rad/sec)	Maximum Wave Slope (Degrees)	Pitch Amplitude (Degrees)	Ratio
4.293	0.139	0.2119	1.52	1.364	0.038	0.1583	4.16
5.85	0.873	0.8856	1.01	1.636	0.346	0.1816	0.52
8.195	1.589	1.343	0.845	1.987	0.931	0.1609	0.172
11.32	1.596	0.949	0.59	2.38	1.34	0.0756	0.056
15.61	1.785	0.3911	0.219	2.84	2.13	0.030	0.014
21.85	1.252	0.2021	0.164	3.422	2.17	0.011	0.005

TABLE G-14 V = 30 kts $\bar{H}_{1/3}$ = 1.0 ft

LIST OF REFERENCES

1. Oceanics Incorporated Report No. 71-84B, A Study of Surface Effect Ship (SES) Craft Loads and Motions, Part I & II., by P. Kaplan, J. Bentson, and T. P. Sargent, August 1971.

2. Boncal, R. and Leo, D. G., XR-3 Surface Effects Ship Test Craft: A Mathematical Model and Simulation Program with Verification, M.S. Thesis, Naval Postgraduate School, December 1973.

3. Finley, R. A., Refinements of the Seal Subroutines and Fan Air Flow Maps for the XR-3 Loads and Motion Program, M.S. Thesis, Naval Postgraduate School, December 1974.

4. Forbes, G. T., Validation of the Nonlinear Six Degrees-of-Freedom Mathematical Model of the XR-3 Captured Air Bubble Surface Effect Ship in Calm Water, M.S. Thesis, Naval Postgraduate School, December 1974.

5. Menzel, R. F., A Study of the Roll and Pitch Transients in Calm Water Using the Simulated Performance of the XR-3 Surface Effect Ship Loads and Motions Computer Program, M.S. Thesis, Naval Postgraduate School, December 1975.

6. St. Denis, M. and Pierson, W. J., "On the Motions of Ships in Confused Seas," SNAME Transactions, v. 61, p. 280-357, 1953.

7. Aerojet General Corp. Report No. 9132FR-1, Surface Effect Ships Craft Dynamics Program Final Report, Volume 2 - Technical Discussion, May 1969.

8. Comstock, J. P., Principles of Naval Architecture, p. 608-610, The Society of Naval Architects and Marine Engineers, 1967.

9. Williams, J., Oceanography, p. 186, Little, Brown & Co., 1962.

10. Pierson, W. J. and Moskowitz, L., "A Proposed Spectral Form for Fully Developed Wind Seas Based on the Similarity Theory of S.A. Kitaigorodskii," Journal of Geophysical Research, v. 69, no. 24, 15 December 1964.

11. Cagle, Lonnie F., Some Performance Characteristics of the Bell 100 Ton Surface Effect Ship, M.S. Thesis, Naval Postgraduate School, June 1973.

12. Brigham, E. O., The Fast Fourier Transform, Prentice-Hall, Inc., 1974.

INITIAL DISTRIBUTION LIST

		No. Copies
1.	Defense Documentation Center Cameron Station Alexandria, Virginia 22314	2
2.	Library, Code 0212 Naval Postgraduate School Monterey, California 93940	2
3.	Department Chairman, Code 62 Department of Electrical Engineering Naval Postgraduate School Monterey, California 93940	2
4.	Professor Alex Gerba, Jr., Code 62Gz Department of Electrical Engineering Naval Postgraduate School Monterey, California 92940	5
5.	Professor George J. Thaler, Code 62Tr Department of Electrical Engineering Naval Postgraduate School Monterey, California 93940	1
6.	Mr. A. W. Anderson PMS.304-31A-1 Surface Effect Ships Project Office P. O. Box 34401 Bethesda, Maryland 20034	6
7.	Lt. Bryant F. Booth III, USN NAVCOMMSTA Box 72 FPO, Seattle, Washington 98777	2